OPTIMIZATION OF THE FAIR TECHNIQUE FOR SPECIFIC BRAIN REGION PERFUSION STUDIES

APPROVED BY SUPERVISORY COMMITTEE

Richard W. Briggs

Roderick William McColl

Vikram D. Kodibagkar

Hanli Liu

Greg Allen

DEDICATION

I would like to thank my mentor Dr. Richard W. Briggs for his help and support for my thesis research work. I also want to thank the members of my Graduate Committee for their time and guidance. I want to appreciate all the people and my family who have given me help, especially those who shared my happiness and sadness.

OPTIMIZATION OF THE FAIR TECHNIQUE FOR SPECIFIC BRAIN REGION PERFUSION STUDIES

by

XIUFENG LI

DISSERTATION

Presented to the Faculty of the Graduate School of Biomedical Sciences

The University of Texas Southwestern Medical Center at Dallas

In Partial Fulfillment of the Requirements

For the Degree of

DOCTOR OF PHILOSOPHY

The University of Texas Southwestern Medical Center at Dallas

Dallas, Texas

November, 2008

OPTIMIZATION OF THE FAIR TECHNIQUE FOR SPECIFIC BRAIN REGION PERFUSION STUDIES

XIUFENG LI, Ph.D.

The University of Texas Southwestern Medical Center at Dallas, 2008

RICHARD W. BRIGGS, Ph.D.

Most of the technical development and applications of ASL (arterial spin labeling) imaging have mainly focused on the superior cortical regions of the brain. However, optimal ASL measurements to quantify cerebral blood flow (CBF) in specific brain regions may require optimized parameters, improved techniques, or new imaging schemes based upon physiological or anatomic characteristics of those brain regions. In this thesis, the advantages of this region-targeted approach are demonstrated by performing quantitative perfusion studies

of two representative brain regions, the cerebellum in the inferior part of the brain and the hippocampus in the mid-brain.

To minimize or eliminate the venous artifacts found in cerebellum perfusion studies using traditional FAIR (flow-sensitive alternating inversion recovery) technique, FAIR ASST (FAIR with active suppression of superior tagging technique), as well as MDS FAIR, (modulated dual saturation pulse trains for FAIR) was developed and compared to PICORE (proximal inversion with a control for off-resonance effects) for quantifying cerebellum perfusion. The data indicate that FAIR ASST yields more robust CBF (cerebral blood flow) measurements.

OPTIMAL FAIR (orthogonally-positioned tagging imaging method for arterial labeling of FAIR) was developed and shown to reduce the heterogeneity of within-slice transit time and to minimize partial volume effects, improving quantitative CBF maps for cerebellum and hippocampus.

These techniques were optimized and applied to the study of perfusion abnormalities in brain regions important to the study of Gulf War Syndrome. Together with regionally optimized parameters, these ASL methods provide more reliable, efficient, accurate, and artifact-free CBF measurements than methods previously available.

TABLE OF CONTENTS

LIST OF FIGURES

LIST OF TABLES

LIST OF DEFINITIONS

CBF – cerebral blood flow

ASL – arterial spin labeling

PASL – pulsed arterial spin labeling

CASL – continuous arterial spin labeling

FAIR – flow-sensitive alternating inversion recovery

PICORE - proximal inversion with a control for off-resonance effects

MDS FAIR - modulated dual saturation pulse trains for FAIR

FAIR ASST - FAIR with active suppression of superior tagging technique

OPTIMAL FAIR - orthogonally-positioned tagging imaging method for arterial labeling of FAIR

CHAPTER 1 Introduction

The perfusion of the cerebral tissue bed is a very important physiological index for evaluating function and viability. In this chapter, a comprehensive literature review is performed about perfusion, perfusion imaging techniques - especially pulsed arterial spin labeling (PASL) methodologies and quantification models, and aspects relevant to the brain regions studied, such as the brain vascular system. One of the most widely used PASL techniques, the flow-sensitive alternating inversion recovery (FAIR) technique, is also discussed in detail. Lastly, the background and specific aims of this thesis research are presented.

1.1 PERFUSION AND CEREBRAL BLOOD FLOW

Tissue perfusion is one important physiological parameter that is widely used to evaluate the delivery rate of nutrients to tissue. Tissue perfusion is calculated as the amount of delivered blood in milliliters per minute per 100 grams of tissue (mL/min/100g). In brain perfusion studies, the brain perfusion is also called cerebral blood flow (CBF) or regional cerebral blood flow (rCBF).

For healthy brain tissue, typical CBF for grey matter is more than two times higher than that of white matter, and the average perfusion of grey matter ranges from 50 to 70 mL/100g/min (Matthew, Andreason et al. 1993; Buxton 2001; Matt A. Bernstein 2004; Ito, Inoue et al. 2006). The entire blood flow to the brain is about 750 to 900 mL/min (Yazici, Erdogmus et al. 2005; Fox 2006).

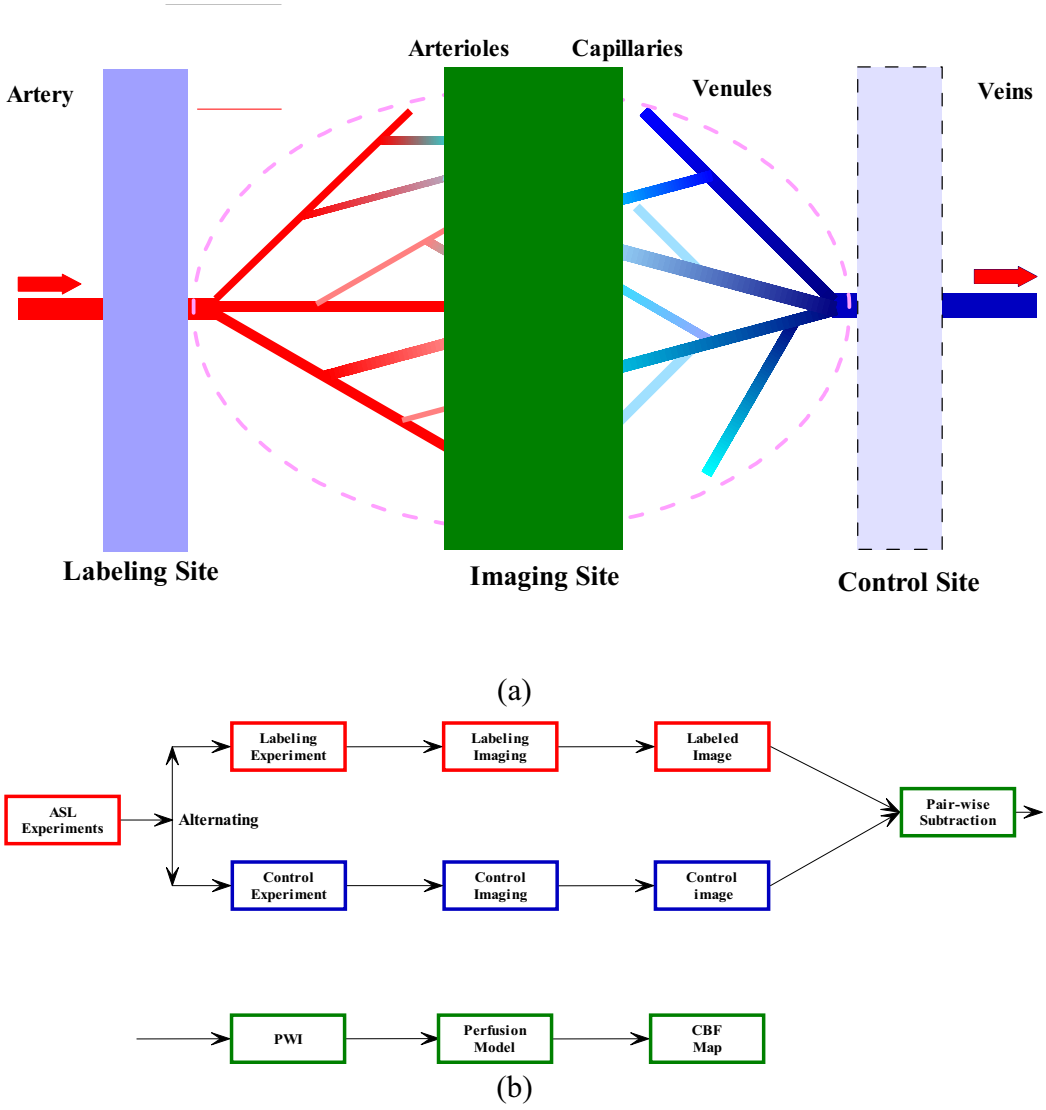

Figure 1-1 Schematic diagram for ASL imaging. (a) The labeling of arterial blood is proximal to the tissue of interest, as shown by the blue plane at left. After a delay to let labeled blood to arrive at the tissue sites, imaging acquisitions will be performed. In some ASL techniques, such as EPISTAR, control experiments will be done using the symmetric labeling RF pulse at the distal site to minimize the MT effects (light blue plane at right). (b) The boxes in red and blue demonstrate how ASL studies will be performed in an alternating way between labeling and control experiments. The boxes in green show the work flow to generate PWI and CBF maps

1.2 PERFUSION IMAGING AND ARTERIAL SPIN LABELING

Tissue perfusion has been studied for a long time by using different imaging methods (Wintermark, Sesay et al. 2005), including the microsphere method (Sapirstein 1958), autoradiography techniques based on the modified Fick law by Kety-Schmidt (Kety and Schmidt 1948), PET (positron emission tomography) (Frackowiak, Lenzi et al. 1980; Raichle, Martin et al. 1983; Jagust, Eberling et al. 1993; Ishii, Sasaki et al. 1998) and SPECT (single photon emission computed tomography) (Ohnishi, Hoshi et al. 1995; Rodriguez, Vitali et al. 2000; Kubota, Ushijima et al. 2005), and magnetic resonance imaging techniques such as bolus tracking (Haase, Matthaei et al. 1986; Rempp, Brix et al. 1994; Ostergaard, Sorensen et al. 1996; Ostergaard, Weisskoff et al. 1996) and arterial spin labeling (ASL) (Detre, Leigh et al. 1992; Alsop and Detre 1996; Wong, Buxton et al. 1997; Buxton, Frank et al. 1998; Edelman and Chen 1998; Wong, Buxton et al. 1998; Buxton 2005).

As a completely non-invasive perfusion imaging technique, ASL has been widely applied both at clinic and in research laboratories. ASL techniques use labeled arterial blood to measurement CBF. The labeling of arterial blood is achieved by using saturation (Detre, Leigh et al. 1992) or inversion pulses (Zhang, Williams et al. 1992) at the site proximal to the tissue of interest(Figure 1-1). In ASL perfusion study, there are two experiments/imaging acquisitions: control experiment and labeling experiment. These two experiments are performed in an interleaved way. In labeling experiment, arterial blood is labeled and labeling images are acquired after a short delay to allow labeled arterial blood to be delivered to brain tissue. In control experiment, no arterial blood is labeled and after the same short delay, control images are acquired. In control

image, MRI signals come from brain tissue and arterial blood. In labeling image, MRI signals come from brain tissue and labeled arterial blood. After pair-wise subtraction, ideally, static brain tissue can be cancelled out to leave only arterial blood signals left. By using proper ASL model, CBF maps can be reconstructed. The pair-wise subtracted image from the control image (no magnetic labeling) and the labeling image is referred to as a perfusion-weighted image (PWI) (Figure 1-1).

The application of inversion RF pulses can generate magnetization effects (MT) (Wolff and Balaban 1989) on tissue, especially in multi-slice ASL perfusion studies in which inversion RF pulses are applied relative to the center of imaging slab, and if the MT effects are not the same between the labeling and control experiments, this MT effects can confound ASL perfusion signals. In tissue, protons can be categorized into two pools: free pool, in which protons are not restricted and mobile, and restricted pool, in which protons are bound to macromolecules or membranes. The application of off-resonance RF pulses can saturate protons in restricted pool but has no effects on protons in free pool. Due to the exchange of protons between free pool and restricted pool, MRI signals can be different between images acquired with and without applied off-resonance RF pulses. Because ASL signals have lower signal level (about 1%), without well-controlled MT effects between two experiments, signals due to MT effects can dominate the subtraction signals, making perfusion measurements not reliable. To minimize the MT effects, some ASL techniques, such as EPISTAR (Edelman, Siewert et al. 1994), usually perform control experiments using the same labeling RF pulses at the symmetric distal sites. Inflow of labeled blood produces a measurable change in the magnetization, which is used for perfusion quantification.

ASL techniques usually fall into two major categories: continuous arterial spin labeling (CASL) and pulsed arterial spin labeling (PASL).

In CASL, the arterial blood is inverted continuously by using flow-driven adiabatic RF pulses with sufficiently long time (1-2 second(s)) to establish the equilibrium/steady-state for the labeled spins between arteries and brain parenchyma before the images are acquired (Williams, Grandis et al. 1993). To achieve adiabatic inversion, some conditions have to be satisfied (Williams, Detre et al. 1992; Zhang, Williams et al. 1993). Depending on the selection of inversion slab gradient strength and RF pulse B1, the labeling efficiency at the labeling site can range from 80% to 90% in CASL (Zhang, Williams et al. 1993; Maccotta, Detre et al. 1997; Marro, Hayes et al. 1997; Utting, Thomas et al. 2003). However, in real practice, due to the limitation from RF amplifier capability and SAR, intermittent RF pulse train is usually used with lower duty cycle, resulting in much lower labeling efficiency (Wang, Zhang et al. 2005). Using a separate coil for the labeling of the arterial blood is another way to perform continuous arterial spin labeling perfusion studies (Silva, Zhang et al. 1995; Zhang, Silva et al. 1995; Zaharchuk, Ledden et al. 1999; Zhang, Nagaoka et al. 2007).

To avoid overestimations of CBF due to labeled blood spins in large arteries, in Ye's study (Ye, Mattay et al. 1997), a weak crusher gradient was used to dephase the fast-flowing labeled spins, showing that as much as 50% of the total blood signal comes from big arteries and the apparent transit time is much delayed with comparison to the transit time measured without using weak crushing gradient. In this study, the four-step acquisition method was proposed to compensate the asymmetry in the magnetization transfer spectrum around the chemical shift to the water signal (Pekar, Jezzard et al. 1996)

and applied in other studies (Ye, Mattay et al. 1997). However, bipolar gradients can not separate fast-flowing and slow-diffusing spins in tissue (Le Bihan, Breton et al. 1988). Furthermore, even a weak crusher gradient with a small b value produces diffusion effects, which might complicate CBF quantification. As another approach to reduce the intravascular artifacts and minimize the sensitivity of CBF estimations to transit time (Zhang, Williams et al. 1992; Kim 1995), a post-labeling delay between the labeling pulse and the image acquisition was inserted (Alsop and Detre 1996).

Although CASL has (e times) higher SNR than PASL under circumstances and produces a better-defined temporal bolus width for CBF quantification, the disadvantages of CASL have limited its applications. CASL has lower temporal resolution due to its long labeling time (Alsop and Detre 1998; Wang, Zhang et al. 2005) and post-bolus delay (Alsop and Detre 1996). The labeling efficiency of CASL has strong dependency on flow velocity. The assumption of steady-state magnetization for labeled blood with CASL also makes the quantification of CBF highly sensitive to other MRI parameters, such as the T1 of brain tissue and exchange time τ_{ex}. At higher fields (3T or 7T systems), due to its higher specific absorption rate (SAR), a transmit/receive head coil has to be used, which limited the coverage of the brain in perfusion studies.

In contrast to CASL, the labeling of arterial blood can be done within tens of milliseconds in PASL. PASL will be introduced in the following section.

1.3 PULSED ARTERIAL SPIN LABELING (PASL)

PASL represents a family of pulse sequences, all of which use the same basic principle but different strategies to perform the labeling and control experiments. According to the symmetry of applied labeling RF pulses relative to the imaging slab, all

PASL techniques can be further categorized into two major types: asymmetric and symmetric PASL techniques.

1.3.1 Asymmetric PASL

The first asymmetric PASL technique is echo-planar imaging with signal targeting by alternating radiofrequency pulses (EPISTAR), proposed by Edelman (Edelman, Siewert et al. 1994). To eliminate venous inflow due to the application of inversion RF pulses on the distal side of the imaging section in control experiment and to take care of asymmetric MT effects, EPISTAR technique was further optimized (Edelman and Chen 1998).

Based on the same schemes by EPISTAR (Edelman and Chen 1998), other asymmetric techniques have been proposed and widely used, mainly including the proximal inversion with a control for off-resonance effects (PICORE) (Wong, Buxton et al. 1998), transfer insensitive labeling technique (TILT) (Golay, Stuber et al. 1999; Pruessmann, Golay et al. 2000), and double inversion with proximal labeling of both tagged and control images (DIPLOMA) (Jahng, Zhu et al. 2003).

1.3.2. Symmetric PASL

The representative symmetric PASL technique is the flow-sensitive alternating inversion recovery (FAIR) technique proposed initially by Kwong (Kwong, Belliveau et al. 1992) and further studied and applied by Kim (Kim 1995) and other researchers (Wang, Tang et al. 2003). In this technique, selective inversion of the imaging section and non-selective inversion of whole brain are performed in labeling and control experiments, respectively. Transmit/receive head coil was dominantly used in early human studies (Schwarzbauer, Morrissey et al. 1996; Kim and Tsekos 1997).

In the selective inversion acquisition, the inversion slab is applied to a region slightly larger than the imaging slab to minimize the edge effects of imperfect inversion pulse profiles. During the selective inversion, the tissue outside of the inversion slab is not perturbed. After a delay, images are acquired using EPI or other fast imaging sequences.

In the non-selective inversion acquisition, global inversion of water protons in the whole head is performed without any slice-select gradient. In some implementations of FAIR, the same gradient waveform can be applied at a different time to spoil the residual magnetization, compensate the eddy current effect, and minimize the differences in gradient waveforms between selective inversion and non-selection inversion acquisitions (Kwong, Chesler et al. 1995).

The selective inversion acquisition of FAIR technique is called labeling experiment, in which the magnetization of labeled blood is not inverted and has a positive z component. The non-selective inversion acquisition of FAIR technique is called control experiment, in which the magnetization of blood water is inverted and has a negative z component. ASL difference signal can be calculated by using the formula: $\Delta M = M_{labeling} - M_{control}$.

Because inversion pulses are symmetrically applied relative to the center of the imaging section, the FAIR technique and other symmetric PASL techniques are very robust against MT effects. Another unique characteristic of symmetric PASL techniques is that they have superior labeling on the distal side in addition to the inferior labeling on the proximal side of the brain tissue of interest. However, spins in big veins, such as

sagittal sinus and straight sinus, may also be labeled and appear as hyper-intense artifacts in neighboring tissue around veins, which will be addressed in detail in this thesis study.

FAIR is a widely used PASL technique with many variants, including un-inverted flow-sensitive alternating inversion recovery (UNFAIR) (Yongbi, Branch et al. 1998; Berr, Hagspiel et al. 1999; Berr and Mai 1999; Tanabe, Yongbi et al. 1999), FAIR excluding radiation damping (Zhou, Mori et al. 1998; Zhou and van Zijl 1999), FAIR with an extra radiofrequency pulse (FAIRER) (Mai and Berr 1999; Mai, Hagspiel et al. 1999), FAIR exempting separate T1 measurement (FAIREST) (Pell, Lythgoe et al. 1999; Pell, Thomas et al. 1999; Lai, Wang et al. 2001), unprepared basis and selective inversion (BASE) (Schwarzbauer and Heinke 1998), FAIR-trueFISP (Schraml, Boss et al. 2007), turbo-FLASH FAIR (Pell, Lewis et al. 2004), and so on.

1.3.3. Improvements on PASL

In most PASL implementations, the temporal bolus width is defined by a separate inversion RF pulse and gradient, and is dependent on the specific blood velocity in the labeling site and labeling slab size. The estimation of the temporal bolus width using the central volume principle (Alsop and Detre 1996) is invalid for the blood in big arteries, and the mean transit time can not be accurately estimated, all of which can cause errors for PASL CBF quantification. To permit quantitative CBF estimations, studies have been conducted using multiple inversion times to provide data for fitting to a perfusion model (Hennig, Nauerth et al. 1986). To simplify CBF quantification, the single-subtraction methods QUIPSS I and II were proposed by Wong (Wong, Buxton et al. 1998). QUIPSS is the acronym for quantitative imaging of perfusion using a single subtraction. According to the results from comparison studies, QUIPSS II is better than

QUIPSS I because QUIPSS I is more sensitive to flow-through effects and not amenable to multiple slice imaging. This method was further improved by Luh (Luh, Wong et al. 1999; Luh, Wong et al. 2000), and the modified method was named Q2TIPS, or QUIPSS II with thin-slice TI1 periodical saturation.

A new form of PASL, velocity-selective ASL (Wong, Cronin et al. 2006), was proposed to reduce the sensitivity to transit time. In this method, only blood spins flowing above a defined cutoff velocity are labeled in the labeling phase and only spins with the velocity below a specific threshold are imaged in the data acquisition phase. In this method, the labeling is not limited to specific spatial locations but is close to the target slice with negligible transit delay. However, it is more sensitive to pulsation (Wu and Wong 2007) and has lower signal-to-noise ratio because of the small amount of labeled blood. Studies (Duhamel, de Bazelaire et al. 2003; Wu and Wong 2006) have been conducted to better understand, evaluate, improve, and apply this scheme.

1.3.4. Advantages and Disadvantages of PASL Techniques

PASL has much higher temporal resolution and higher labeling efficiency than CASL. CBF estimation with PASL is less sensitive to T1 values of brain tissue than with CASL. PASL also has lower subtraction error level due to the imperfection of inversion profiles. SAR is not an issue for PASL even at ultra-high field.

A significant disadvantage of PASL is its lower SNR, making more averages necessary. When performing CBF quantifications with PASL sequences using QUIPSS II or Q2TIPS schemes, the temporal bolus width definition can be poorer than with CASL, due to the variation of velocity across cardiac cycle and space.

1.4 RECENT DEVELOPMENT OF FAIR TECHNIQUE AND ITS LIMITATIONS

The original FAIR technique has been adapted to the latest advances of MRI scanner hardware and to perform quantitative perfusion studies using the single blood compartment perfusion model. However, when applied to perfusion studies in specific brain regions, the FAIR technique exhibits some limitations that compromise reliable CBF estimations.

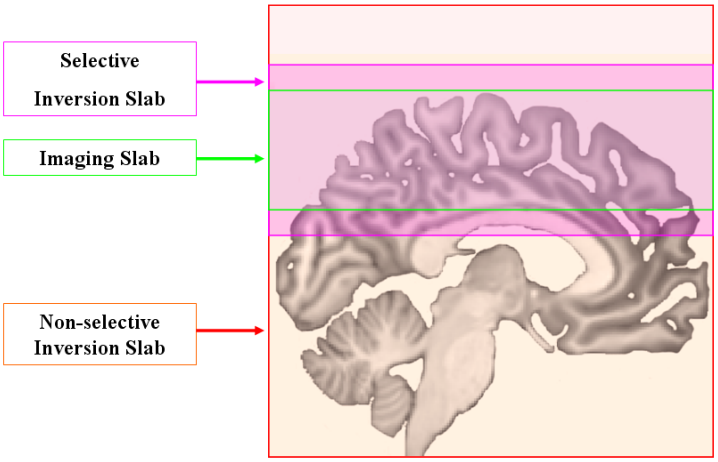

Figure 1-2 Schematic diagram for FAIR technique (refer to Appendix D for the information about the anatomic image)

1.4.1 Original FAIR Technique

FAIR is a symmetric PASL technique, and originally used selective inversion and non-selective inversion for control and labeling imaging as demonstrated in Figure 1-2. The selective and non-selective inversion RF pulses were typically hyperbolic secant pulses with duration about 15 ms (Frank, Wong et al. 1997). To avoid slice profile imperfections at the edges or minimize substantial subtraction errors due to the transition regions of the inversion slabs, the selective inversion slab is made wider than the imaging slab. The non-selective inversion is achieved by using the same hyperbolic secant pulse without slab selective gradient. In those earlier studies, transmit/receive head coil was dominantly used. However, the use of transmit/receive head coil for ASL perfusion studies may give lower labeling efficiency at the edge of the head coil. Due to the limited size of the transmit/receive head coil, to have enough arterial blood labeled, larger

labeling slab has to be used, making ASL perfusion studies mainly restricted to the superior part of the brain. The position of imaging slices shown in Figure 1-3 is the typical setup for PASL studies.

With parallel imaging, multiple channel phased array coils are used for signal reception, while the body coil is typically used as the transmit coil. But non-selective inversion with body-coil produces extra problems for FAIR. One of them is that the repetition time has to be long enough to allow the complete relaxation of labeled spins before the next non-selective inversion. Otherwise, the labeling efficiency or the signal-to-noise ratio of the perfusion map will be lower. More importantly, CBF quantification model assumes that in the labeling experiment of the FAIR technique, the blood outside of the imaging slab should be fully relaxed. To avoid this complication, global pre-saturation was proposed by Pell (Pell, Thomas et al. 1999) to make the label and control experiments have identical initial longitudinal magnetization and improve the time efficiency for short TR. An even worse problem for body coil transmission is that the very long bolus duration from the non-selective inversion will present labeled spins in larger arteries of the imaged slice(s) during signal acquisition, generating spurious hyper-intense signals in both perfusion-weighted images and CBF maps and resulting in the overestimation of cerebral blood flow.

1.4.2 Temporally-confined FAIR

To simplify CBF quantification using single subtraction method and FAIR technique, FAIR with QUIPSS II (Wang, Licht et al. 2003) scheme was implemented to help define relatively accurate temporal width of the bolus by conducting saturations at the labeling site after a user-specified labeling time following the selective and non-

selective inversion (Figure 1-3). However, because large saturation slab size was used (Wang, Licht et al. 2003), the profile of saturation pulse can not match the profile of inversion pulse very well with contaminations due to the interference between the saturation slab and the imaging slab, making CBF estimation in the inferior slices unreliable. In addition, although two (Wang, Licht et al. 2003) or more (Gunther, Oshio et al. 2005) saturation pulses were used, the saturation may not be complete. To avoid these problems, FAIR with Q2TIPS method had better be used, which will be addressed in the Chapter 2.

QUIPSS II and Q2TIPS techniques have been used mainly with a transmit/receive head coil, in which the spatial size of the non-selectively labeled bolus is limited by the extent of the head coil. When this technique is applied using the body coil as a transmitter and a phased array head coil as a receiver for parallel imaging, non-selective inversion will generate an excessively large bolus, causing CBF to be overestimated due to intense intravascular artifacts from the residual signal of the excess bolus in the imaging slice(s) during signal acquisition. Furthermore, because of the dependence of transit time of the residual of the bolus upon individual brain geometry, the inter-subject variability of CBF can be also higher.

1.4.3 Spatially-confined FAIR

To overcome these difficulties, Zhang et al. implemented and evaluated spatially-confined FAIR by conducting comparisons with FAIR using global non-selective inversion and a diffusion-weighted gradient, and FAIR using global non-selective inversion with QUIPSS II in the superior part of the brain (Zhang, Song et al. 2005). In spatially-confined FAIR, the non-selective inversion in the labeling experiment

is replaced by a large selective inversion slab created with a weaker than normal slice-selective gradient. Their results indicate that QUIPSS II overestimates the CBF due to large vessel effects and that spatially-confined FAIR gives CBF values similar to those obtained from global non-selective inversion with a diffusion-weighted gradient. Spatially-confined FAIR can also help facilitate perfusion studies in the inferior part of the brain, which is impossible for both PASL and CASL techniques using a transmit/receive head coil.

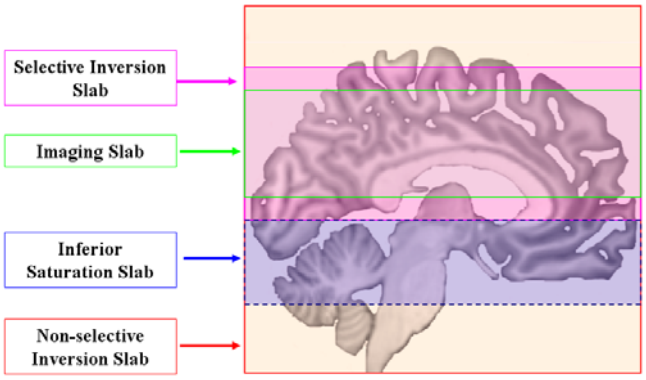

Figure 1-3 Schematic diagram for FAIR QUIPSS II (refer to Appendix D for the information about the anatomic image)

1.4.4 Limitations of FAIR

However, there are still some unsolved problems with FAIR and similar sequences. First, the intrinsic two-sided labeling generates significant venous artifacts due to inflowing spins from the superior inversion slab in perfusion studies using limited coverage, especially when such studies are focused on the mid-brain and inferior parts of the brain containing large veins, such as the occipital lobe with sagittal sinus and the cerebellum with transverse and straight sinuses. Second, the two-sided labeling of FAIR can introduce additional potential confounds for CBF quantification using single subtraction methods when limited coverage imaging slabs are used and imaging slice(s)

contain curved or tortuous arteries that going through the imaging slice(s) and come back. For accurate CBF quantification, this superior inflow should be included in the model. More simplistically, if the single subtraction method and single blood compartment model are used, the temporal width for the superior bolus should also be defined, as usually done for the inferior bolus with QUIPSS II or Q2TIPS. However, this may affect the bolus defined in the inferior side of imaging slab, making CBF quantification using FAIR in this circumstance problematic.

1.5 ASL MODELS AND PASL CBF QUANTIFICATION

Although perfusion-weighted maps give a qualitative picture of cerebral perfusion, quantitative estimation of cerebral blood flow (CBF) requires that the data be modeled appropriately. Depending upon whether the labeled blood is freely diffusible or undergoes restricted diffusion, a single-, two- or multiple-compartment model may be used.

1.5.1 ASL Models for Perfusion Quantification

Two approaches have been proposed independently by Detre (Detre, Leigh et al. 1992) and Buxton (Buxton, Frank et al. 1998) to model the perfusion magnetization evolution in the brain. Detre's model, based on a modified Bloch equation, was applied initially to CASL data. Buxton's model, based on a linear response model to the bolus delivery, was used for PASL studies. These two approaches are equivalent (Parkes 2005) if the same assumptions are made for both models. However, the essential assumption taken by both models that blood water is freely diffusible (100% extraction) is not true. Although the exchange time (τ_{ex}) was included later in the model (Alsop and Detre 1996) to account for the restricted diffusion of blood water, it is very difficult to accurately

measure the exchange time using flow weighting or diffusion weighting gradients (Le Bihan, Breton et al. 1988). Silva (Silva, Zhang et al. 1997) suggested using the extraction fraction of blood water to correct the single-compartment model. Recently, restricted permeability of the capillaries has been included in the single-compartment model (Zhou, Wilson et al. 2001; Parkes and Tofts 2002), assuming that the permeability changes as a function of travel distance in the capillary bed (St Lawrence, Frank et al. 2000; Ewing, Cao et al. 2001).

Recent theoretical studies have shown that the single blood compartment model is relatively accurate and more practical (Parkes and Tofts 2002; Buxton 2005; Parkes 2005) than multiple-compartment models for ASL perfusion studies. Further discussion of models and CBF quantification methods for perfusion studies using PASL techniques follows.

1.5.2 Single Blood Compartment (or Microsphere) Model for PASL

By assuming plug flow or a rectangular bolus and based on the general linear model by Buxton (Buxton, Frank et al. 1998) with the assumption that no exchange occurs during the experiment time, the three phases of the single blood compartment model can be expressed as the following:

$$\Delta M(t) = 0 \qquad 0<t<\Delta t \qquad (1.1)$$

$$= 2\alpha M_{ob} f (t-\Delta t)\exp(-t/T_{1b}) \qquad \Delta t<t<\tau+\Delta t \qquad (1.2)$$

$$= 2\alpha M_{ob} f \tau \exp(-t/T_{1b}) \qquad \tau+\Delta t<t \qquad (1.3)$$

In the above equations, ΔM(t) is the measured perfusion-weighted ASL signal in a specified ROI or voxel at inversion time t, Δt is the transit time, τ is the bolus

duration, f is the cerebral blood flow, T1b is the longitudinal relaxation time of the blood, M0b is the fully relaxed magnetization of the blood, and α is the labeling efficiency (0.95 for the hyperbolic secant pulse used in thesis work). When inversion time is shorter than blood transit time, no ASL signals can be acquired. When inversion time is longer than transit time but shorter than transit time pulse total bolus duration, ASL signals increases due to the dominant accumulation of labeled arterial blood. When the inversion time is longer than transit time plus total bolus duration, ASL signals will decrease due to the longitudinal relaxation or possible out flow effects. There are four unknown parameters: M_{0b}, Δt, τ, and f. To estimate CBF (f) or other unknown parameters, multiple inversion experiments and model fitting are usually performed (Wong, Buxton et al. 1997; Buxton 2005). Perfusion images are acquired at different inversion times and ASL signals from defined regions of the acquired perfusion-weighted images are fitted to the model. The multiple inversion experiment is time-consuming and thus often impractical on a routine basis. To overcome this difficulty, single-subtraction quantification methods and corresponding ASL techniques, such as QUIPSS II (Wong, Buxton et al. 1998) and Q2TIPS (Luh, Wong et al. 1999), were proposed, in which a relatively accurate temporal bolus width (TI_1) is defined by the ASL sequence. The single blood compartment model can be simplified as the following:

$$f = \frac{\Delta M}{2\alpha M_{0b} TI_1 e^{-(TI_2/T_{1b})}} \tag{1.4}$$

$$M_{ob} = M_0 / \lambda \tag{1.5}$$

ΔM is the measured ASL difference signal between labeling and control images, TI_2 is

the total inversion time equal to the sum of TI_1 and post-bolus delay, M_0 is the measured tissue proton density, and λ is the brain blood/tissue partition coefficient (assumed to be 0.9). To use this simplified single blood compartment model for CBF quantification, the following conditions should be satisfied:

$$TI\ 1<\tau \tag{1.6}$$

$$TI2>TI1 + \Delta t \tag{1.7}$$

1.5.3 Parameter Measurements in Perfusion Quantification

Several other parameters must be known or measured before CBF can be quantitatively estimated. Some are global parameters (they remain the same across the brain), such as T_{1b} and M_{0b}; others vary across the brain as local parameters, such as Δt and τ. Accurate measurements of these parameters to maximize the accuracy of CBF quantification in different situations (baseline, activation, aging or disease) is an important part of current research in ASL.

1.5.3.1 Measurement of M_{0b}

In all ASL perfusion quantifications, the equilibrium magnetization of arterial blood, M_{0b}, has to be measured. There are two primary ways to estimate it: two-step blood signal measurement (Wong, Buxton et al. 1997; Wong, Buxton et al. 1998) and using the tissue equilibrium magnetization (Wang, Licht et al. 2003).

The first method uses the ratio (R) between blood magnetization (M_{0b}) in the sagittal sinus and the magnetization of white matter (M_{0wm}), after correction for the different transverse relaxation times for white matter and blood:

$$M_{0b} = RM_{0wm} \exp((1/T_{2wm}^{*} - 1/T_{2b}^{*}) * TE) \tag{1.8}$$

In the above equation, T_{2wm}^{*} represents the transverse relaxation time of white matter, T_{2b}^{*} represents the relaxation time of the blood and TE represents the echo time. To obtain the ratio R, a proton density image can be obtained using a T_2*-weighted (short TE, long TR) gradient echo sequence and one slice that goes through sub-cortical white matter and remains vertical to the sagittal sinus. The ratio R can be calculated from average intensities of ROIs drawn in white matter and in sagittal sinus. However, sometimes measurements performed in the sagittal sinus may not be stable due to the fast flow of venous blood. Recently, CSF has been considered as a more stable reference for the measurement of M_{0b} (Wu, Fernandez-Seara et al. 2007).

The second method measures the proton density of brain tissue (M_{0t}) using the same sequence as that used in ASL data acquisition. To calculate the blood magnetization maps (M_{0b}), the tissue proton density maps (M_{0t}) are divided by the brain blood/tissue partition coefficient (λ):

$$M_{0b} = M_{0t} / \lambda \tag{1.9}$$

1.5.3.2 Bolus Duration (τ) and Transit Time (Δt) Estimation

The usual way to estimate transit time is to perform perfusion studies at different delay times and perform model-fitting for the experiment data. Bolus duration can be also estimated using multiple inversion experiments. By incorporating small-amplitude bipolar gradient in the ASL sequence, the apparent transit time or the assumed arrival time at small arterioles and capillaries can also be estimated (Ye, Mattay et al. 1997; Yang, Frank et al. 1998).

1.5.4 Selection of Model and Complexity

There are many factors that can affect the quantification of ASL perfusion, including field strength, tissue type, and experimental parameters such as post-bolus delay and inversion time. At 1.5T and 3.0T, the assumption of a two-compartment model with no exchange (Parkes and Tofts 2002) yields relatively accurate CBF values in grey matter. However, this model requires the acquisition of a T_1 map, which is often not practical, especially in a clinical setting. The single blood compartment model is accurate within 10% for grey matter and 20% for white matter with TR $\leq$ 3 s (Parkes and Tofts 2002; Parkes 2005).

A number of physiological processes can reduce the accuracy of CBF quantification using ASL techniques. For example, recent studies by Wu (Wu, Mazaheri et al. 2007) showed that flow dispersion and cardiac pulsation can affect the quantification of CBF. Subject-dependent cerebrovascular geometry can affect the temporal bolus width and transit time, resulting in large variance of the regional perfusion for the same brain substructure. Pathology also affects CBF and its measurement, necessitating calibration experiments to optimize bolus width and transit time specific to individual groups (e.g., stroke subjects) and even individuals.

In practice, as long as the underlying conditions of the selected model are satisfied, the quantification of CBF will be relatively consistent across subjects and studies.

1.6 BRAIN VASCULAR SYSTEM

The human brain is extremely dependent upon a continuous and sufficient blood supply to maintain its normal activities. Four major arteries supply blood to the brain: two carotid arteries and two vertebral arteries, branches of which form a special structure in the middle part of the brain, called the circle of Willis. The circle of Willis equalizes

the distribution of blood and ensures adequate perfusion of all parts of the brain when one of the four arterial vessels is obstructed.

1.6.1 Blood Supply Based on Carotid Arteries

The carotid arteries are the most important blood supply source for the brain, contributing nearly 80% of total brain perfusion (Lars Edvinsson 2002; Haines 2004). Four small artery pairs branch from the carotid arteries after they enter the cranial cavity: the anterior cerebral arteries, the middle cerebral arteries, the anterior choroidal arteries and the posterior communicating arteries. Anterior arteries supply blood for the frontal pole and medial aspects of frontal and parietal lobes. The middle cerebral arteries supply most of the blood for the lateral aspects of the cerebral hemispheres and irrigate some neural foci in the deep brain region, such as the putamen and the globus pallidus. Anterior choroidal arteries and their branches supply blood for the choroid plexus and many small cerebral structures, including the anterior portion of the hippocampus, the tail of the caudate nucleus, and the amygdala. As the last branches of anterior cerebral arteries, posterior communicating arteries are responsible for the perfusion of other brain structures, such as the genu of the corpus callosum and the rostral thalamus.

1.6.2 Blood Supply Based on Vertebral and Basilar Arteries

There are two vertebral arteries, which have three pairs of branches before they fuse together to form the basilar artery. Basilar arteries are further divided into two posterior cerebral arteries (Lars Edvinsson 2002; Haines 2004). The posterior inferior cerebellar arteries branch from the vertebral arteries, supplying blood to irrigate the cerebellum and the choroid plexus of the fourth ventricle. The anterior inferior cerebellar arteries irrigate the rostral portion of the inferior surface of the cerebellum. Superior

cerebellar arteries branch from the basilar artery to irrigate the superior parts of the cerebellum. Two posterior cerebral artery branches from the basilar artery and are connected to the carotid arteries by the posterior communicating arteries. These posterior cerebral arteries supply the blood for the inferior and medial aspects of the temporal and occipital lobes. Branches of arteries from the temporal lobes also supply blood to hippocampus bodies and tails.

1.6.3 Versatile Blood Supplies for Specific Brain Regions

Blood supply for specific brain regions can come from several different artery branches, or even different major blood supply sources. For example, blood supply for the cerebellum is mainly via three pairs of feeding arteries: the superior cerebellar artery (SCA), the anterior inferior cerebellar artery (AICA) and the posterior inferior cerebellar artery (PICA). As another example, the blood supply for the hippocampus is mainly from posterior cerebral arteries and to a lesser degree from anterior choroidal arteries. For the hippocampus bodies and tails, blood supplies are completely via branches (medial and lateral posterior choroidal arteries) from the posterior cerebral arteries. For the hippocampus head, blood supply is also from branches arising from the anterior choroidal artery.

1.6.4 Venous Drainage

The removal of the metabolic by-products from the tissue is mainly via veins. In the brain, the major fraction of the blood flows out of the brain via the transverse sinus veins. Blood drained from the cortex is collected by the superior sagittal sinus, while blood drained from the sub-cortex exits mainly via the straight sinus, which connects with other veins or sinuses, such as the inferior sagittal sinus, posterior veins of corpus

callosum, and the superior cerebral vein. The sagittal sinus and the straight sinus connect with the transverse sinus, which becomes the sigmoid sinus and ends in the internal jugular veins.

Generally, no sharply delineated drainage territories exist in the cerebral venous system. For some brain regions, the drainage of the blood shows some local specificity. For example, the hippocampus head, and body and tail all drain blood via the temporal horn or inferior ventricular veins. In the cerebellum, there are three major drainage veins (superior cerebellar, inferior cerebellar, and posterior cerebellar veins) to collect the blood from the anterior superior parts of the cerebellum, the anterior inferior parts and the posterior parts of the cerebellum, respectively. The superior cerebellar vein joins to the straight sinus, the inferior cerebellar vein joins to the jugular veins, and the posterior cerebellar vein connects to the inferior part of the sagittal sinus.

1.7 THESIS RESEARCH

Although most ASL studies to date have utilized axial labeling and imaging planes, cerebrovascular geometry suggests that slice orientations should ideally be region-specific. Furthermore, both the arterial sources and pathways suggest that optimization of parameters should also be tailored to the specific brain region of interest. To better facilitate quantitative ASL perfusion studies in specific brain regions, the development of brain region-targeted ASL techniques for improved or novel ASL imaging schemes and parameter optimizations was chosen as the topic for this thesis research.

For demonstration, two brain regions were selected for region-targeted perfusion studies: the cerebellum in the inferior part of the brain, and the hippocampus in the mid-brain. These two regions not only have specific geometric and cerebrovascular features

that suggest a targeted approach, as just described, but also are important for Gulf War illness research, as will be further discussed later. To simplify CBF quantification using the single subtraction method and the single blood compartment model, FAIR with Q2TIPS was implemented as the basic ASL technique for quantitative perfusion studies and further developments (see Chapter 2).

1.7.1 Brain Region-targeted ASL Techniques for Cerebellum and Hippocampus Perfusion Studies

In the past 15 years, most of the technical development and applications of the MR technique of arterial spin labeling (ASL) have focused on the superior part of the brain, especially superior cortex. Less attention has been focused on other regions of the brain, especially smaller mid-brain and lower brain structures, such as hippocampus, thalamus, pons and cerebellum. Typical ASL sequences for perfusion studies of the superior part of the brain utilize a slab of axial image slices, generally parallel to AC-PC direction and mostly beginning from the middle, horizontal level of the thalamus to the top surface of the cortex. To achieve more reliable and accurate perfusion quantification of smaller mid-brain and inferior brain structures, based on the specific blood supply patterns and anatomic characteristics of these regions, new region-targeted ASL sequences with optimized parameters are necessary. Thus, unlike traditional ASL methods for imaging brain perfusion more globally and generally, these region-targeted approaches to ASL perfusion studies are specially customized ASL techniques in terms of optimized ASL parameters and even specifically designed imaging schemes based on both physiological and anatomic characteristics, and have potentials to make perfusion studies more reliable - with more accurate and artifact-free CBF measurements, more efficient - by using more

suitable slice geometry and placement, and more sensitive to CBF changes - due to reduced partial volume effects and lower variability of perfusion measurements.

1.7.2 ASL Parameter Optimization for Brain Region-targeted ASL

For PASL, important parameters that need to be tuned include temporal bolus width (TI_1) and the post-bolus delay. The temporal bolus width defined by the sequence should be shorter than the bolus duration determined by the labeling slab size. Proper bolus duration can be estimated by performing multiple inversion experiments using the FAIR technique (Wong, Buxton et al. 1997; Buxton 2005). The post-bolus delay should be long enough to avoid intravascular artifacts. However, if the post-bolus delay is too long, the SNR of perfusion images will be decreased. By observing the time at which intravascular artifacts disappear in multiple inversion studies using a selected temporal bolus width and maximal number of inferior saturation pulses, the proper post-bolus delay can be estimated (Wang, Licht et al. 2003; Campbell and Beaulieu 2006).

Other parameters also need to be verified for reliable or optimal perfusion studies. For example, if the blood flow velocity of the labeling region is low, a short TR value may result in lower labeling efficiency and artificially low CBF estimations, due to incomplete refreshing of labeled blood at the labeling site. To minimize heat deposition, the minimal number of inferior saturation pulses requisite with adequate saturation should be used for the ASL technique with Q2TIPS (Luh, Wong et al. 1999). The minimal number of inferior saturation pulses can be estimated by performing perfusion studies using a selected temporal bolus width and post-bolus delay but varied number of inferior saturation pulses. Optimized values for these parameters can vary with different targeted brain regions.

1.7.3 New Imaging Schemes for Brain Region-targeted ASL

1.7.3.1 Improvements of Traditional FAIR

Without considering region-specific physiological and/or anatomical features, traditional FAIR with Q2TIPS can be used for quantitative perfusion studies in specific brain regions. However, as mentioned earlier, traditional FAIR has limitations and cannot provide reliable CBF measurements when applied to specific regions, such as the cerebellum. Therefore, new imaging methods have to be designed for these areas.

1.7.3.2 Perfusion Studies Using New Schemes

In perfusion studies of the superior part of the brain, the major blood flow direction is along the foot-head direction, and ascending imaging acquisition order is used. The major purpose of using ascending acquisition order is to minimize the heterogeneity of transit time within imaging slices. In addition, it also permits the labeled bolus destined for distal slices to have more time to travel through the vascular tree into small arterioles or the capillary bed when proximal slices are acquired. Uniform transit time is more important for multi-slice ASL perfusion studies using the single blood compartment model, with the assumption that labeled blood spins stay mainly in the vascular space. For appreciable heterogeneity of within-slice transit time, a longer post-bolus delay has to be used to make sure labeled blood has reached small arterioles or capillaries, especially for tissues with longer transit times. However, labeled blood for other tissue regions with shorter transit times will have more chance to be exchanged into brain tissue, and the overall SNR for perfusion signals in these areas will be lower.

The cerebellum and the hippocampus are two brain regions that have their own specific blood supply pattern. Blood supply for the cerebellum is mainly via three pairs of

feeding arteries: the superior cerebellar artery (SCA), the anterior inferior cerebellar artery (AICA) and the posterior inferior cerebellar artery (PICA). These arteries are branches from vertebral arteries or the basilar artery. Their orientations are nearly perpendicular to their predecessors. Because of this blood flow pattern that is first vertical and then horizontal and the higher blood velocity in bigger vertical arteries than that in smaller horizontal arteries, there is a greater spread of effective transit times along the anterior-posterior direction than along the foot-head direction in the cerebellum. Therefore, it was hypothesized that a better image acquisition scheme for the cerebellum would be to use coronal, rather than axial, imaging slices with acquisition order along the anterior-posterior direction, to make the with-slice transit time more uniform. Furthermore, using coronal slices for cerebellum perfusion studies using FAIR can also help to avoid the venous artifacts from the superior labeling slab. Since the basilar arteries and the superior segment of the vertebral artery are perpendicular to the three major horizontal arteries, the labeling should be kept as usual in the axial orientation.

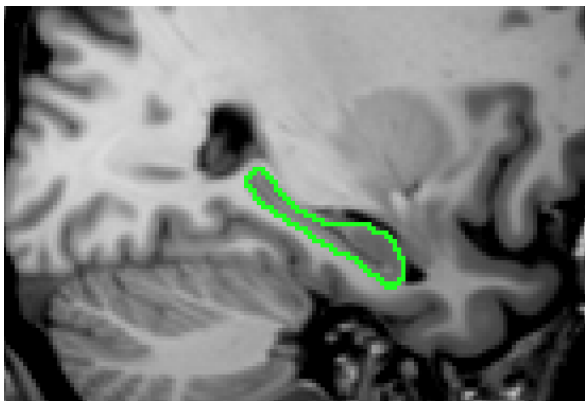

Figure 1-4 Sagittal view of hippocampus (refer to the appendix D for the information about the anatomy image).

The hippocampus also has its own specific blood supply characteristics. The blood supply for hippocampus is mainly via posterior cerebral arteries and to a lesser degree via anterior choroidal arteries. For the hippocampus bodies and tails, the transit time is longer

in the tail than in the body. For the hippocampus head, the transit time for labeled blood from the anterior choroidal artery may be shorter than that for labeled blood from posterior cerebral arteries, since the blood velocity in carotid arteries is higher than that in posterior arteries (Yazici, Erdogmus et al. 2005). Therefore, it was hypothesized that acquisition along the anterior-posterior direction in oblique coronal slices would be optimal for the hippocampus.

Partial volume effects can also compromise accurate CBF quantification. Thicker slices than commonly used for anatomic images are typically used for ASL to obtain sufficient SNR and permit fewer image slices and a shorter study time. However, a different imaging scheme than commonly used can sometimes be used to reduce partial volume effects. For example, by making imaging slices perpendicular to the anterior-posterior direction of the hippocampus, and by using higher in-plane resolution, partial volume effects can be reduced. The anatomic structure of the hippocampus is unique. The arc-shaped hippocampus is like a seahorse. Each hippocampus has an enlarged head and narrow body and tail. The total length of the hippocampus ranges from 40 mm to 45 mm, while its cross-sectional size in the right-left direction is 15 to 20 mm wide for the head and only about 10 mm wide for the body. The thickness of the hippocampus body and tail along the foot-head direction is even smaller: 2 mm to 6 mm. The change of shape along the anterior-posterior direction is relatively slow. In Figure 1-4, the hippocampus region is emphasized by a green contour line.

1.7.4 Significance of Cerebellum and Hippocampus Perfusion Studies

The study of cerebellum perfusion is important in both basic neuroscience and clinic contexts. Many diseases involve the cerebellum. In ataxia, the sensorimotor

cerebellum is impaired. In cerebellar cognitive affective syndrome (CCAS), the pathology is in the lateral hemisphere of the posterior cerebellum (involved in cognitive processing) or in the vermis (limbic cerebellum) (Manto 2002). Veterans with Gulf War Syndrome, especially those with Syndrome II, exhibit behavior disorders correlated with significant differences in regional cerebellum CBF changes between resting state and cholinergic challenge state [Haley et al., unpublished results]. Reliable cerebellum CBF estimation is also valuable to facilitate the translation of ASL techniques to clinical application. For example, in some Alzheimer's Disease studies, PET and SPECT techniques use the cerebellum as a routine reference for CBF normalization, with the assumption that cerebellar cortices are less involved in Alzheimer's disease, especially for mild-to-moderate Alzheimer's disease patients.

In two recent ASL perfusion studies (Fernandez-Seara, Wang et al. 2005; Gunther, Oshio et al. 2005), whole-brain coverage, in which the cerebellum was included, was achieved using a single-shot 3D GRASE sequence. However, cerebellum CBF was not carefully studied and reported. In the work by Günther, only the superior part of the cerebellum was covered and only overall grey matter and white matter CBF were evaluated for slices that covered the superior part of the brain. In the work by Fernández-Seara, although nearly the whole cerebellum was covered, cerebellum perfusion was greatly affected by magnetization transfer effects due to closely placed continuous flow-driven adiabatic pulses, making the estimation of cerebellum CBF unreliable. No quantitative cerebellum CBF measurements were reported in this study. In the recent ASL perfusion study by Andreas Boss using True-FISP FAIR (Boss, Martirosian et al. 2007), a single slice was placed across the temporal lobe and middle part of the

cerebellum. A CBF map was shown, but no specific CBF estimation was performed or reported for the cerebellum. In addition, since True-FISP is not a single-shot sequence, the inversion time is not proper for CBF quantification due to the fact that each phase encoding step has its own inversion time. Furthermore, no inferior saturation pulses were used in this study, so intravascular artifacts and inflow effects due to the 300 ms acquisition time for the single slice reduced ASL image quality, making CBF quantification questionable. For True-FISP FAIR, it is impossible to perform multi-slice perfusion studies.

The hippocampus has a critical role in learning and memory, regulation of emotional behavior, certain aspects of motor control, and regulation of hypothalamic functions (Duvernoy 2005). Veterans with Gulf War Syndrome suffer disorders in motion control and memory loss indicative of hippocampus damage (Hom, Haley et al. 1997; Haley 1999). A ^{1}H MRS study revealed lowered NAA/Cho and NAA/Cr in the hippocampus of veterans ill with Gulf War Syndrome compared to normal controls (Menon, Nasrallah et al. 2004). Abnormal hippocampus resting state CBF and CBF regulation upon pharmacologic challenge has recently been shown in Gulf War Syndrome veterans [Haley et al., unpublished results]. Performing perfusion studies on the hippocampus can provide information about its physiological characteristics and be valuable for diagnostics (Alsop, Casement et al. 2008). By performing dynamic perfusion studies for functional imaging, deeper insights into the functional role of the hippocampus can be achieved (Fernandez-Seara, Wang et al. 2007).

Thus although the cerebellum and the hippocampus are two important brain regions with their own specific characteristics in terms of physiology and functional

anatomy, no systematic quantitative perfusion studies using PASL have been reported for these two regions. Performing quantitative perfusion studies using PASL for these two regions is thus new and of fundamental significance.

1.7.5 Thesis Research Aims, Hypothesis and Performed Studies

The primary aim of this thesis research is to develop new and improved methods for ASL perfusion studies that address the unique properties and characteristics of specific brain regions for optimizing the parameters and protocol; this is referred to as region-targeted ASL. A secondary aim is to provide representative demonstrations of the advantages of this approach by performing quantitative perfusion studies on selected brain regions (the cerebellum and the hippocampus), showing that when ASL perfusion studies are focused on specific brain regions, more reliable and/or more efficient CBF measurements, and maybe higher sensitivity to CBF changes, are possible.

The central hypothesis is that brain region-targeted ASL techniques represent a new and valuable approach with unique features that will enable improved regional CBF estimations.

To achieve these aims, numerous studies have been performed, including sequence design, implementation and evaluation, ASL optimization, and quantitative perfusion studies. For example, to perform more reliable cerebellum perfusion studies using FAIR, modulated dual saturation for FAIR (MDS FAIR), FAIR with active suppression of superior tagging (FAIR ASST), an orthogonally-positioned tagging imaging method for arterial labeling of FAIR (OPTIMAL FAIR), and MDS OPTIMAL FAIR were implemented and evaluated.

MDS FAIR is a passive method to minimize venous artifacts from superior labeling of FAIR. Technical aspects and evaluation results are described in Chapter 3. Those evaluation studies indicate that MDS FAIR cannot effectively minimize venous artifacts in some situations, such as perfusion studies on whole cerebellum, and poses a problem associated with the definition of temporal bolus width for the superior bolus when MDS FAIR is combined with Q2TIPS for quantitative CBF estimations.

FAIR ASST is an active method to eliminate venous artifacts by destroying the superior labeling effects of FAIR at the labeling stage. Since only the inferior bolus is used for CBF quantification, the FAIR ASST technique can effectively remove venous artifacts and at the same time avoid the dilemma about the definition of temporal bolus width for the superior labeled blood. FAIR ASST technique development and evaluation studies are described in Chapter 4. Quantitative perfusion studies of the cerebellum using FAIR ASST and PICORE are compared in Chapter 5.

(MDS) OPTIMAL FAIR uses imaging slices that are perpendicular to the labeling slab for perfusion studies where proximal feeding arteries branch perpendicular to distal feeding arteries. (MDS) OPTIMAL FAIR can effectively avoid venous artifacts by utilizing coronal or oblique coronal imaging slices for cerebellum perfusion studies. Acquiring imaging slices along the anterior to posterior direction using (MDS) OPTIMAL FAIR can reduce the heterogeneity of transit time within perfusion imaging slices. (MDS) OPTIMAL FAIR can also help minimize the partial volume effects in the perfusion studies of the cerebellum and the hippocampus by using more proper slice orientation and high in-plane resolution. The description of this technique and its initial

application for cerebellum perfusion are described in Chapter 6. Its application to hippocampus perfusion studies is described in Chapter 7.

Before performing these quantitative perfusion studies of the cerebellum and the hippocampus, ASL optimization studies were performed for the selection of proper ASL parameters. These ASL parameters mainly include defined temporal bolus width, post-bolus delay and the minimum number of inferior saturation pulses. Possible TR effects were also evaluated.

In Chapter 2, general aspects and methods for the ASL studies performed are presented. These general aspects include descriptions of MRI equipment, ASL study protocols, subject recruitment, and data processing and analysis.

CHAPTER 2 General Aspects of Performed Studies

For all performed ASL studies, there are some common aspects. These common aspects are described once in this chapter to avoid the unnecessary redundancy in the description of each study. Descriptions about subjects, sequence development and MRI system are provided at the beginning. Study protocol and imaging parameters for routine sequences are given in the second section. In the third section, methods for data processing and analysis are introduced with a little more emphasis on iterative model fitting of multiple inversion experiment data. In the fourth section, implemented basic FAIR sequences, spatially-confined FAIR and spatially-confined FAIR with Q2TIPS, are addressed in detail. In the last section, the experiment designs for ASL optimization studies are described.

2.1 GENERAL DESCRIPTIONS ABOUT SUBJECTS AND MRI SYSTEM

2.1.1 Subjects

All recruited healthy adults have been required to refrain from caffeine (coffee, tea, caffeine-containing soft drinks) within 8 hours before the studies (Cameron, Modell et al. 1990; Mathew and Wilson 1991; Stubbs and Macdonald 1995; Field, Laurienti et al. 2003; Lunt, Ragab et al. 2004; Blaha, Benes et al. 2007). All studies were performed roughly at the same time of the day. The time varies for different studies. Consent forms were obtained from all participants according to a protocol approved by the UT Southwestern institutional review board.

2.1.2 Sequence Development and MRI System

To perform these studies, research sequences have been designed and implemented using Siemens IDEA (integrated development environment for applications) platform with version VB13. All research sequences have been tested and simulated in IDEA environment with the digital signal processing (DSP) tool and further verified using phantoms before their applications on human subjects. Particularly, the position and size of saturation and inversion slabs were verified by positioning them into a coronal imaging slice.

All the studies were performed on a 3T Siemens Trio TIM whole-body scanner with 60 cm diameter magnet bore and SQ gradients. The maximum gradient strength is 45 mT/m in the z direction and 40 mT/m in the x and y directions, with maximum slew rate 200 mT/m.ms and 200 μs rise time to maximum amplitude. The body coil was used for transmission, and the Siemens 12-channel phased array receive-only head coil was used for imaging.

2.2 STUDY PROTOCOL AND GENERAL IMAGING PARAMETERS

2.2.1 Protocol

All studies were planned in advance using Auto-Align, Siemens' online co-registration and study planning tool, by using a standard head atlas that comes with the Auto-Align package. Due to subject-dependent brain geometry, manual translation adjustment is helpful to ensure consistent slice position relative to selected anatomy landmarks across subjects. These adjustments were performed by using the acquired T1-weighted high-resolution anatomic images for more accurate reference. The landmark used for each study is different, which will be described for each study. Slice orientation was always kept intact as determined by Auto-Align, which ensures better consistency

for slice orientation across subjects. The Auto-Align scout was run at the beginning of the MR session, followed by the usual gradient echo scout or localizer and then the T1-weighted high-resolution anatomic imaging acquisition using MPRAGE. The planned ASL scans were played out, followed by gradient echo imaging (GRE) scan with high in-plane resolution. This GRE volume matched the ASL imaging slab in terms of slice orientation and slice thickness. The accuracy of co-registration between the lower-resolution ASL series and the T1-weighted high-resolution anatomic MPRAGE images can be improved by using these high-resolution GRE images in an intermediate alignment step. This approach was applied for all performed ASL perfusion studies using OPTIMAL FAIR technique of the thesis research work.

2.2.2 General MRI Parameters

Anatomic T1-weighted Imaging

The Siemens T1-weighted high-resolution anatomic imaging sequence MPRAGE was used with the following typical parameters: TR/TE = 2250/4 ms, TI = 900 ms, FA = 9 degrees, imaging volume of view = 230 x 230 x 160 mm^3, matrix size = 256 x 256 x 160, imaging resolution = 0.9 x 0.9 x 1.0 mm^3, bandwidth = 160，GRAPPA iPAT factor = 2 with 24 reference lines and triple mode, partial Fourier (PF) = 7/8, slice over sampling = 10%, slice orientation = sagittal, phase encoding direction = anterior-posterior, total imaging time = 4:38 min.

M_{0b} Measurements

For any performed perfusion studies in which the measurements of the magnetization of the blood (M_{0b}) are needed, the method that uses the measurements of the magnetization of brain tissue (M_{0t}) and blood-tissue partition coefficient (λ) was used.

In each perfusion study, exactly the same sequence was used with all other parameters kept the same except that longer TR (equal to 8 seconds) was used to have proton density images of brain tissue.

2.3 DATA PROCESSING

2.3.1 CBF Reconstruction

All ASL image series were pre-processed using SPM 2 to evaluate possible large motions for each subject. Mean image of ASL series was always generated for later co-registration purpose. Whenever the translational motion variation was larger than 1 mm and the rotational variation around any axis larger than 1 degree, motion correction was used. Images with motions larger than 2 mm in translation and 2 degrees in rotation around any axis were excluded from the analysis. Each ASL label-control image series was processed by pair-wise subtraction to generate a perfusion-weighted imaging series. Each perfusion-weighted imaging series was further averaged to produce a mean perfusion weighted image. To facilitate CBF quantification, two acquired M_0 images for each series were averaged to obtain a mean M_0 image. The mean perfusion-weighted image and the mean M_0 image were used for the CBF calculation using the single blood compartment model.

2.3.2 ROI-based CBF Analysis

To get tissue masks separately for grey matter, white matter and CSF based on the probability maps from SPM 2, 0.75 was used as probability threshold. To obtain CBF for a specific brain region, for example, the cerebellum, a hand-drawn ROI on a high-resolution anatomic image was used to produce a binary regional mask. By performing Boolean operation between the binary mask and the obtained overall segmentation maps

from high-resolution anatomic image, constrained segmentation maps can be generated. In perfusion studies of the hippocampus, segmented ROIs of the hippocampus were generated by using one of FSL software tools - FIRST. The suggested segmentation mode for the hippocampus was used for hippocampus segmentation. Manual adjustments were performed when hippocampus segmentations are not satisfactory even after edge correction.

To keep the generated CBF maps intact for quantitative accuracy, the so-called original imaging space analysis approach was used, in which ROIs and the corresponding anatomic images were aligned with CBF maps. Those constrained segmentation masks as well as overall segmentation masks for gray matter, white matter, and CSF, or segmented ROIs were co-registered with the mean image of the ASL scan series, using the transformation matrix of the co-registration between the high-resolution anatomic image and the mean image of the ASL scan series. To improve the quality of co-registrations in perfusion studies using OPTIMAL FAIR technique, the high-resolution anatomic image was first co-registered to the high-resolution GRE image and then further co-registered to the ASL series. To reduce interpolation errors, during the co-registration between T1-weighted high-resolution anatomic images and GRE images, the option “co-register only” in SPM 2 was used. In multiple inversion or multiple post-bolus delay ASL experiments, high-resolution anatomic images were co-registered to each ASL series respectively to ensure accurate co-registration of ROIs for each ASL measurement. When performing co-registration between constrained masks and ASL series, the constrained binary masks had voxels with values other than 0 and 1 due to the interpolation. Some of those voxels with value between 0 and 1 may go beyond the interested tissue regions. To

further conservatively limit the generated ROIs to ensure the mean CBF is from the region of interest, a threshold was used based on visual inspection for each subject.

2.3.3 Iterative Model-fitting of Multiple Inversion Experiment Data

Table 2-1 Typical parameter ranges and initial guesses in iterative non-linear least-squares model-fitting

	Unknown Parameters			
	Transit Time (ms)	**Bolus Duration (ms)**	**M_{0b} (a.u.)**	**CBF (mL/100g/min)**
Low Limit	0	0	1400	0
Up Limit	1500	2000	2000	120
Initial Guess	500	800	1500	60

The values set for M_{0b} are mainly based on our previous ASL study results.

To facilitate ASL optimization studies using multiple inversion experiments, an iterative nonlinear least-squares model-fitting program was implemented in MatLab 7.0 to fit ASL signals from the defined ROIs to the three-phase of single blood compartment model. To make the iterative reconstruction process converge faster, initial guesses and limited ranges were provided for the unknown parameters. The typical ranges and initial guesses for four unknown parameters are listed in Table 2.1. If necessary, these parameter ranges can be manually adjusted to see if model-fitting residuals can be further minimized. Also, by fixing one parameter value (for example, temporal bolus width) and estimating other parameters, numerical simulation results can be obtained for specific situations. As an additional constraint, only non-negative CBF values were allowed during the data analysis of multiple inversion experiments; negative signals at very early inversion times were forced to zero. To produce higher SNR and more stable ASL time course values, mean ASL signal from two or more slices were sometimes used for model fitting.

2.4 IMPLEMENTATION OF BASIC FAIR SEQUENCES

To facilitate the thesis research work, basic FAIR sequences, including spatially-confined FAIR and spatially-confined FAIR with Q2TIPS, were implemented. All of these sequences were all tested with phantoms and further evaluated on human subjects before their applications. These sequences form the basis for the newly-developed sequences in the thesis research work.

2.4.1 Spatially-confined FAIR

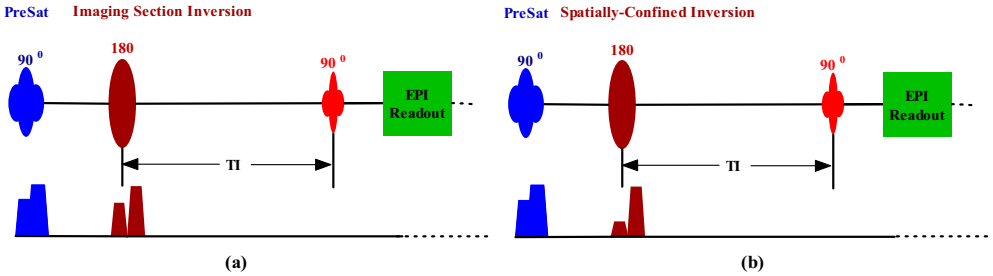

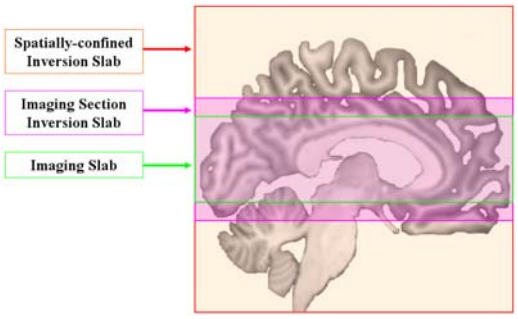

(c)

Figure 2-1 Diagram for spatially-confined FAIR sequence: (a) labeling experiment, (b) control experiment and (c) spatial definitions of spatially-confined inversion slab, imaging section inversion slab and imaging slab. Pre-saturation (indicated by PreSat) pulse is used in this implementation. TI is the total inversion time measured from the end of hyperbolic inversion pulse to the beginning of excitation pulse of EPI sequence (refer to Appendix D for the information about the anatomic image).

With the wide applications of parallel imaging technique, the standard configuration for brain MRI imaging is to use multiple channel phased-array head coil as the receiver and body coil as the transmitter. Spatially-confined FAIR is suitable for ASL

perfusion studies using such a coil configuration. The spatially-confined FAIR sequence was implemented as illustrated in Figure 2-1. The only difference between labeling and control experiments is the amplitude of the slice selective inversion gradients. In labeling experiment, stronger slice selective gradient is used for the inversion of imaging section, in which larger slab than real imaging slab is usually used. In control experiment, a weaker slice selective gradient is used to invert a much larger slab, the size of which is the sum of imaging section and spatial bolus width. In this implementation, the same hyperbolic secant pulse as in other studies (Wang, Licht et al. 2003) was used. The duration of this hyperbolic secant pulse is 15.36 ms with 22 μT RF amplitude, 95% labeling efficiency and slice-selective reference gradient for a 100 mm inversion slab is 0.7 mT/m. For selective inversions with different slab sizes (e.g., the wider spatially-confined inversion slab in labeling experiment and the narrower imaging section inversion in the control experiment of FAIR), automatically calculated gradients with appropriate amplitudes are played out with this hyperbolic secant pulse. To ensure good saturation for imaging sections with different widths, a series of optimized sinc pulses were selected for this purpose. Each sinc pulse is an optimized sinc RF pulse proper for a range of slab size. The slab size covered by this series of sinc RF pulses ranges from 1 mm up to 150 mm. Proper sinc RF pulse is automatically determined by sequence program according to the current imaging section size. After the saturation RF pulse, a standard spoiler gradient with duration about 7 ms will be played out along both slice and readout directions to dephase the magnetization. Gradient echo planar imaging sequence is used as imaging readout. The imaging section and spatially-confined inversion RF

pulses are applied symmetrically relative to the center of imaging slab. The spatial definitions for imaging slab, imaging section, and spatially-confined inversion slab are

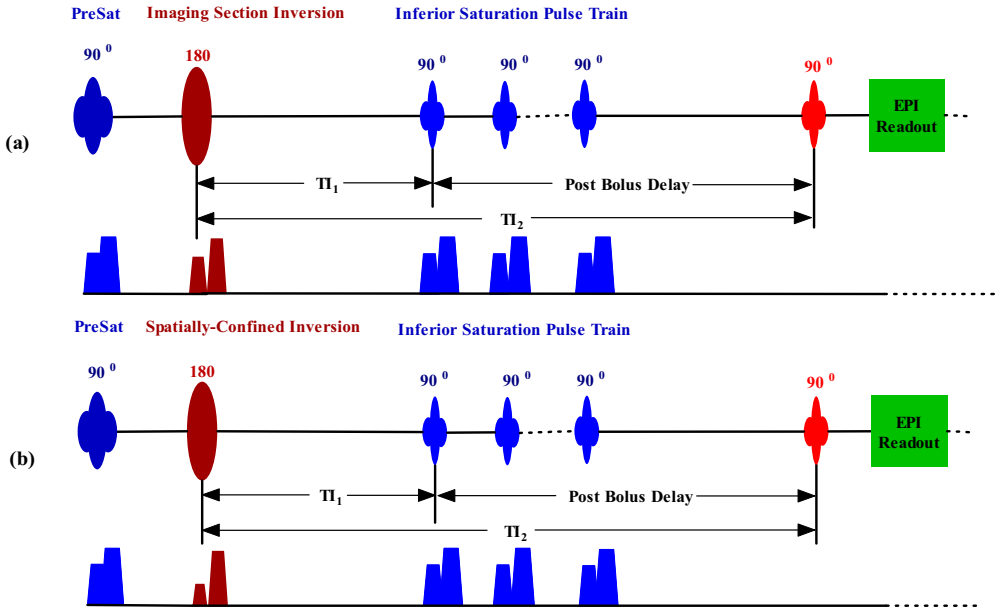

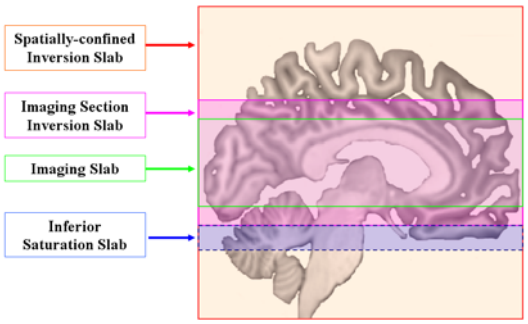

(c)

Figure 2-2 Diagram for spatially-confined FAIR with Q2TIPS: (a) labeling experiment, (b) control experiment and (c) spatial definitions of spatially-confined inversion slab, imaging section inversion slab, imaging slab and inferior saturation slab. Pre-saturation (indicated by PreSat) pulse is used in this implementation. TI_2 is the total inversion time measured from the end of hyperbolic inversion pulse to the beginning of excitation pulse of EPI sequence (refer to Appendix D for the information about the anatomic image).

illustrated in Figure 2-1.

2.4.2 Spatially-confined FAIR with Q2TIPS

To facilitate CBF quantification using single subtraction method and single blood compartment model, the temporal width of the bolus has to be defined in the sequence by using inferior saturation pulses. Q2TIPS scheme was selected as the method for this purpose. The spatially-confined FAIR with Q2TIPS was implemented as showed in Figure 2-2. The added inferior saturation pulse train performs a series of saturations immediately after a delay (TI_1), which is the temporal bolus width specified by the user. The saturation pulses are applied just below the imaging section. The saturation pulse is default sinc pulse with 2.56 ms duration and 512 sample points. After each saturation pulse, a standard spoiler gradient with duration about 7 ms is played out to dephase the magnetization. The total duration for each saturation including both RF pulse and corresponding spoiler gradient is about 10 milliseconds. The slab thickness of the saturation pulse, the time interval between two saturation pulses and the number of saturation pulses can be determined by the user. Typically, in all performed studies of the thesis research, 20 mm slice thickness was used to minimize the interference between saturation slab and imaging slab. Using 20 mm saturation slice thickness, saturation pulses with time interval equal to 25 ms can effectively saturate the blood with velocity as high as 80 cm/s in theory, making such saturation pulse train fast enough even when using large arteries for blood labeling.

2.5 EXPERIMENT DESIGNS FOR ASL OPTIMIZATION STUDIES

Experiments for ASL optimizations are challenging due to long study time. Especially for multiple inversion experiments, ASL signals have to be measured at

several inversion time points. From the point of view of model fitting, the more inversion time points, the more accurate and robust for parameter estimation.

However, the study time is constrained by the fact that subjects usually can not keep holding very still for a very long time. To minimize the total study time, thicker imaging slices are typically used to decrease the number of measurements while keeping enough SNR for perfusion-weighted images. To further increase SNR and reduce the oscillation of ASL signals, for any defined ROI, ASL signals from more than one imaging slice can be averaged together.

In the following, experiment designs for ASL optimization studies are described by using the implemented basic sequences as examples. When new imaging sequences were used for ASL optimization studies, the same schemes were utilized except that new imaging sequences have extra sequence components (MDS FAIR and FAIR ASST) or use imaging slices with different orientation (OPTIMAL FAIR).

2.5.1 Multiple Inversion Experiments

To estimate transit time and bolus duration, multiple inversion experiments can be performed to have ASL signals measured at several different inversion time points. In the multiple inversion experiments, spatially-confined FAIR sequence was used. ASL scans for different inversion time points were performed in a randomized order for each subject. Typical labeling size is used: 90 mm (labeling size = (spatially-confined inversion slab size – imaging section)/2).

2.5.2 Multiple Post-bolus Delay Experiments

To estimate proper post-bolus delay time, spatially-confined FAIR with Q2TIPS sequence was used. In this kind of experiments, proper bolus width is selected and

defined by inferior saturation pulse train. For ASL scans with different post-bolus delays, inferior saturation pulses will be applied during the whole delay period.

In principle, ASL signals should be measured after all of the bolus have be delivered to imaging sites, and this delay time should be longer than the sum of estimated transit time and sequence-defined bolus duration. However, sometime, intravascular artifacts can be still obvious even when the post-bolus delay time is longer than the sum of estimated transit time and total bolus duration because labeled blood spins have not been cleared from big surface arteries. Therefore, to avoid intravascular arteries, the proper delay time is usually determined with the help of visual inspection of perfusion-weighted images acquired at different delay times. The quantitative CBF signals will also stay relatively stable when most of the labeled blood has arrived at small arterioles or capillary bed.

2.5.3 TR Effects and Sufficient Inferior Saturation

If labeled blood can not be cleared from labeling site before the next application of labeling pulse, both SNR of perfusion-weighted images and the labeling efficiency will be lower. If the typical value for labeling efficiency parameter is used in CBF quantification, perfusion will be underestimated. There is more chance for this to happen when short TR is used. However, shorter TR is preferred with no doubt since the total study time can be greatly reduced, which is more important for ASL perfusion studies at clinic.

Before using short TR values in ASL perfusion studies, the possible adverse effects associated with TR should be evaluated first by comparing CBF

estimations using different TR values. In these experiments, inferior saturation pulse train will be performed during the whole post-bolus delay.

Even though performing inferior saturation pulse train during the whole post-bolus delay does not have SAR issue, minimized RF radiation is preferred. To estimate the minimal/sufficient number of inferior saturation pulses, ASL perfusion studies can be performed using varied number of inferior saturation pulses to see when there is no obvious drop for CBF measurements. Visual inspection can also help ensure sufficient suppression of labeled blood residues. If the number of inferior saturation is far from enough, in multiple-slice acquisition, spurious ASL signals will be observed due to the inflow of labeled blood residues.

CHAPTER 3 MDS FAIR

As mentioned in the previous chapter, although FAIR is very suitable for multi-slice perfusion studies, its superior labeling slab can generate problems especially when perfusion studies are focused on the inferior part of the brain with limited coverage. In this chapter, this problem of FAIR will be demonstrated with the results from perfusion studies using traditional spatially-confined FAIR with Q2TIPS. After that, MDS FAIR technique will be introduced in detail. The performed evaluation studies for two MDS FAIR techniques, MDS FAIR I and II, are reported at the end.

3.1 VENOUS ARTIFACTS OF TRADITIONAL FAIR

It is well-known that FAIR technique can not reject venous inflow due to its superior labeling slab. When perfusion studies are performed with limited coverage, such as single slice perfusion study, and especially when perfusion studies are focused on the inferior part of the brain, artifacts from labeled venous blood in sinuses can become quite conspicuous, making CBF estimations in neighboring tissue unreliable.

In Figure 3.1, perfusion-weighted images from our preliminary perfusion studies of the cerebellum are presented. These perfusion-weighted images were obtained by using traditional spatially-confined FAIR with Q2TIPS. MRI parameters used for low resolution perfusion study are the same as those used in the first evaluation study of MDS FAIR I (see Section 3.3). MRI parameters for the high-resolution perfusion study are as the following: TR/TE = 2500/12 ms, field of view (FOV) = 180 x 180 mm^2, matrix size = 72 x 72, slice thickness/gap = 3.5/0.7 mm, the number of imaging slices = 16, imaging resolution = 2.5 x 2.5 x 3.5 (+0.7 mm slice gap) mm^3, the number of measurements = 180,

iPAT GRAPPA factor = 2 with 24 reference lines using CP mode, partial Fourier (PF) = 7/8, acquisition order = ascending (foot to head), imaging section inversion slab size = imaging slab size + 20 mm, spatially-confined inversion slab size = imaging slab size + 200 mm, temporal bolus width (TI_1) /post-bolus delay = 800/1000 ms, inferior saturation pulse number = 20, inferior saturation slab size = 20 mm, inferior saturation pulse interval = 25 ms.

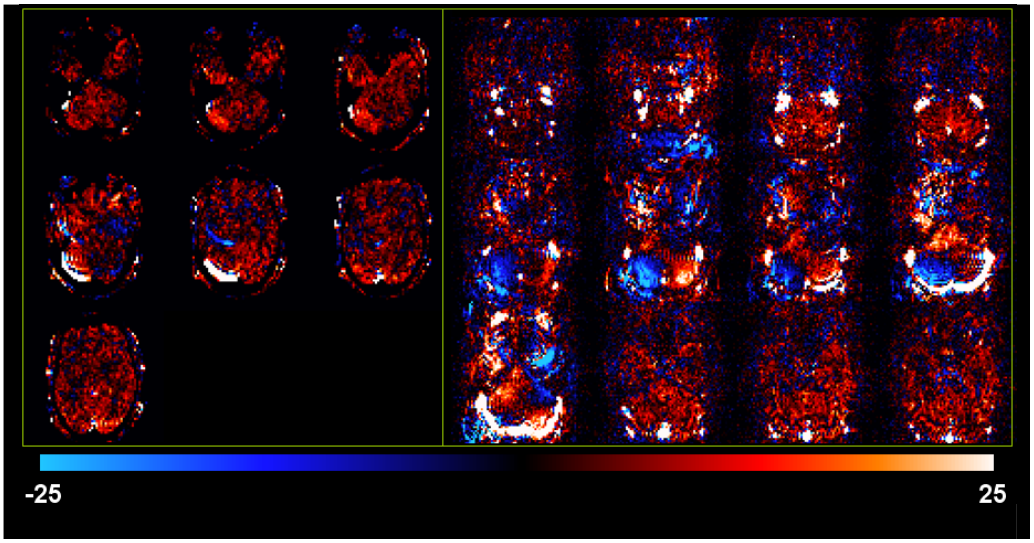

Figure 3-1 Perfusion-weighted images from cerebellum perfusion studies using spatially-confined FAIR with Q2TIPS: (a) low resolution (in-plane resolution = 2.97 x 2.97 mm^2, slice thickness/gap = 5/1 mm) and (b) high resolution (in-plane resolution = 2.5 x 2.5 mm^2, slice thickness/gap = 3.5/0.7 mm).

Artifacts generated by labeled venous blood from the superior labeling of traditional FAIR gave hyper-intense signals in sinuses in the perfusion-weighted images. When lower resolution was used, these hyper-intense signals from sinuses can affect ASL signals in the neighboring tissue via partial volume effects. To minimize the partial volume effects between the sinus and cerebellum tissue, high in-plane resolution should

be used. However, these hyper-intense signals also behave like ringing artifacts, aliasing into neighboring tissues.

Due to these venous artifacts, perfusion-weighted images near transverse sinuses have asymmetric perfusion signals between the left and right lobes of the cerebellum: one side with dominant sinus had much higher ASL signals while the other side had obvious signal loss. When high imaging resolution was used for cerebellum perfusion studies, these artifacts became even worse: as showed by the imaging slices that contain the transverse sinuses, one side of the cerebellum had only negative ASL signals while the other side had very higher ASL signals.

These artifacts are mainly from the frequency or phase errors in imaging reconstruction due to the fast flow and oscillation of labeled venous blood across space and time.

The superior labeling slab can be pushed out of the brain by using many redundant slices, and the venous artifacts from the superior labeling can be avoided. However, this method is not preferred for high-resolution perfusion studies in the inferior part of the brain. If I want to perform high-resolution cerebellum perfusion study using slice thickness equal to 3.5 mm or even less, to avoid venous artifacts, at least 40 imaging slices have to be used for typical subject's head. Using so many slices, perfusion study time has to be increased greatly due to increased TR. If high in-plane resolution is used with thinner slices too, for example, 2.5 x 2.5 x 3.5 mm^2, TR will be further increased due to increased TE. Even by using parallel imaging technique GRAPPA with accelerator factor equal to 2 and partial Four transform at the same time, for imaging resolution 2.5 x 2.5 x 3.5 mm^2, shortest TE is still around 44 ms, and TR will be longer than 3.5 s. For

perfusion studies using such resolution, to have enough SNR, at least 200 measurements have to be acquired, which will take more than 12 minutes. On the other hand, if I can remove venous artifacts and use only necessary imaging slices for cerebellum perfusion study, study time can be greatly reduced. For the same resolution, 16 slices will be sufficiently cover cerebellum tissue for most subjects, which will reduce the total study time to less than 8 minutes. ASL imaging technique is very sensitive to motions. Shorter scan time can help minimize motion artifacts, making CBF measurements more reliable.

To solve these problems, MDS FAIR technique was proposed to suppress the venous artifacts of traditional FAIR.

3.2 MDS FAIR SEQUENCES

Using modulated dual saturation pulse trains for spatially-confined FAIR (MDS FAIR) is a passive solution to suppress venous artifacts. In this method, one saturation pulse train added on the superior side of imaging section can help to suppress the labeled venous blood. Depending on the start time for this superior saturation pulse train, two versions of MDS FAIR technique have been implemented: MDS FAIR I and MDS FAIR II.

Similar to the automatic compensation of MT effects by inferior saturation pulses in Q2TIPS, MT effects induced by the added superior saturation pulses can be nicely removed for imaging slices after pair-wise subtraction since superior saturation pulses are performed exactly in the same way for both control and labeling experiments. Smaller saturation slab had better be used for the superior saturation pulses too since smaller saturation slab can not only help avoid the interference between imaging slab and superior saturation slab but also reduce the heat deposition.

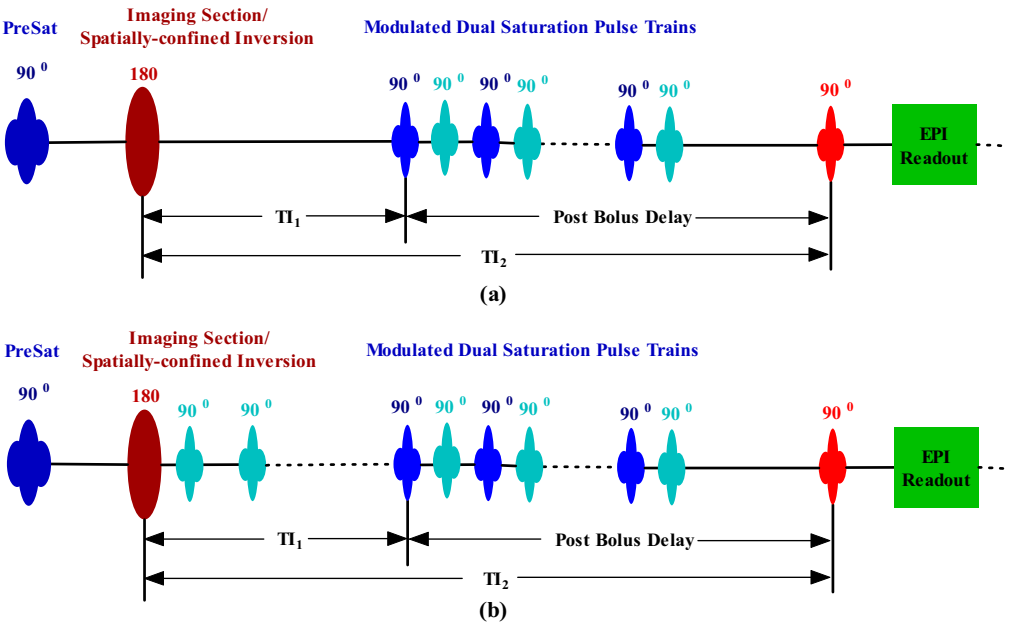

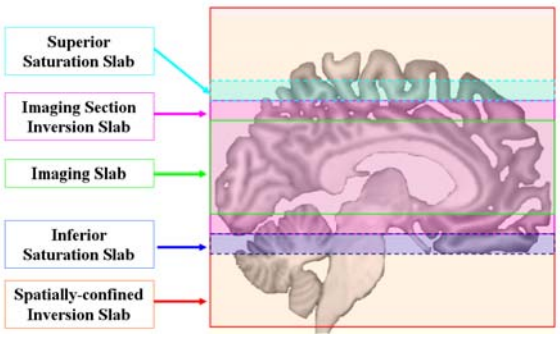

Figure 3-2 Sequence diagrams for MDS FAIR techniques: (a) MDS FAIR I, (b) MDS FAIR II and (c) spatial definitions for different slabs of MDS FAIR techniques. Superior saturation pulses and corresponding saturation slab are showed in cyan, inferior saturation pulses and corresponding saturation slab are indicated by dark blue. The superior and inferior saturation pulses are performed in an interleaved way with inferior saturation pulses run first (refer to Appendix D for the information about the anatomic image).

3.2.1 MDS FAIR I

In MDS FAIR I, the superior saturation pulse train begins immediately after a time equal to the user-defined temporal bolus width (TI_1). The sequence diagram for MDS FAIR I is showed in Figure 3-2 (a). The spatial definitions for different slabs are illustrated in Figure 3-2 (c). One saturation pulse train (dark blue ones in Figure 3-2 (a)) is exactly the same as the one used in spatially-confined FAIR with Q2TIPS (Figure 2-2), performing inferior saturations using a thinner slice slab (dark blue slab in Figure 3.2 (c)) on the inferior side of imaging slab to help define the temporal bolus width (TI_1) and eliminate the residues of labeled blood after TI_1. The number of inferior saturation pulses can be specified by the user within the defined post-bolus delay period (TI_2-TI_1). The added periodical saturation pulse train (cyan ones in Figure 3.2 (a)) is played out using similar thinner slice slab (cyan slab in Figure 3-2 (c)) on the superior side of the imaging section to suppress labeled venous blood. In MDS FAIR I, the inferior and superior saturation pulses are performed in an interleaved way with inferior saturation pulses run first. The saturation slab thickness for two saturation pulse trains can be different. But to be simple, the same typical slab thickness (20 mm) has been used for our performed studies to minimize the interference between the superior saturation slab and imaging slab. The superior saturation pulses use the same RF pulse as that used for the inferior saturation pulses of spatially-confined FAIR with Q2TIPS. The number of superior saturation pulses after TI_1 can be specified separately as long as the total duration will not exceed user-defined post-bolus delay (TI_2-TI_1). The interval between one pair of superior or inferior saturation pulses in our studies is usually 25 milliseconds.

3.2.2 MDS FAIR II

MDS FAIR II will be exactly the same as MDS FAIR I except that one extra pulse train was added during the labeling time period (TI_1). That is, this superior saturation pulse train begins just after the inversion pulses and lasts until the beginning of post-bolus delay. Sequence diagram for MDS FAIR II and spatial definitions for different slabs are illustrated in Figures 3-2. The number of superior saturation pulses before TI_1 is determined by the sequence automatically by dividing TI_1 with the user-specified pulse interval. In our studies, the same pulse interval was used for this added superior saturation pulse train as before: 25 milliseconds.

By performing earlier and longer superior saturations, MDS FAIR II may be able to suppress the venous artifacts more effectively.

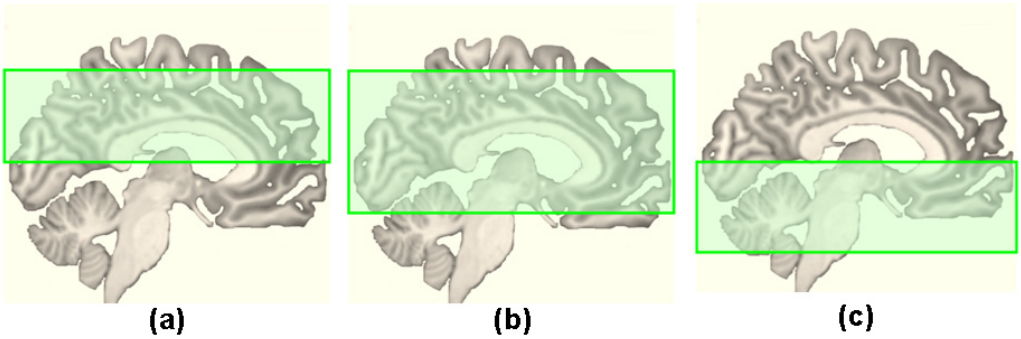

Figure 3-3 Imaging slice positions for MDS FAIR I evaluation studies: (a) smaller coverage and low resolution in the superior part of the brain, (b) larger coverage and low resolution in the middle part of the brain and (c) smaller coverage and low resolution in the inferior part of the brain (refer to Appendix D for the information about the anatomic image).

3.3. MDS FAIR EVALUATION STUDIES

3.3.1 MDS FAIR I Evaluation Studies

To evaluate the effectiveness of MDS FAIR I technique in terms of the suppression of venous artifacts, three experiments have been performed using different coverage, positions and imaging resolutions (Figure 3-3). For comparison purpose, these experiments were performed by using both traditional FAIR (spatially-confined FAIR with Q2TIPS) and MDS FAIR I, two healthy male adults aged 38 and 39 years were recruited for this evaluation study.

Materials and Methods

In the first evaluation study, smaller coverage and low-resolution images (Figure 3-3 (a)) were used in perfusion studies in the superior part of the brain. ASL perfusion imaging parameters are listed in the following: TR/TE = 3000/9.6 ms, FOV = 220 x 220 mm^2, matrix size = 74 x 74, in-plane resolution = 2.97 x 2.97 mm^2, slice thickness/gap = 5/1 mm, the number of imaging slices = 7, the number of measurements = 60, slice acquisition order = ascending, iPAT GRAPPA factor = 2 with 24 reference lines using CP mode, partial Fourier (PF) = 7/8, imaging section inversion slab size = imaging slab size + 20 mm, spatially-confined inversion slab size = imaging slab size + 200 mm, temporal bolus width (TI_1)/post-bolus delay = 700 /1000 ms. The same setup was used for two saturation pulse trains: saturation pulse number = 40, saturation slab size = 20 mm, saturation pulse interval = 25 ms.

In the second evaluation study, the same imaging parameters were used as those in the first evaluation study except that sixteen slices were used to have a larger coverage (Figure 3-3 (b)).

In the third evaluation study, MDS FAIR I was tested under a more critical situation by using the same MRI parameters as in the first evaluation study: perfusion studies in the inferior part of the brain with smaller coverage.

For all other aspects of materials and methods used in performed studies, please refer to the descriptions in Chapter 2.

Results and Discussion

One representative subject's perfusion-weighted images are presented in Figures 3-4, 3-5 and 3-6 from the evaluation study one, two and three respectively. To emphasize the subtraction errors due to labeled venous artifacts, both positive and negative ASL signals are presented by using color-coded images with dynamic range from -25 to 25.

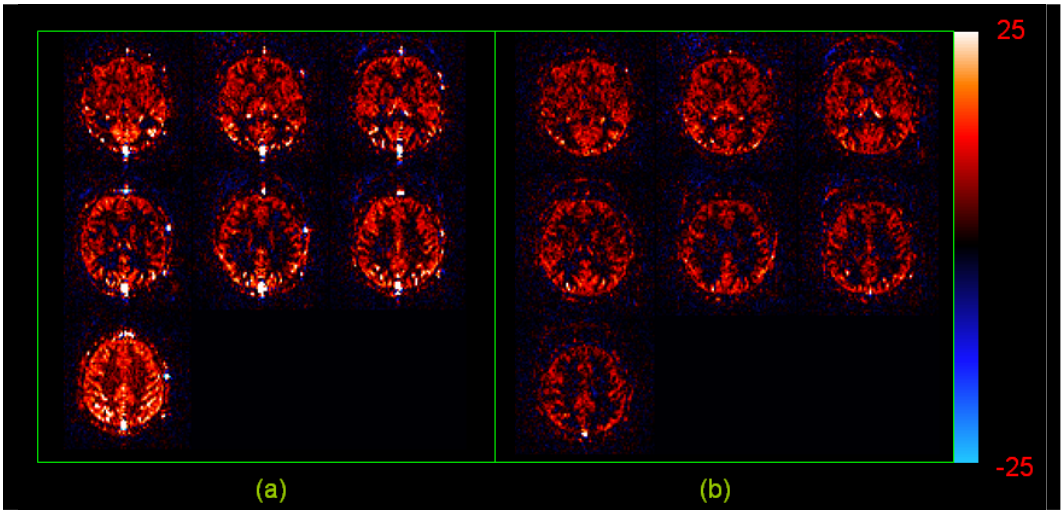

Figure 3-4 One typical subject's perfusion-weighted imaging maps from MDS FAIR I evaluation studies using smaller coverage and low resolution at the superior part of the brain: (a) traditional FAIR and (b) MDS FAIR I

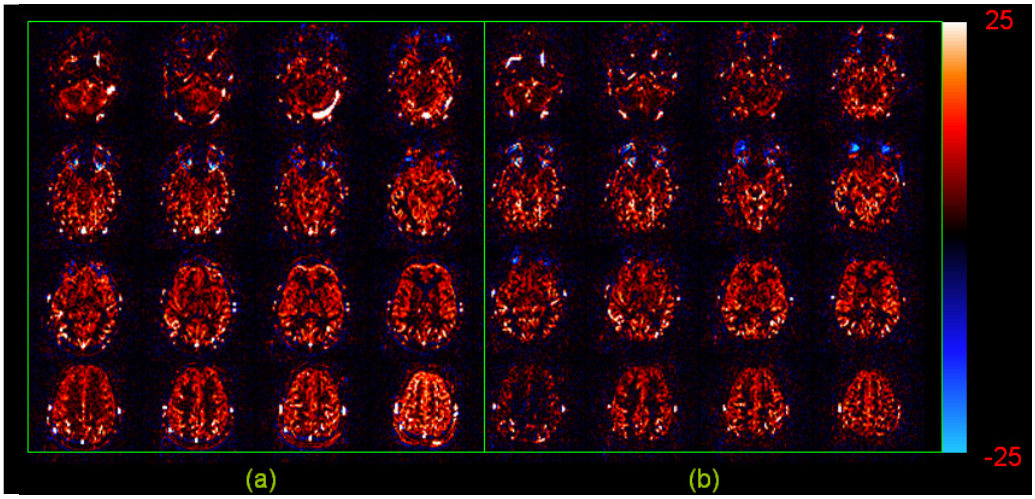

Figure 3-5 One typical subject's perfusion-weighted imaging maps from MDS FAIR I evaluation studies using large coverage and low resolution: (a) traditional FAIR and (b) MDS FAIR I

The study results from MDS FAIR I evaluation study one (Figure 3-4) indicated that MDS FAIR I could relatively well suppress venous artifacts. Only a tiny amount of venous signals can be observed in the most superior slice acquired using MDS FAIR I. For perfusion imaging under such a situation, it should be easier for MDS FAIR I to suppress venous artifacts since the amount of labeled blood is less, and the effective labeling region of superior labeling slab can be covered by superior saturation slab. Even if there are some residuals of labeled venous blood, since the venous blood flow velocity is relatively low, they may have less chance to flow into imaging slices before all imaging slices have been acquired. In contrast, perfusion-weighted imaging maps obtained using traditional FAIR had obvious hyper-intense venous artifacts and the superior slices gave higher perfusion signals than inferior or middle imaging slices. Based on these results, it is obvious that superior bolus can contribute to ASL signals in a large extend, especially for superior slices.

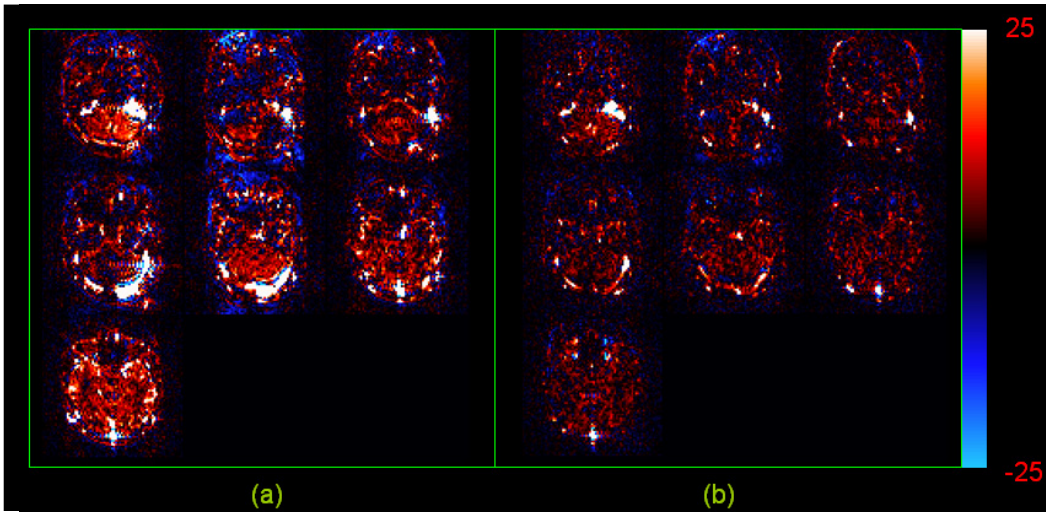

Figure 3-6 One subject's perfusion-weighted imaging maps from MDS FAIR I evaluation studies using smaller coverage and low resolution at the inferior part of the brain: (a) traditional FAIR and (b) MDS FAIR I

When large imaging slab was used, MDS FAIR I also worked well; huge venous artifacts observed around transverse sinus has been suppressed and perfusion signals in cerebellum area become more uniform due to reduced venous artifacts (Figure 3-5). Higher perfusion signals were also observed for superior slices acquired using traditional FAIR.

Study results from evaluation study three showed that venous artifacts could not be effectively suppressed when perfusion studies were performed in the inferior part of the brain with smaller coverage: the venous artifacts in the inferior slices were minimized a little bit while the venous artifacts in the superior slices were relatively well suppressed. These study results indicated that those labeled venous blood must have already flown into the imaging section before the beginning of superior saturation pulse train. Therefore, earlier superior saturation had better be performed.

In these evaluation studies, totally eighty saturation pulses were performed for each measurement, but the observed specific absorption rate (SAR) was less than 45% of the permitted maximum level.

These study results indicated that the superior inflow have large contributions to perfusion signals, which means symmetric PASL techniques, like traditional FAIR, will give higher CBF estimations than asymmetric PASL techniques when limited coverage was used for perfusion studies. The superior inflow can contain both venous drainage and arterial blood. In some brain regions, such as super cortex, the superior bolus for perfusion study using smaller coverage will mainly have labeled arterial blood signals from the superior side. In some other brain regions, such as the cerebellum, the superior bolus will mainly contain labeled venous blood, which behaves as artifacts and should be avoided.

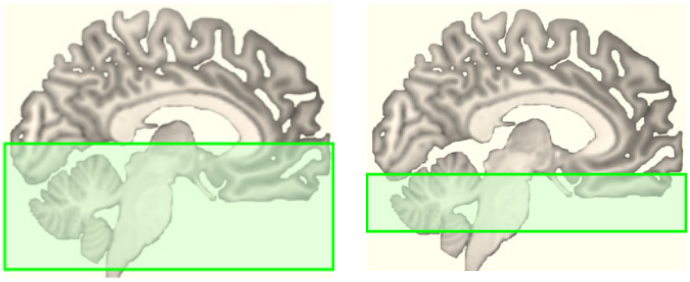

Figure 3-7 Imaging slice positions for MDS FAIR II evaluation study (left) and cerebellum perfusion study using MDS FAIR I and II (right) (refer to Appendix D for the information about the anatomic image).

The possible argument for MDS FAIR I is that the modulated superior saturation pulse train may kill defined bolus from the inferior side due to the tortuous path of some blood arteries, making the perfusion study questionable, which will become even worst for single slice perfusion study. Of course, this argument also faces the dilemma whether the labeled superior bolus has to be temporally defined for a specific bolus width.

Conclusions

Although MDS FAIR can help suppress venous artifacts for perfusion studies in the superior part of the brain or in deep brain region under specific situations, MDS FAIR I can not effectively suppress venous artifacts for perfusion studies in the inferior part of the brain. Better techniques had better be designed to facilitate reliable perfusion studies in the inferior part of the brain.

3.3.2 MDS FAIR II Evaluation Studies

Two studies were performed with complete focus on cerebellum area: MDS II evaluation study and quantitative cerebellum perfusion study using MDS FAIR techniques.

In the quantitative cerebellum perfusion study, for comparison purpose, traditional spatially-confined FAIR with Q2TIPS, MDS FAIR I and MDS FAIR II were used. To minimize study time and corresponding physiological oscillation, intermediate imaging resolution was used. Imaging slice positions for both studies are showed in Figure 3-7. Three healthy adults (two male subjects aged at 38 and 39 years and one female subject aged at 28 years) were recruited for the evaluation study. Six healthy adults (four male subjects with age range 27-40 years and two female subjects with age range 27 – 28 years) took part in the initial cerebellum perfusion study.

Materials and Methods

In the evaluation study, higher imaging resolution was used with the following MRI parameters: TR/TE = 3000/11 ms, FOV = 160 x 160 mm^2, matrix size = 64 x 64, in-plane resolution = 2.5 x 2.5 mm^2, slice thickness/gap = 5/1 mm, the number of imaging slices = 10, the number of measurements = 140, slice acquisition order = ascending, iPAT

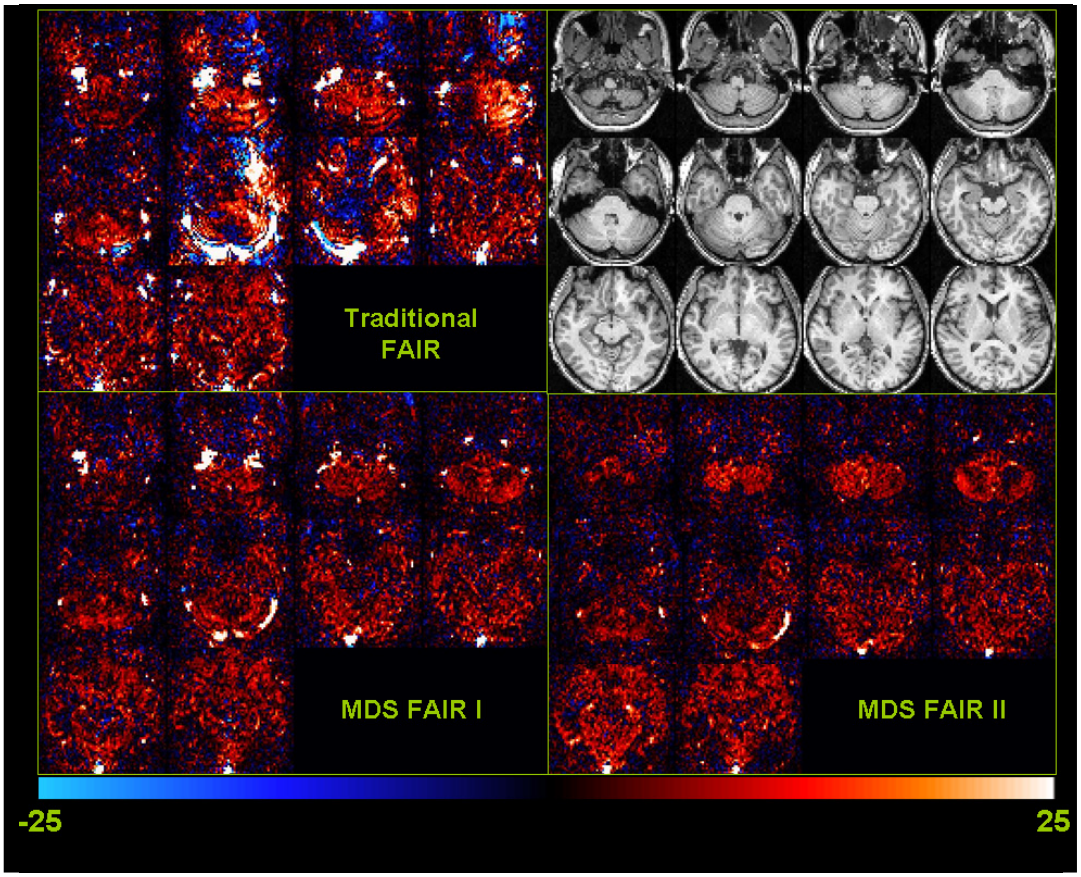

Figure 3-8 One representative subject's perfusion-weighted imaging maps from evaluation studies using smaller coverage and high resolution in the inferior part of the brain.

GRAPPA factor = 2 with 24 reference lines using CP mode, partial Fourier (PF) = 7/8, imaging section inversion slab size = imaging slab size + 20 mm, spatially-confined inversion slab size = imaging slab size + 200 mm, temporal bolus width (TI_1) /post-bolus delay = 800/1000 ms. For superior and inferior saturation pulses, the following parameters were used: saturation slab size = 20 mm, saturation pulse interval = 25 ms, superior saturation pulse number = 72, inferior saturation pulse number = 40.

MRI parameters used for cerebellum perfusion study are exactly the same as those in previous study except the following ones: TR/TE = 2500/9 ms, FOV = 240 x 240 mm^2,

matrix size = 68 x 68, in-plane resolution = 3.5 x 3.5 mm^2, slice thickness/gap = 5/1 mm, the number of imaging slices = 4, the number of measurements = 60. Quantitative cerebellum perfusion estimations were obtained from this study.

For all other aspects of materials and methods used in these performed studies, please refer to the descriptions in Chapter 2.

Results and Discussion

Perfusion-weighted images from one subject of MDS FAIR II evaluation study are displayed in Figure 3-8. Perfusion-weighted images from MDS FAIR I showed that a little improvement was achieved in terms of minimized venous artifacts. For the first several inferior imaging slices, the amount of venous signals are less, and the perfusion-weighted imaging signals in those slices become a little more uniform. Signal loss in slices 6 and 7 was recovered relatively well. MDS FAIR II gave more improvements: venous artifacts disappeared completely for the four most inferior imaging slices, perfusion signals became much more uniform and signal loss have been better recovered. However, venous artifacts are still obvious for middle and superior slices. Ringing-like artifacts still have adverse effects on perfusion signals in the neighboring tissue. The results from MDS FAIR II indicated that although superior saturation was performed during the whole inversion time (TI_2), labeled venous blood could not be suppressed completely. During the time for performing imaging acquisition of inferior slices, the residues of labeled venous blood flew into superior imaging slices, generating those observed artifacts. The observed SAR level for MDS FAIR II was still around 50% of the permitted maximum level for all subjects.

The study results from cerebellum perfusion studies using four imaging slices are displayed in Figures 3-9 to 3-10. In Figure 3-9, one representative subject's perfusion weighted imaging maps are presented for three FAIR methods: traditional FAIR method, MDS FAIR I and MDS FAIR II. No venous artifacts were observed for perfusion-weighted imaging maps from MDS FAIR II. CBF analysis was only performed for MDS FAIR I and II methods. The CBF estimations, inter-subject variability and calculated CBF ratio are presented in Figure 3-10 for two MDS FAIR methods. MDS FAIR I technique tends to give a little higher CBF estimations for both grey and white matter and much larger inter-subject variability. The CBF ratio from MDS FAIR I is larger than that from MDS FAIR II. Due to the limited coverage used in this study, superior bolus can contribute to CBF signals for MDS FAIR I and II. MDS FAIR II had more superior labeled blood suppressed by performing earlier and longer superior saturation, and should have lower CBF estimations. Single-tailed paired t tests showed significant difference for grey matter CBF measurements between MDS FAIR I and MDS FAIR II ($p = 0.029$). The higher CBF estimations from MDS FAIR I can also come from the contaminations from incompletely suppressed venous artifacts. The amount of labeled blood and venous artifacts due to the superior labeling are all subject dependent, and this may be the reason why MDS FAIR I gives larger inter-subject variability than MDS FAIR II.

Conclusions

MDS FAIR II is a better technique than MDS FAIR I in terms of more reliable CBF estimations for perfusion studies in the inferior part of the brain. However, when

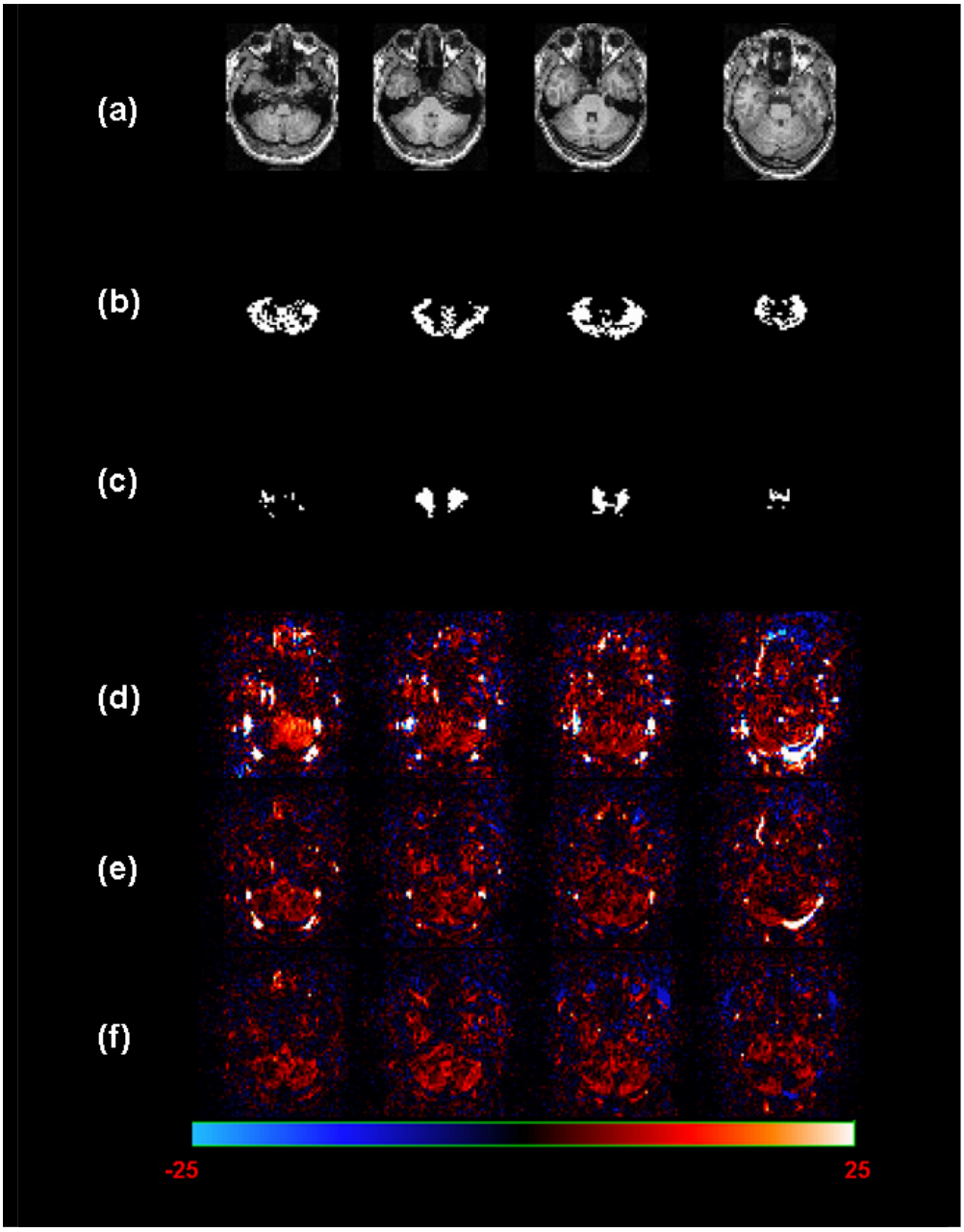

Figure 3-9 One typical subject's cerebellum perfusion study results using tradition FAIR, MDS FAIR I and II: (a) co-registered anatomic images, (b) cerebellum grey matter segmentation maps, (c) cerebellum white matter segmentation maps, (d) perfusion-weighted imaging maps from traditional FAIR, (e) perfusion-weighted imaging maps from MDS FAIR I and (f) perfusion-weighted imaging maps from MDS FAIR II.

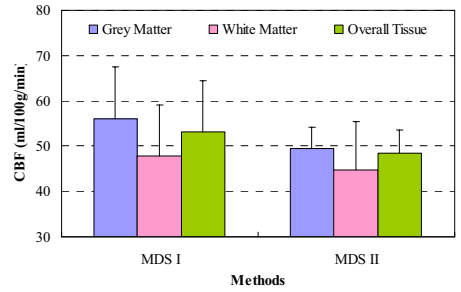

(a)

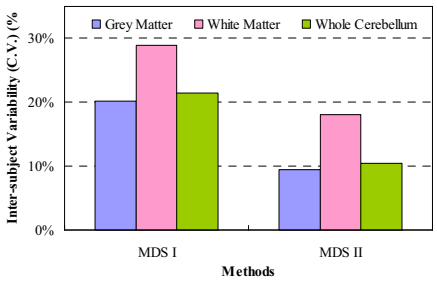

(b)

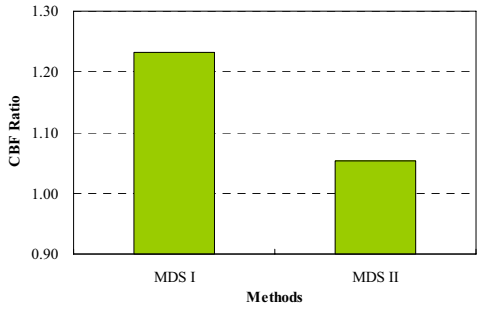

(c)

Figure 3-10 Cerebellum perfusion study results using MDS FAIR I and II: cerebellum CBF estimations (a), inter-subject variability as coefficient of variance (C.V.) (b) and CBF ratio between grey matter and white matter (c).

large coverage is used, for example, in the perfusion study of whole cerebellum, MDS FAIR II can not suppress the venous artifacts very well any more.

Compared to MDS FAIR I, MDS FAIR II also face the dilemma about the definition of temporal bolus width for the superior bolus, and have more possibility to kill bolus defined from the inferior side, especially for very small coverage in specific brain region.

3.4 SUMMARY

To suppress the venous artifacts of traditional FAIR technique, MDS FAIR techniques, by using modulated saturation pulse trains on both inferior and superior sides of imaging section for FAIR, were proposed to passively saturate labeled venous blood before the acquisition of perfusion imaging slices. Depending on the start time of the

superior saturation pulse train, two versions of MDS FAIR sequences were implemented and evaluated.

MDS FAIR I can help suppress venous artifacts for perfusion studies in the superior part of the brain or perfusion studies using large coverage, but can not effectively suppress venous artifacts for perfusion studies in the inferior part of the brain. By performing superior saturation pulses earlier, MDS FAIR II can effectively suppress venous artifact for perfusion studies in the inferior part of the brain when relatively smaller coverage was used. These two techniques all face dilemma about the temporal bolus width definition for the superior bolus.

To overcome the limitations of MDS FAIR technique in perfusion studies in the inferior part of the brain, even better techniques have to be designed and implemented. In the next chapter, an active approach for the suppression of the superior tagging of traditional FAIR will be described.

CHAPTER 4 FAIR ASST

To facilitate more reliable perfusion studies in the inferior part of the brain, especially cerebellum perfusion studies, an active approach for the suppression of venous artifacts of FAIR, FAIR with active suppression of superior tagging (FAIR ASST), was proposed, implemented and evaluated. In this chapter, the description of FAIR ASST technique will be followed by the report of three evaluation studies.

4.1 FAIR ASST SEQUENCE

In contrast to MDS FAIR techniques, in which the labeled venous blood spins from the superior tagging of FAIR were suppressed using periodical superior saturation pulses before imaging acquisition, FAIR ASST techniques will actively suppress the labeled venous blood signals at the labeling stage. This can be achieved by performing several superior saturation pulses around the inversion pulses (both imaging section inversion and spatially-confined inversion pulses) in both labeling and control experiments with larger saturation slab size which will depend on the size of labeling slab in the superior side (Figure 4-1). Before the inversion pulses, one or more superior saturation pulses can be performed to decrease the initial magnetization intensity that inversion pulses will work on. After the inversion pulses, one or more superior saturation pulses can be performed to further destroy the magnetization in labeling or control experiments. For CBF quantification purpose, Q2TIPS scheme can also be used with FAIR ASST, which is referred as FAIR ASST with Q2TIPS. To be brief, FAIR ASST is used in the following to refer to FAIR ASST with Q2TIPS if there is no specific declaration.

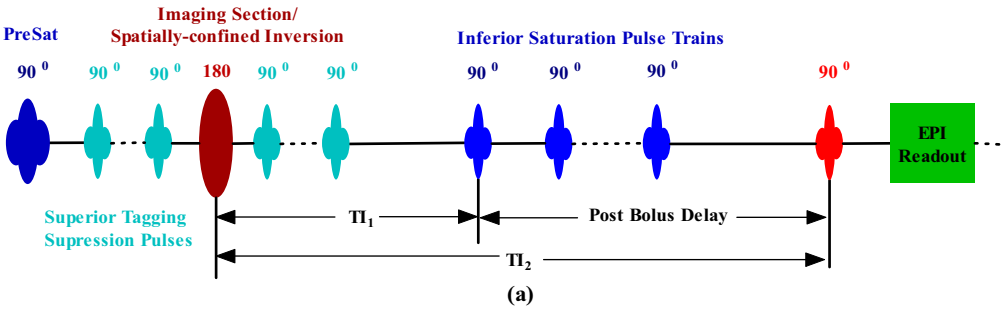

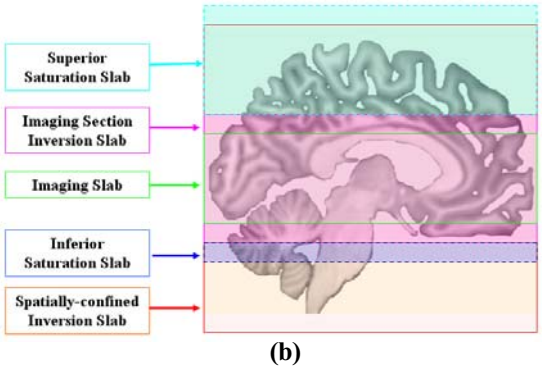

Figure 4-1 Diagram for sequence FAIR ASST with Q2TIPS (a) and spatial definitions for different slabs (b). Superior tagging suppression pulses and corresponding saturation slab are displayed in cyan, inferior saturation pulses and corresponding saturation slab are indicated by dark blue. The superior tagging suppression slab is larger than the defined superior labeling slab to ensure the transition part of the labeling slab can be also suppressed (refer to Appendix D for the information about the anatomic image).

The superior saturation effects are achieved by performing 90-degree RF pulse saturation and standard spoiler gradient. There are many ways to perform the superior saturations, especially the post-inversion superior saturations. The situation here is complicated due to different RF pulses, labeling and control experiments, and the flow of labeled venous blood so that it is difficult to predict signal evolutions precisely and correctly. Therefore, empirical approach was taken here to figure out better methods.

To better discriminate different FAIR ASST methods, three modes were defined according to the features of post-inversion superior saturations: 0, 1 and 2. In mode 0,

there is no phase difference between the first two post-inversion superior saturation pulses in both control and labeling experiments. Mode 1 is the same as mode 0, except that there is a 180-degree phase difference between the first two post-inversion superior saturation pulses in the control experiment. In mode 2, the first two post-inversion superior saturation pulses are always performed with a 180-degree phase difference in the control experiment, and only the second one is followed by a spoiler gradient in both control and labeling experiments. In modes 1 and 2, after the first two post-inversion superior saturation pulses, any additional user-defined post-inversion superior saturation pulses are applied in the same way as in mode 0: saturation and spoiling. FAIR ASST methods with single post-inversion superior saturation pulse were put under mode 0. In Table 4-1, the comparisons between three modes of FAIR ASST are listed. In all implemented FAIR ASST methods, each pre-inversion superior saturation pulse has a following spoiler gradient.

Table 4-2 Comparisons of implemented three modes of FAIR ASST technique

FAIR ASST Modes	Phase Difference for the First Two PSSP in Control Experiment (degree)	Spoiler Gradient (s) for the First Two PSSP	Consideration of Source of Residues
0	0	after each	incomplete dephase
1	180	after each	incomplete dephase
2	180	after the second	flow effects

PSSP: post-inversion superior saturation pulses

FAIR ASST methods from different modes are different in terms of physical principles. For FAIR ASST methods from modes 0 and 1, if the first two post-inversion superior saturations can completely saturate labeled venous blood (complete dephase), the residual of labeled venous blood using methods from these two modes will be zero. Otherwise, the residual from the methods of mode 0 will be much larger than that from

the methods of mode 1. This is because for the methods from mode 1, the residual of labeled venous blood spins from both control and labeling experiments will point to the same direction due to the 180- phase difference between the first two post-inversion superior saturation pulses in the control experiment. As another possibly good approach, mode 2 uses the first two post-inversion superior saturation pulses to rotate the magnetization of the blood by 180 degrees in the labeling experiment while the first two post-inversion superior saturation pulses keep the magnetization point to the original direction in the control experiment, making the magnetizations from both labeling and control experiments point to the same direction. If labeled venous blood dose not flow very fast, relatively less residual can be generated by the methods from mode 2 due to longer RF radiation before spoiling and following saturations. However, effective FAIR ASST methods from three modes perhaps may not give significantly different CBF measurements if the residues due to underlying physical differences are subtle. To help understand the possible magnetization residues after two post-inversion superior saturation pulses, for both control and labeling experiments, the directions of the magnetization in the superior labeling site are listed in Table 4-2 for each mode as well as the initial state.

To simplify the representation of these methods, a coding scheme is used to indicate the mode number and the number of pre-inversion and post-inversion superior saturation pulses: for method XYZ, X represents the mode number, Y represents the pre-inversion superior saturation pulse number and Z represents the post-inversion superior saturation pulse number. For mode 2, the last digit only represents the number of extra user-defined post-inversion superior saturation pulses in addition to the initial two phase-

inverted superior saturation pulses. FAIR ASST method 000, in fact, is the traditional FAIR method (spatially-confined FAIR with Q2TIPS).

Table 4-3 Directions of initial magnetization and magnetization residues at the superior labeling site after the first two post-inversion superior saturation pulses for each mode

ASL Experiments	Magnetization Directions			
	Initial	Mode 0	Mode 1	Mode 2
Control	↓	↕	↓	↓
Labeling	↑	↓	↓	↓

The saturation pulses and spoiler gradient used for superior saturation are the same as those used for imaging section pre-saturation. The spoiler gradients in the superior saturation pulses run along slice and readout directions simultaneously.

4.2 EVALUATION STUDIES FOR FAIR ASST

Three studies have been performed to evaluate different FAIR ASST methods. The initial evaluation study is a kind of screening study to sort out possible effective FAIR ASST methods. In the second evaluation study, the found effective methods were further tested under a little more critical situation. Since the venous artifact is the worst in the inferior part of the brain, the first two evaluation studies were performed using the imaging slab in pink in Figure 4-2. In the third study, quantitative perfusion studies were performed using three imaging slabs as showed in Figure 4-2. In addition to the inferior imaging slab used in the two previous evaluation studies, two other imaging slabs were used to evaluate the possible side-effects of superior saturation pulses of FAIR ASST using green imaging slab, and especially the superior labeling effects of traditional FAIR on CBF quantifications using yellow imaging slab. The yellow imaging slab covers the

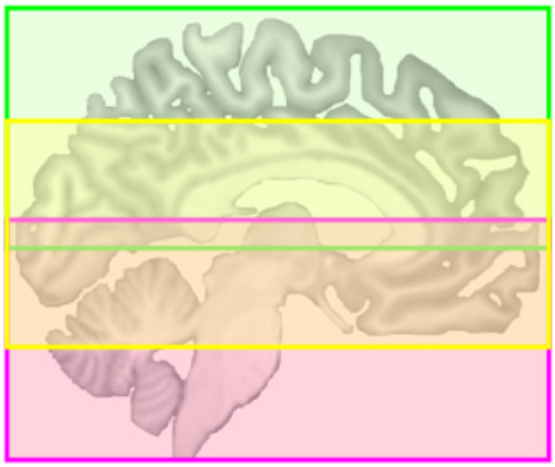

Figure 4-2 Imaging slab positions for evaluation studies for FAIR ASST. Three slabs are used to have important brain structures covered completely in each slab. For example, cerebellum is covered by the inferior slab in pink (refer to Appendix D for the information about the anatomic image).

mid-brain area begun from the parahippocampal gyrus to the top of the caudate. The green imaging slab mainly covers the superior cortex.

When performing quantitative perfusion studies in the superior part of the brain, traditional FAIR will not have venous blood labeled since the superior labeling slab will be outside the brain. Therefore, by comparing the CBF estimations using traditional FAIR method and effective FAIR ASST methods in the superior part of the brain, I can evaluate if the added superior saturation pulse train of FAIR ASST technique has some side effects on CBF estimations. By comparing CBF measurements in the deep brain region, the superior inflow effects from traditional FAIR on CBF estimations can be evaluated. CBF estimations using traditional FAIR can be higher than those using FAIR ASST methods since labeled venous blood can be wrongly accounted as real perfusion, which may also provide us some clues why some measured CBF values using traditional FAIR are much higher than usual physiological values estimated by using other imaging techniques (Wang, Alsop et al. 2002; Wang, Licht et al. 2003; Donahue, Lu et al. 2006)

and why there are sometimes discrepancies between CBF measurements using different ASL techniques.

4.2.1 Materials and Methods

4.2.1.1 Evaluation Study I

In this study, total 23 combinations of pre-inversion and post-inversion superior saturation pulses were evaluated to narrow down to the more robust methods (see Table 4-3): only methods with total number of superior saturation pulses less than 5 were tested thoroughly. Two male healthy adults aged at 38 and 39 years took part in this initial evaluation study.

MRI parameters used for this study are as the following: TR/TE = 2500/9.0 ms, FOV = 220 x 220 mm^2, matrix size = 64 x 64, resolution = 3.44 x 3.44 mm^2, the number of imaging slices = 10, slice thickness/slice gap = 5/1 mm, the number of measurements = 60, iPAT GRAPPA factor = 2 with 24 reference lines using CP mode, partial Fourier (PF) = 7/8, ascending acquisition order, temporal bolus width (TI_1) /post-bolus delay = 800/1000 ms, inferior saturation number = 20 with 25 ms interval using 20 mm saturation slab, superior saturation slab size = 100 ms, superior saturation pulse interval = 25 ms, imaging section inversion slab equal to imaging slab size plus 20 mm, spatially-confined selective inversion slab equal to the imaging slab size plus 100 mm on each side of imaging slab. Traditional FAIR method (000) was also used in this study as a control for the comparison.

4.2.1.2 Evaluation Study II

(a)

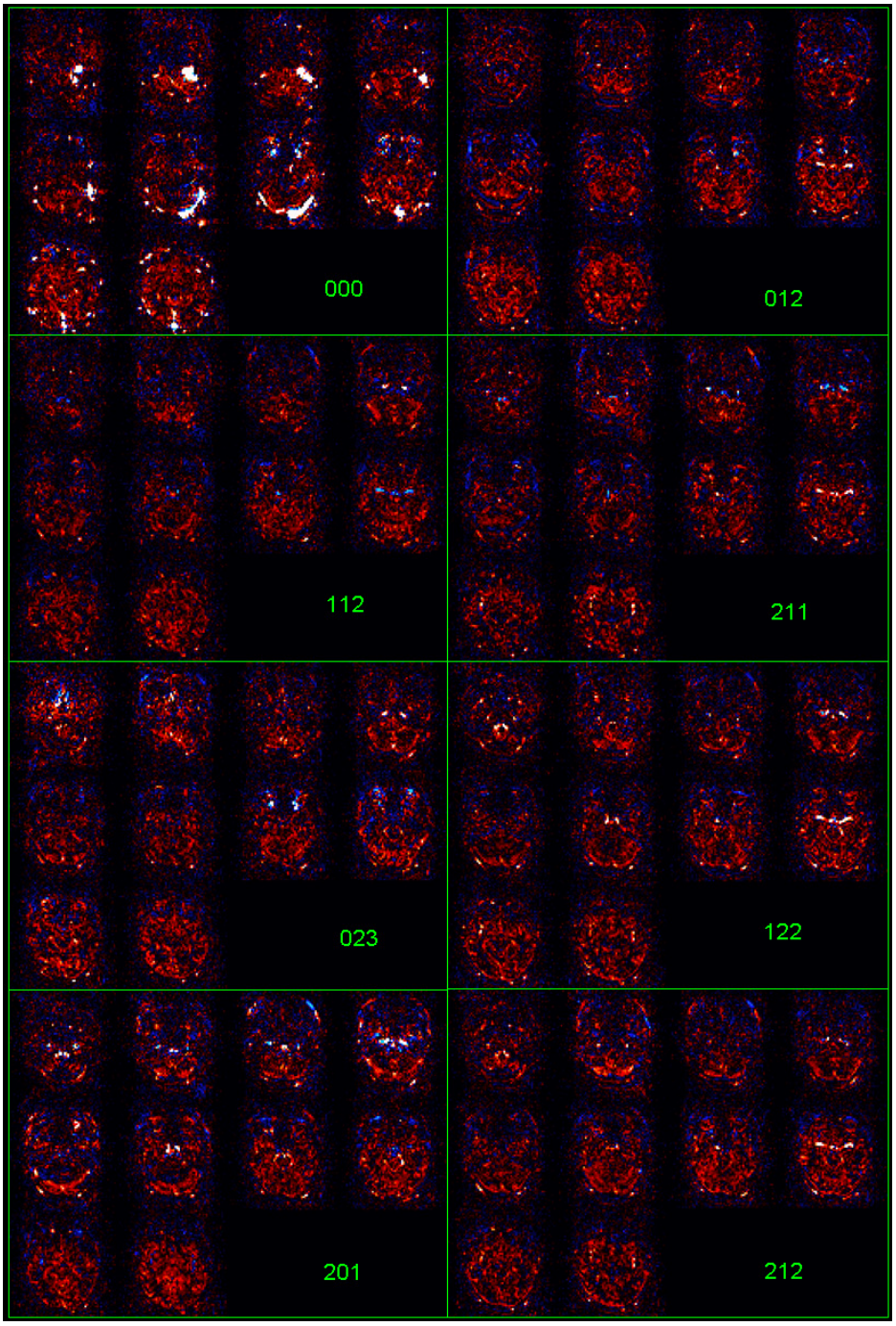

(b)

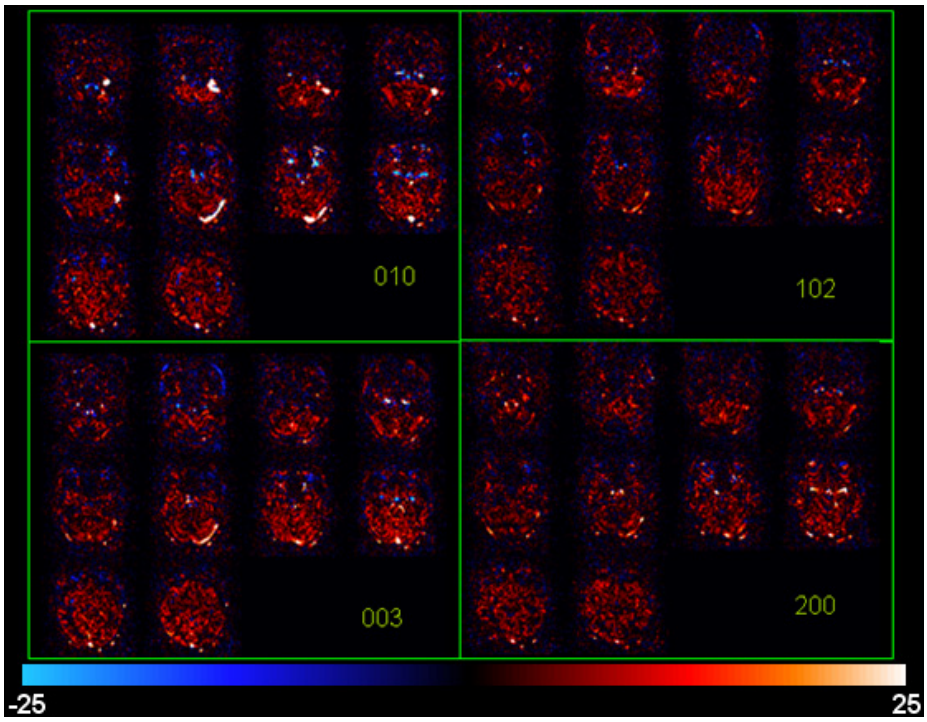

Figure 4-3 One representative subject's perfusion-weighted imaging maps from FAIR ASST evaluation study I: (a) traditional FAIR and selected effective FAIR ASST methods, and (b) four non-effective FAIR ASST methods

Totally three healthy male adult subjects (age range, 28-39 years) took part in this study. In this evaluation study, four found effective FAIR ASST methods (012, 112, 211 and 023), as well as traditional FAIR method (000), were further tested using isotropic imaging resolution. All other MRI parameters used for this study are the same as those used in the previous study except the following ones: TR/TE = 2500/9.2 ms, FOV = 230 x 230 mm^2, matrix size = 66 x 66, resolution = 3.5 x 3.5 mm^2, the number of imaging slices = 16, slice thickness = 3.5 mm with 20% gap, the number of measurements = 110.

4.2.1.3 Evaluation Study III

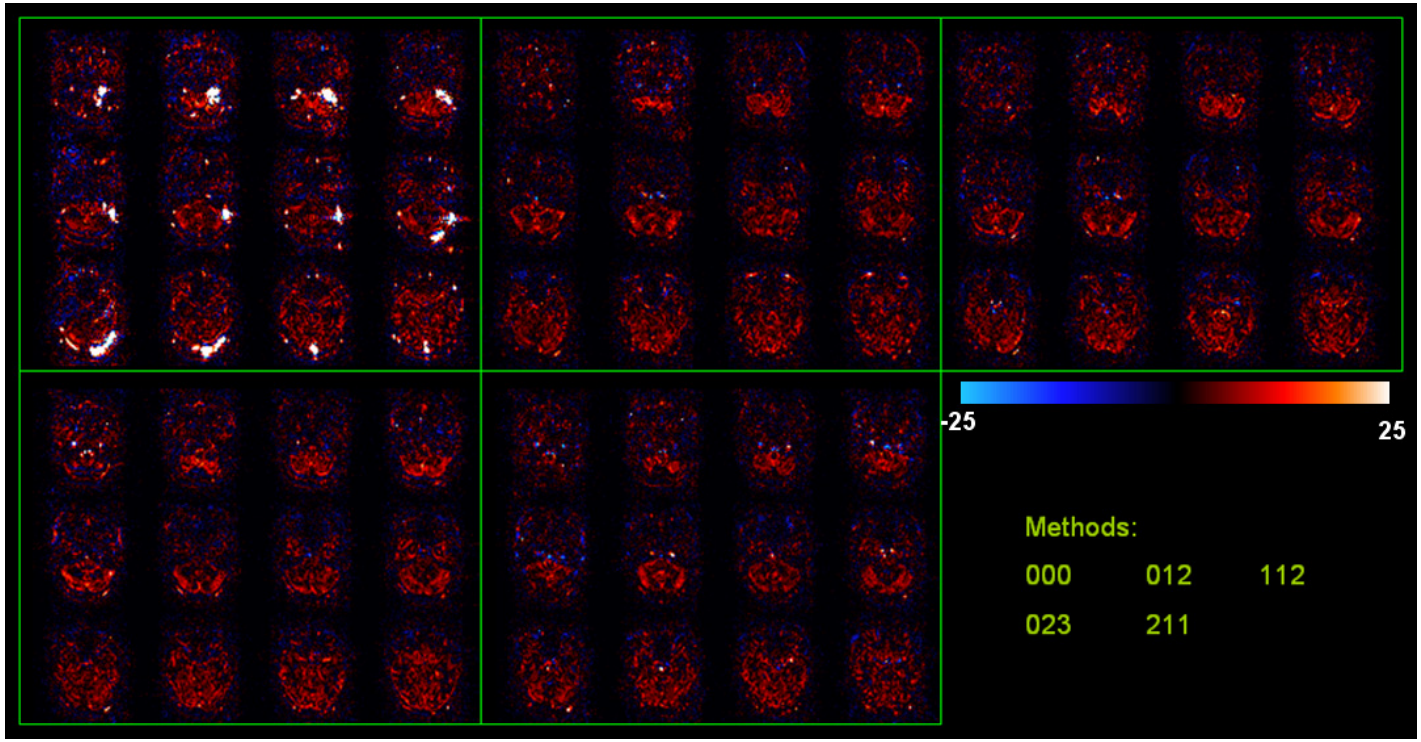

Figure 4-4 One representative subject's perfusion-weighted imaging maps from FAIR ASST evaluation study II. Only inferior twelve slices out of sixteen are displayed.

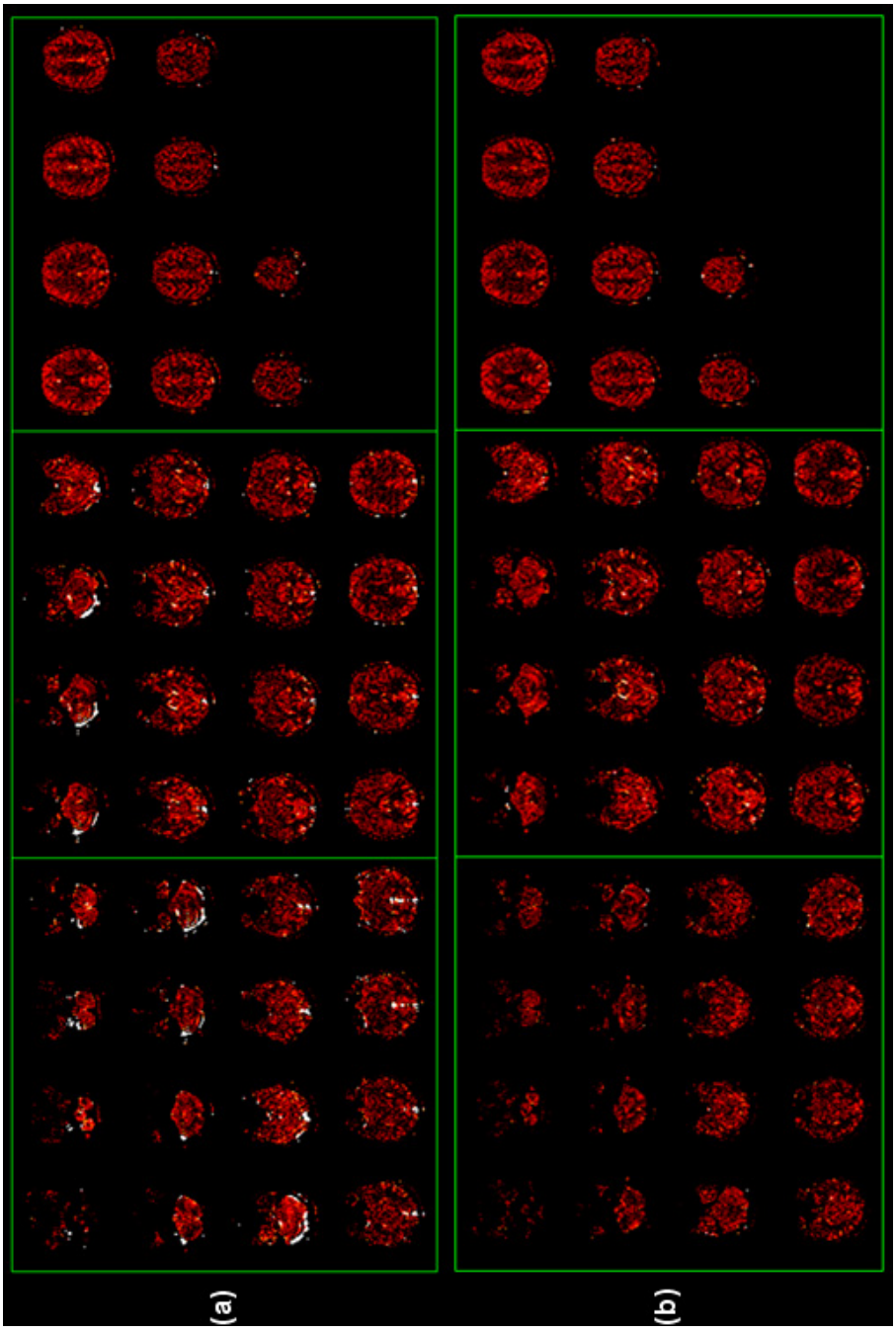
(a)
(b)

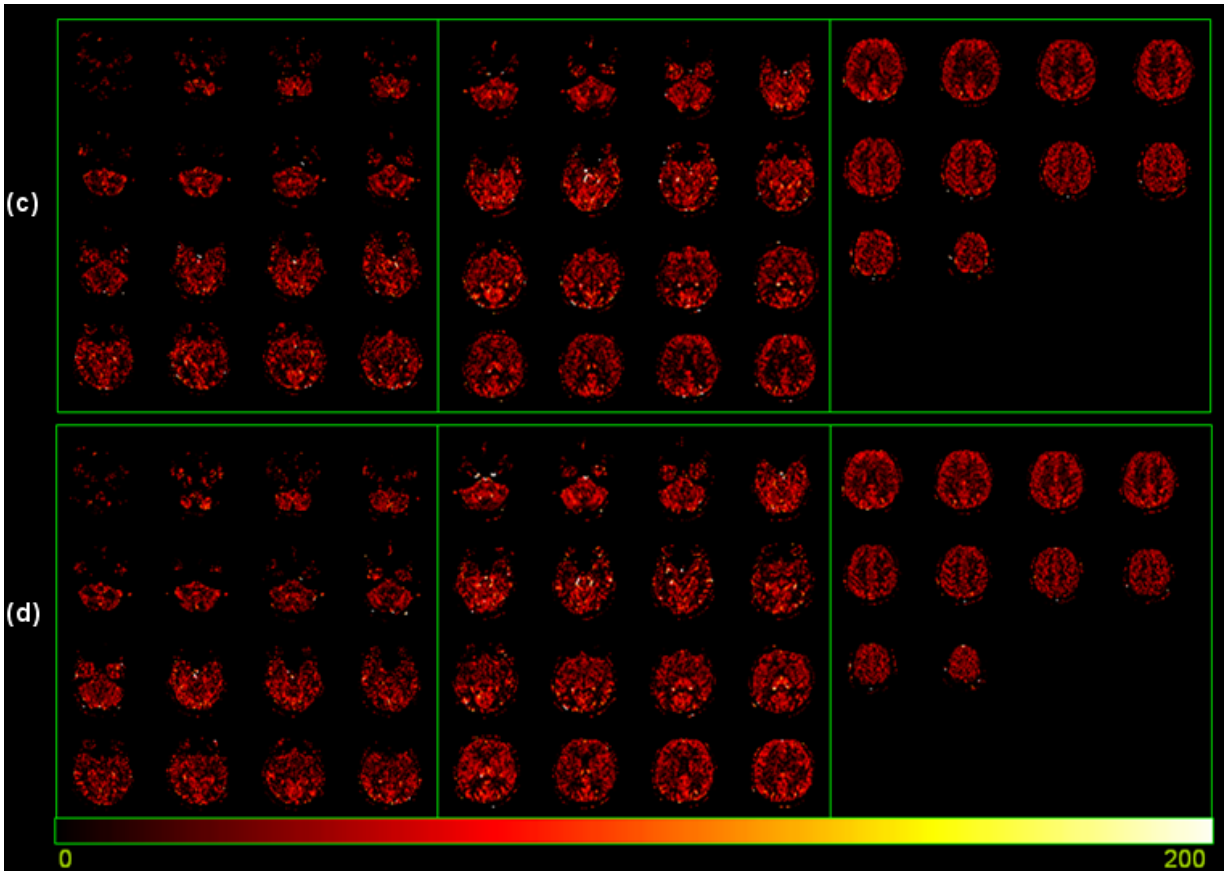

Figure 4-5 One representative subject's CBF maps for the control and three FAIR ASST methods on three parts of the brain from evaluation study III. From top to bottom are CBF maps for the control method and FAIR ASST 012, 112 and 211 methods . The unit for the color bar is the unit of CBF: mL/100g/min).

Table 4-4 Effectiveness of tested FAIR ASST methods

Mode No.	colored 3 digit representation of tested FAIR ASST methods											
0	000	001	002	003	010	011	012	013	020	021	022	023
1	102	103	112	113	122	123						
2	200	201	202	210	211	212						

Note: methods in black — not effective for all subjects, methods in green — effective across all subjects, methods in orange — not effective across subjects, method 000 (in red) — traditional FAIR method.

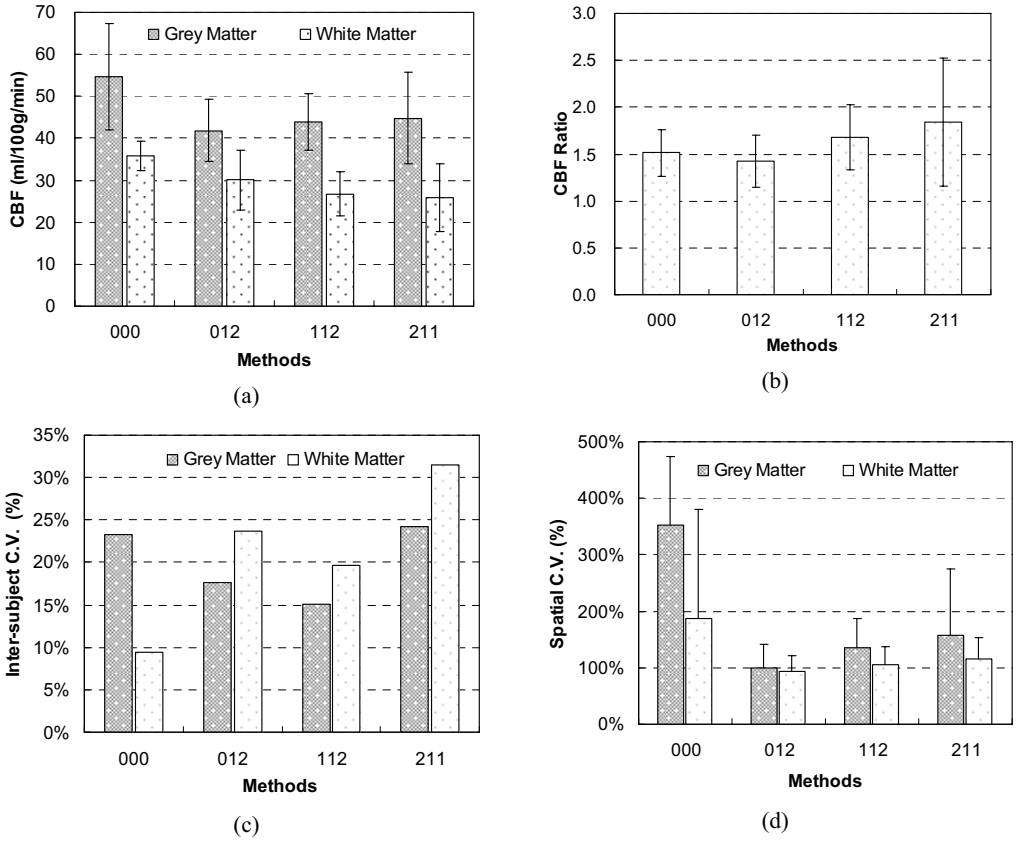

Figure 4-6 The analysis results for the evaluation study in the cerebellum: (a) CBF estimations, (b) CBF ratio between grey matter and white matter, (c) inter-subject variability and (d) spatial variability

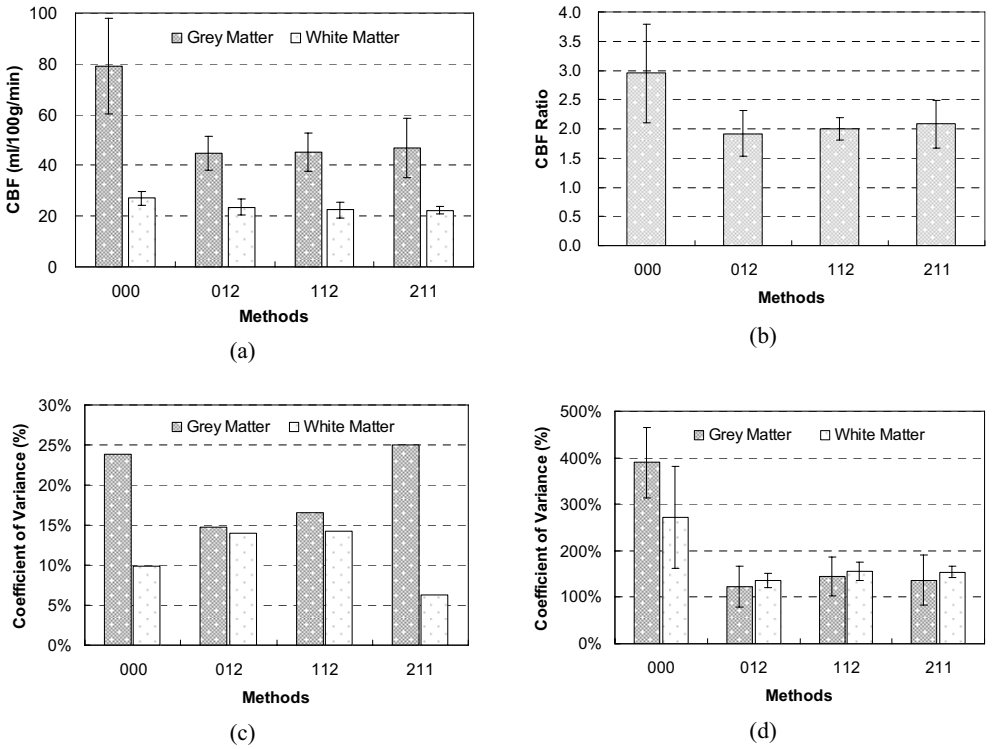

Figure 4-7 The analysis results for the evaluation study in the inferior part of the brain: (a) CBF estimations, (b) CBF ratio between grey matter and white matter, (c) inter-subject variability and (d) spatial variability

Quantitative perfusion studies were performed using three effective FAIR ASST methods (012, 112, and 211) on three parts of the brain with the comparison to the control method (000). Totally five healthy male adults (age range, 26-40 years) took part in this quantitative perfusion study. MRI parameters used in this study were exactly the same as those in the previous study.

Since for perfusion studies in the inferior part of the brain, especially in the cerebellum, the artifacts usually makes ASL signals wrongly co-registered between the left and right sides of the cerebellum, Asymmetry index (A.I.) analysis was performed for

cerebellum CBF measurements from those slices that cover the middle part of the cerebellum. The A.I. was calculated using the following formula:

$$|A.I.| = \frac{|(CBF_{right} - CBF_{left})| * 100}{CBF_{right} + CBF_{left}} (\%)$$

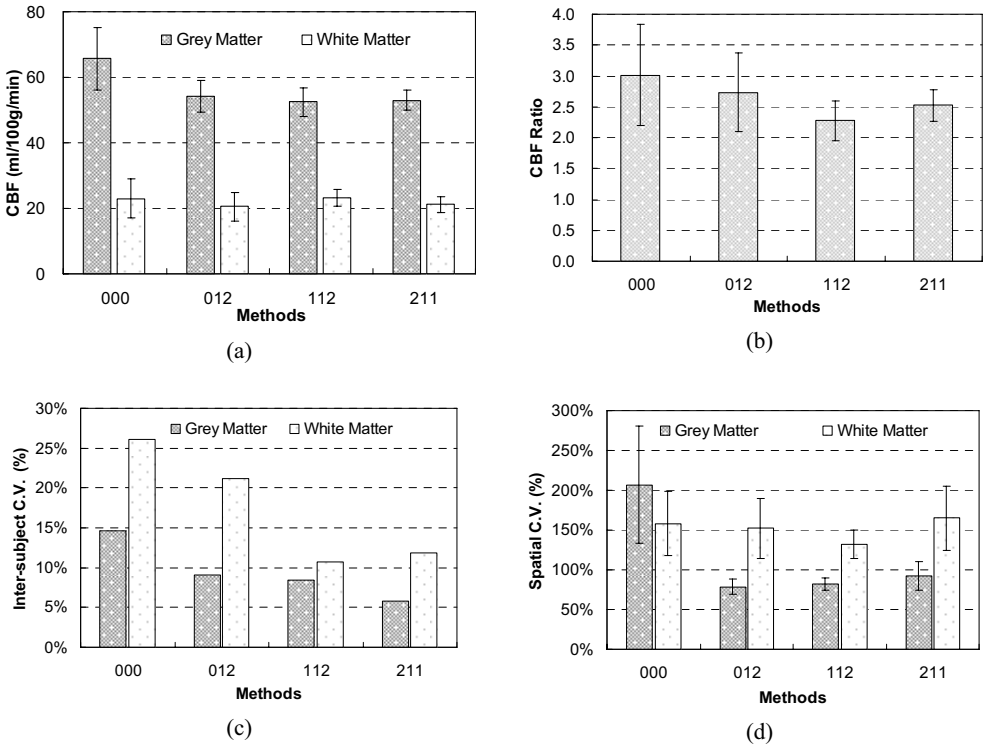

Figure 4-8 The analysis results for the evaluation study in deep brain region: (a) CBF estimations, (b) CBF ratio between grey matter and white matter, (c) inter-subject variability and (d) spatial variability

For some subjects, A.I. is negative while for some other subjects A.I. can be positive, which is due to the fact that the dominant transverse sinus varies between the left and right sides of the cerebellum across subjects. To simplify the presentation of A.I. analysis results, absolute values of A.I. were used.

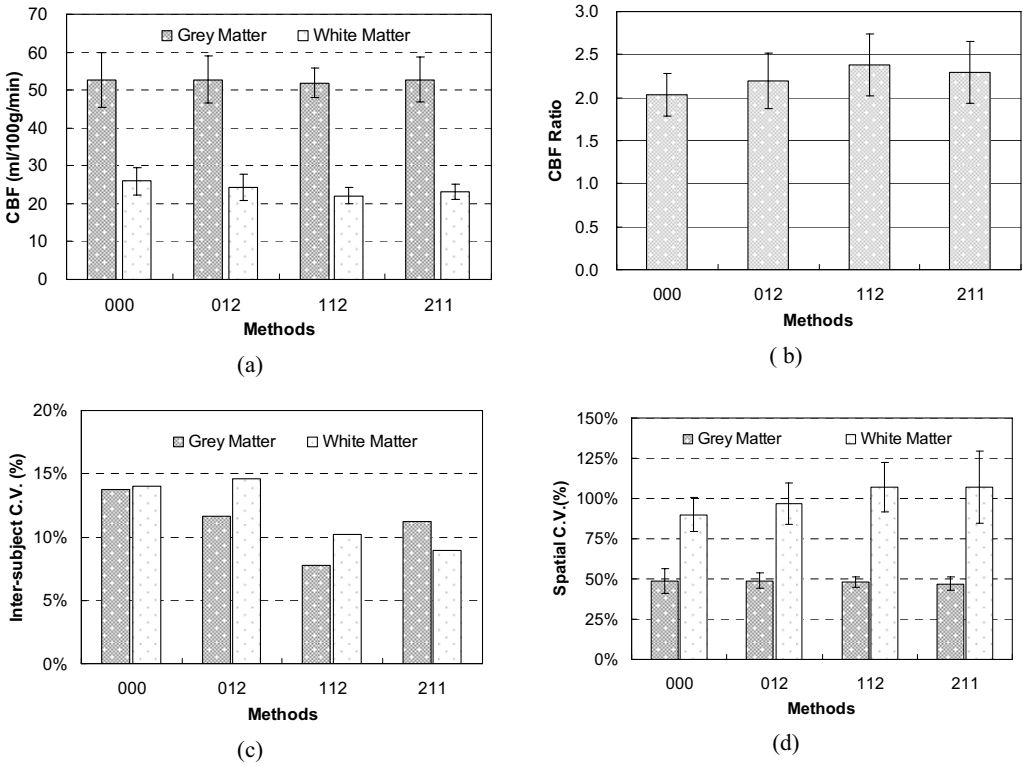

Figure 4-9 The analysis results for the evaluation study in the superior part of the brain region: (a) CBF estimations, (b) CBF ratio between grey matter and white matter, (c) inter-subject variability and (d) spatial variability

For all other aspects of materials and methods used in these three performed studies, please refer to the descriptions in Chapter 2.

4.2.2 Results and Discussion

Study results from evaluation study I are summarized in Table 4-3 by using different colors for the coding digits of the tested methods. These study results indicated that many of the tested methods worked well (those methods with coding digits in green) across subjects. Interestingly, only pre-inversion saturations or only post-inversion saturations could not robustly and successfully suppress the superior tagging of FAIR (for example, the methods 010, 003, 102 and 200). One typical subject's perfusion-weighted

images from selected effective and non-effective methods are displayed in Figure 4-3. Methods that did not work well for all subjects are indicated by using orange. The coding digits for the control method are presented in red. All other methods, with dark coding digits, could not completely suppress the superior tagging of FAIR. Some FAIR ASST methods can effectively suppress venous artifacts but they tend to have adverse edge effects, such as method 201. Although both FAIR ASST methods 210 and 211 are effective, method 211 has following saturation that can further decrease subtraction errors. Therefore, FAIR ASST method 211 was selected for further testing.

The study results from the second evaluation study showed that the selected methods effective in the previous study also worked well under more demanding conditions. One representative subject's perfusion-weighted imaging maps for selected methods are displayed in Figure 4-4. Although FAIR ASST methods with more superior saturation pulses (for example, 023) can also successfully achieve our aim, those effective methods with minimal number of saturation pulses are safer for subjects and thus preferred.

The CBF analysis results for perfusion studies in the cerebellum are presented in Figure 4-6 and Tables A-1-1 to A-1-6. The study results indicated that for both grey matter and white matter, traditional FAIR method (FAIR ASST 000) gave much higher CBF estimations than those from other FAIR ASST methods (about 25% higher relative to CBF estimations by FAIR ASST methods). The CBF measurements from the other three methods are very comparable for both grey and white matters (see Figure 4-6 (a) and Table A-1-1). For cerebellum grey matter CBF estimations, performed t tests found significant differences between traditional FAIR method and other three methods, but no

significant differences were found between FAIR ASST methods 112 and 211 (see table A-1-2). For cerebellum white matter CBF estimations, although no significant difference was found between traditional FAIR method and FAIR ASST method 012, significant differences were found between traditional FAIR or FAIR ASST method 012 and FAIR ASST methods 112 or 211.

The CBF ratios from FAIR ASST methods 112 and 211 tends to be higher although no consistent significant differences were found between methods 112 or 211 and other methods (000 or 012) (see Figure 4-6 (b) and Table A-1-2).

The analysis results for the inter-subject variability evaluation indicated that FAIR ASST method 112 may be the best one among the three effective FAIR ASST methods since it gave us the lowest C.V. for both grey matter and white matter CBF measurements across subjects (see Figure 4-6 (c)). The perfusion uniformity evaluation results by spatial coefficient of variance indicated that CBF measurements by traditional FAIR method have great variance across space. Performed t tests showed significant difference between traditional FAIR method and any of the other three methods, but no significant differences were found between any two of the other three methods (see Figure 4-6 (d) and Tables A-1-3 to A-1-6).

The above observations from cerebellum perfusion analysis were held the same for data analysis results of CBF measurements in the inferior part of the brain (see Figure 4-7 and Tables A-1-7 and A-1-12). The grey matter CBF measurement by traditional FAIR was much higher than that by FAIR ASST methods (about 75% higher relative to those by FAIR ASST methods). CBF ratio of CBF measurements using traditional FAIR technique was also pretty higher. FAIR ASST 112 method gave lower inter-subject and

spatial variability for CBF measurements in the inferior part of the brain. Performed t tests results showed that traditional FAIR is significantly different from the three FAIR ASST methods for all evaluated aspects.

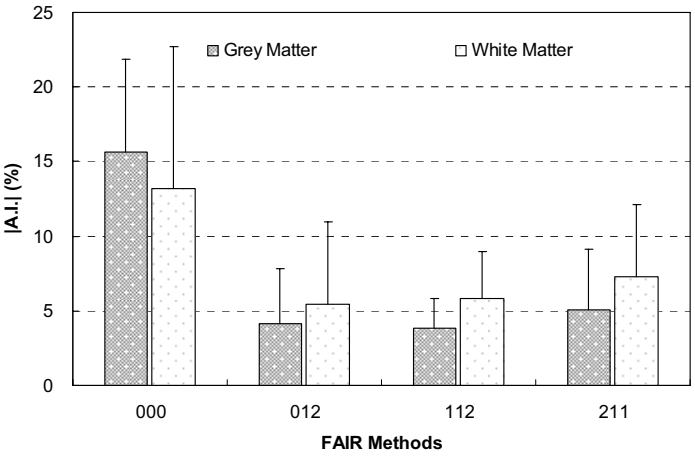

Figure 4-10 Asymmetry index (A.I.) analysis for cerebellum CBF measurements from four imaging slices near transverse sinuses

The CBF analysis results for perfusion studies in the deep brain region are presented in Figure 4-8 and Tables A-1-13 to A-1-18. Grey matter CBF estimation by traditional FAIR method (000) was also higher than that by any other FAIR ASST method, which means, even in deep brain region, contributions from superior inflow is very large (still about 25% higher relative to CBF estimations using three effective FAIR ASST methods). FAIR ASST 112 method still gave lower inter-subject and spatial variability for CBF measurements in the deep brain. Performed t test results showed that traditional FAIR is significantly different from FAIR ASST methods in terms of grey matter CBF estimation. No significant differences were found between FAIR ASST methods 112 and 211.

In Figure 4-9 and Tables A-1-19 to A-1-24, the CBF analysis results for perfusion studies in the superior part of the brain are presented. Four FAIR methods are comparable

to each other in all evaluated aspects. That is, no significant differences were found between any two FAIR methods in terms of grey and white matter CBF estimations, CBF ratio, and spatial variability. Although both FAIR ASST methods 112 and 211 gave relatively lower inter-subject variability, but CBF estimations by using these two methods are very close to those from two other methods.

To quantitatively evaluate the extend ASL signals are wrongly registered between left and right lobes of the cerebellum with the assumption that cerebellum perfusion is symmetric, asymmetric index analysis was perform for cerebellum CBF measurements from middle four slices. The selected four slices contain the majority of cerebellum white matter. The analysis results are showed in Figure 4-10 and Tables A-1-25 to A-1-26. CBF measurements from all four FAIR methods are not symmetric between left and right lobes. Especially, |A.I.| of cerebellum grey matter from traditional FAIR method is significantly higher than that from any of the other methods. CBF |A.I.| of cerebellum white matter from traditional FAIR is obvious higher those from other methods although no significant difference was found with five subjects' data.

The possible reasons for the large asymmetry of cerebellum CBF measurements using traditional FAIR can be due to the fact that usually, transverse sinus are only dominant in one side for nearly all people, and therefore the artifacts generated by the labeled venous blood will be asymmetric. The measured smaller asymmetry of cerebellum CBF measurements using effective FAIR ASST methods can be due to the imperfection of the suppression of the venous effects by these methods.

Motions from all subjects in FAIR ASST evaluation study III were very small due to the good cooperation of subjects and well padding (see Figures A-1-1 to A-1-3). No significant differences were found for both translation and rotation motions between any two of four methods (data not showed). Therefore, the effects from motions on the above analysis results should be neglectable.

Compared to MDS FAIR, FAIR ASST can avoid the dilemma about the temporal width definition for superior bolus. By destroying superior tagging of FAIR, FAIR ASST methods only use the inferior bolus for CBF quantification, which is quite reasonable because superior bolus is not pure arterial blood but contains labeled venous blood. For perfusion studies in specific brain regions, such as pons and cerebellum, the major component of the superior bolus is labeled venous blood. More importantly, the venous blood generates adverse imaging artifacts for perfusion studies in the inferior part of the brain.

Very large superior saturation slab is used in FAIR ASST, and the interference between superior saturation slab and imaging section does exist. However, the pre-inversion superior saturation pulses behave like pre-saturation, and the superior saturation pulses after inversion pulses can be done within tens of milliseconds, leaving little chance for these superior saturation pulses to affect labeled blood spins from the inferior bolus that is tens of millimeters away. Superior saturation pulses do not have MT effects issue since they are conducted exactly in the same way for both control and labeling experiments.

4.2.3 Conclusions

FAIR ASST methods can help suppress the adverse effects from the superior inflow of labeled blood due to the superior labeling slab of FAIR, greatly improving the reliability of CBF measurements in the inferior part of the brain, for example, the quantification of cerebellum perfusion.

Study results from perfusion studies in the deep brain region indicated that superior inflow does have contributions to CBF estimations even in the middle part of the brain, and that estimated CBF values obtained using traditional FAIR tend to be much elevated, explaining in large part why CBF values estimated using traditional FAIR technique are usually higher. This inflow should contain both labeled arterial blood and venous blood. In the inferior part of brain, especially in the cerebellum, most of the labeled blood signals are venous spins in sinuses, and they behave as artifacts.

FAIR ASST methods do not have side effects on CBF measurements, which can be supported by the CBF analysis results from the perfusion studies in the superior part of the brain using four different FAIR methods.

Significant differences were found between traditional FAIR and effective FAIR ASST methods (112 or 211), among which FAIR ASST method 112 may be a better one. In fact, since no significant differences were found between these two methods (112 and 211) for all aspects, any one of these two methods can be freely selected for future perfusion studies.

4.3 SUMMARY

The performed evaluation studies for FAIR ASST techniques indicated that the tested effective FAIR ASST methods, especially 112 and 211, are superior to traditional FAIR method in terms of the robustness and reliability of CBF measurements, particularly for perfusion studies in the inferior part of the brain. No side effects on quantitative perfusion studies were found for the added superior saturation pulses.

CHAPTER 5 Cerebellum Perfusion Studies Using FAIR ASST and PICORE

As an important application of FAIR ASST technique, quantitative cerebellum perfusion study using FAIR ASST was performed. Since asymmetric PASL techniques, such as PICORE, do not have superior labeling and corresponding venous artifacts, it is valuable to have these two methods compared by performing quantitative cerebellum perfusion studies. To make sure proper ASL parameters are used for the quantitative cerebellum perfusion study, three-session ASL optimization studies were performed in advance.

5.1 OPTIMIZATION STUDIES USING FAIR ASST

As emphasized in Chapter one, ASL parameters optimized for perfusion studies in the superior part of the brain may be not suitable anymore for perfusion studies in other parts of the brain. To ensure proper ASL parameters selected for quantitative cerebellum perfusion study, three-session perfusion studies have been performed: (1) multiple inversion experiment, (2) multiple post-bolus delay experiment, and (3) perfusion studies for TR effects evaluation and the estimation of minimal inferior saturation pulse number. In all of these performed studies, FAIR ASST method 112 was used. ASL optimization was mainly focused on cerebellum grey matter since single blood compartment model is more accurate for grey matter CBF quantification (Parkes and Tofts 2002; Parkes 2005). Each study was performed in one session. Total 10 male adults were recruited for these optimization studies. Three healthy adults took part in the first session of the study, four healthy adults participated in the second session of the study, and three healthy adults

were recruited for the third session of the study. The age range for all subjects is 26 to 39 years.

The imaging slab position used for all performed optimization studies is illustrated in Figure 5-1. The imaging slab was planned to make sure the first inferior slice begin to cover the lower edge of the cerebellum. The imaging slices were oriented to be parallel to the long axial of cerebellum white matter to minimize the mixture between grey matter and white matter.

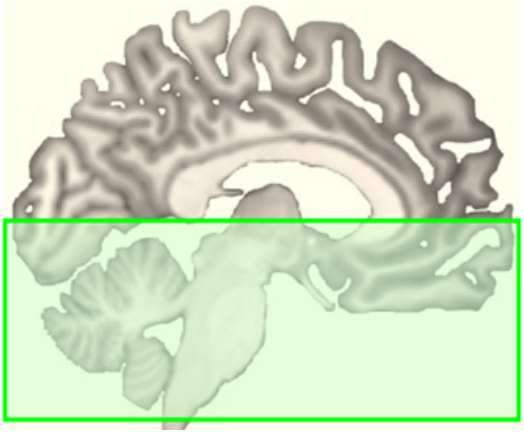

Figure 5-1 The imaging slab position used for cerebellum perfusion studies (refer to Appendix D for the information about the anatomic image).

5.1.1 Multiple Inversion Experiment

Materials and Methods

MRI parameters used in this study are as the following: TR/TE = 4000/9.2 ms, FOV = 230 x 230 mm^2, matrix size = 66 x 66, in-plane resolution = 3.48 x 3.48 mm^2, the number of imaging slice = 12, slice thickness = 5 mm with 20% gap, the number of measurements = 60, iPAT GRAPPA factor = 2 with 24 reference lines using CP mode, partial Fourier (PF) = 7/8, ascending acquisition order, superior saturation slab size = 100 mm, imaging section inversion slab size = imaging slab size + 20 mm, spatially-confined selective inversion slab size = imaging slab size + 200 mm. The inversion time was randomly varied with values: 50 ms, 300 ms up to 3300 ms with 300 ms step. FAIR ASST 112 method was used with inferior saturation pulse train turned off.

For all other aspects of materials and methods used in these three performed studies, please refer to the descriptions in Chapter 2.

Results and Discussion

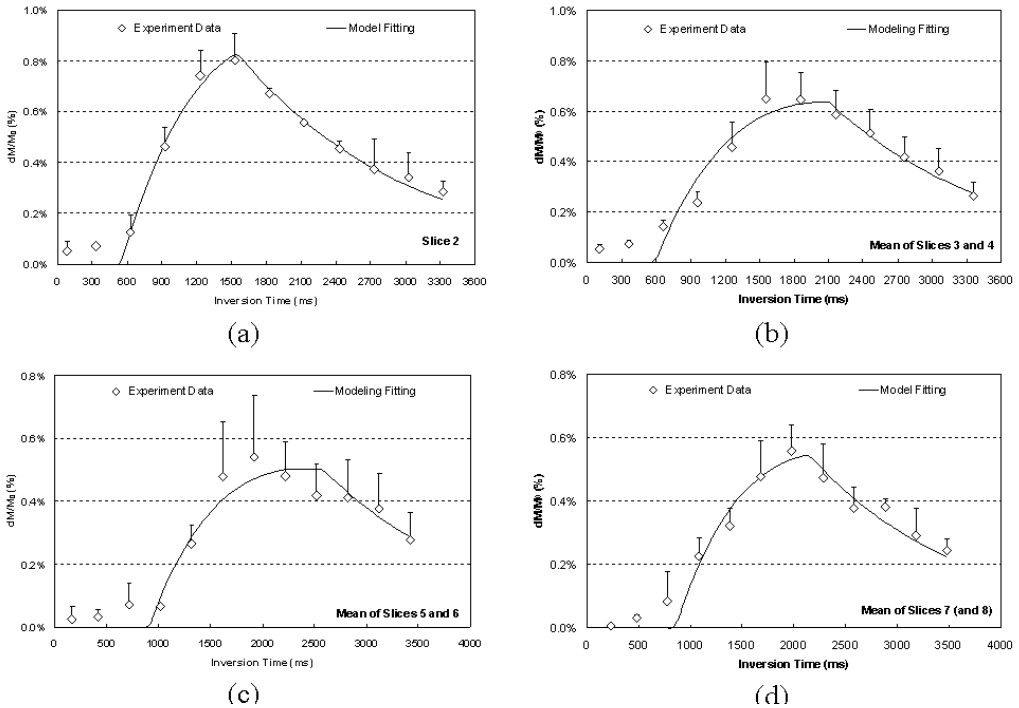

Figure 5-2 Cerebellum grey matter ASL signal changes with the inversion time for (a) slice 2, (b) slices 3 and 4, (c) slices 5 and 6 and (d) slices 7 (and 8)

In Figures 5-2 and 5-3, group mean grey and white matter ASL signals were plotted as a function of the inversion time for four groups of slices. The error bar represents group variance. The model-fitting curves for each slice group are also presented. The estimated bolus durations for slice groups are presented in Figure 5-4. The estimated transit times for slice groups are displayed in Figure 5-5. These transit times are already corrected by including the slice acquisition time spent on previous slices.

These results indicated that although all cerebellum tissue (or all imaging slices) utilizes the same labeled bolus, the estimated bolus durations and transit times varied across slices. For example, the estimated bolus durations varied from 1000 ms up to 1332 ms. The variability can be due to the variation of ASL signals across slices and the different irrigating arteries for different territories or the different extends of bolus dispersions when blood flew into different regions of the cerebellum. This can also be due to model-fitting errors for different slice groups. The similar phenomenon happened for cerebellum white matter: differences of estimated bolus durations between different groups of slices were observed. Of course, in principle, the model fitting for white matter should be less accurate.

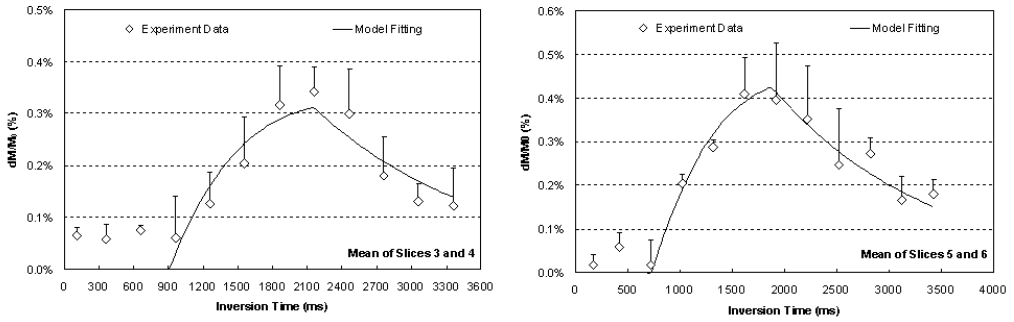

Figure 5-3 Cerebellum white matter ASL signal changes with the inversion time for (a) slices 3 and 4, and (b) for slices 5 and 6

Relatively larger inter-subject variability was observed for the estimations of bolus durations and transit times for both grey matter and white matter. To be conservative, shorter bolus duration and longer transit time should be assumed for quantitative cerebellum perfusion studies. For example, 800 ms can be used for the temporal bolus width conservatively. Long enough post-bolus delay has to be selected to make sure labeled blood spins have been delivered to the imaging slices with longest transit time,

for example, middle slices 5 and 6. The proper post-bolus delay will be further determined later by performing multiple post-bolus delay experiment.

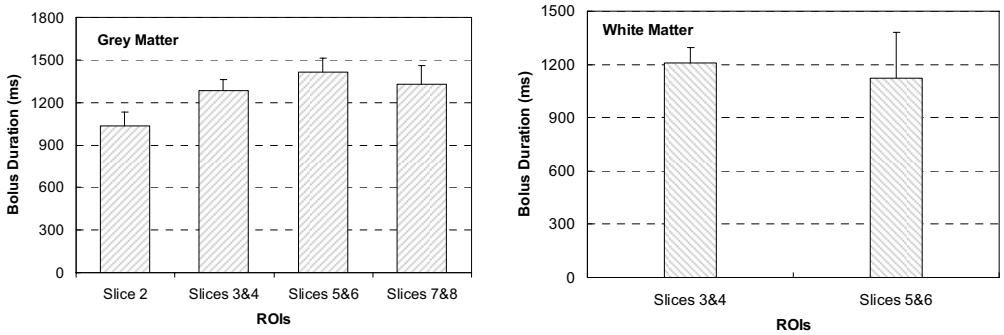

Figure 5-4 Bolus duration estimations for cerebellum grey matter and white matter

The estimated CBFs for cerebellum grey matter and white matter are presented in Figure 5-6. CBF ratio from this study is about 1.47 ± 0.37 and the coefficients of variance for grey matter and white matter are 0.08 and 0.21 respectively. The observed non-consistent increase of estimated transit times may be due to the fact that blood velocity in large vertical arteries, vertebral and basilar arteries, is higher than that in small horizontal arteries that are branches of vertebral and basilar arteries. Other data analysis results

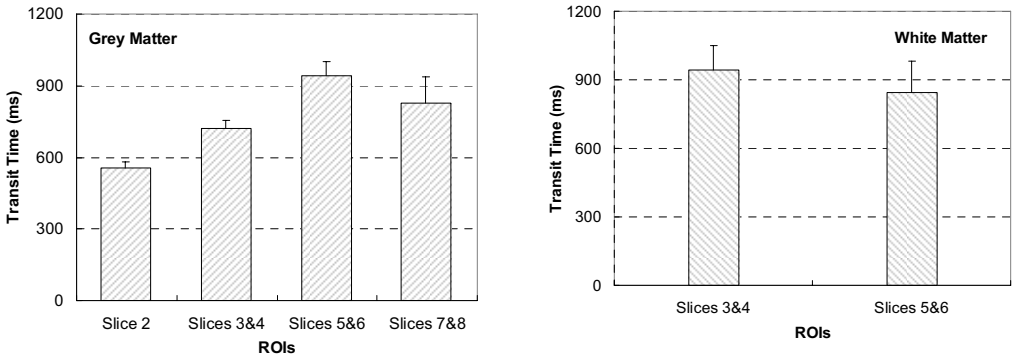

Figure 5-5 Transit time estimations for cerebellum grey matter and white matter

indicated that transit time within axial slices has larger heterogeneity (refer to appendix B).

Conclusions

Based on the multiple inversion experiment results, temporal bolus width less than or equal to 800 ms is proper for quantitative cerebellum perfusion studies using FAIR ASST with Q2TIPS scheme.

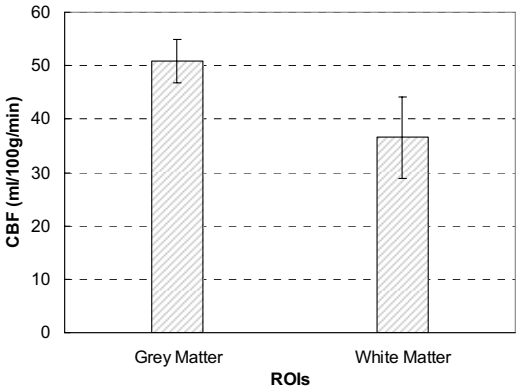

Figure 5-6 CBF estimations for cerebellum grey matter and white matter

5.1.2 Multiple Post-bolus Delay Experiment

Materials and Methods

In this study, FAIR ASST with Q2TIPS scheme (Figure 4-1) was used. All other MRI parameters used in this study are the same as those used in the previous studies except parameters mentioned in the following. The temporal bolus width was fixed as 800 ms while the post-bolus delay was varied from 0 ms to 1400 ms by using 200 ms as an increment. Post-bolus delay time was

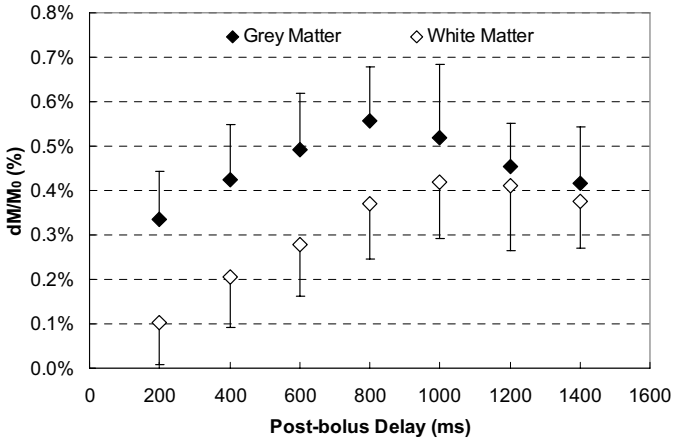

Figure 5-7 ASL signal changes with post-bolus delay for cerebellum grey matter and white matter

randomized for each subject during this study. During each delay time, the possible maximal number of inferior situation saturations were performed by using pulse interval equal to 25 ms and 20 mm saturation slab size. TR equal to 3000 ms was used for this study.

Study Results and Discussion

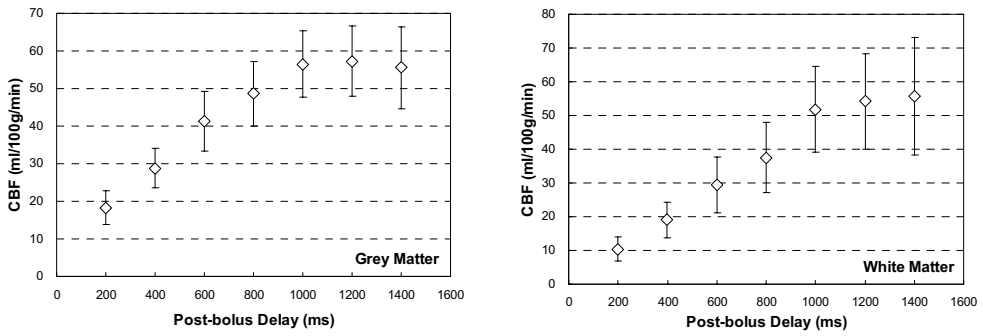

Figure 5-8 Cerebellum CBF changes with post-bolus delay for grey matter and white matter

Figure 5-7 shows that after 800 ms for overall grey matter and 1000 ms for overall white matter, ASL signals begun to decrease, which implies that proper post-bolus delay time can be 1000 ms. Usually arteries in white matter are major small arteries. When labeled blood spins have been delivered to white matter, labeled blood in grey matter should have reached small arteries since the blood is supplied for grey matter first and white matter later. The calculated CBFs for overall cerebellum grey and white matters are displayed in Figure 5-8. After 1000 ms post-bolus delay, both grey matter and white matter CBFs basically reached the plateau. Perfusion-weighted imaging maps from one representative subject are displayed in Figure 5-9. At short delay times, many spurious signals showed up, which mainly came from big arteries. After 1000 ms delay, the perfusion-weighted

imaging maps became very uniform without obviously spurious signals. After even longer delay, such as 1200 ms, as showed in Figure 5-9, the perfusion-weighted imaging maps appeared more uniform but SNR became very lower.

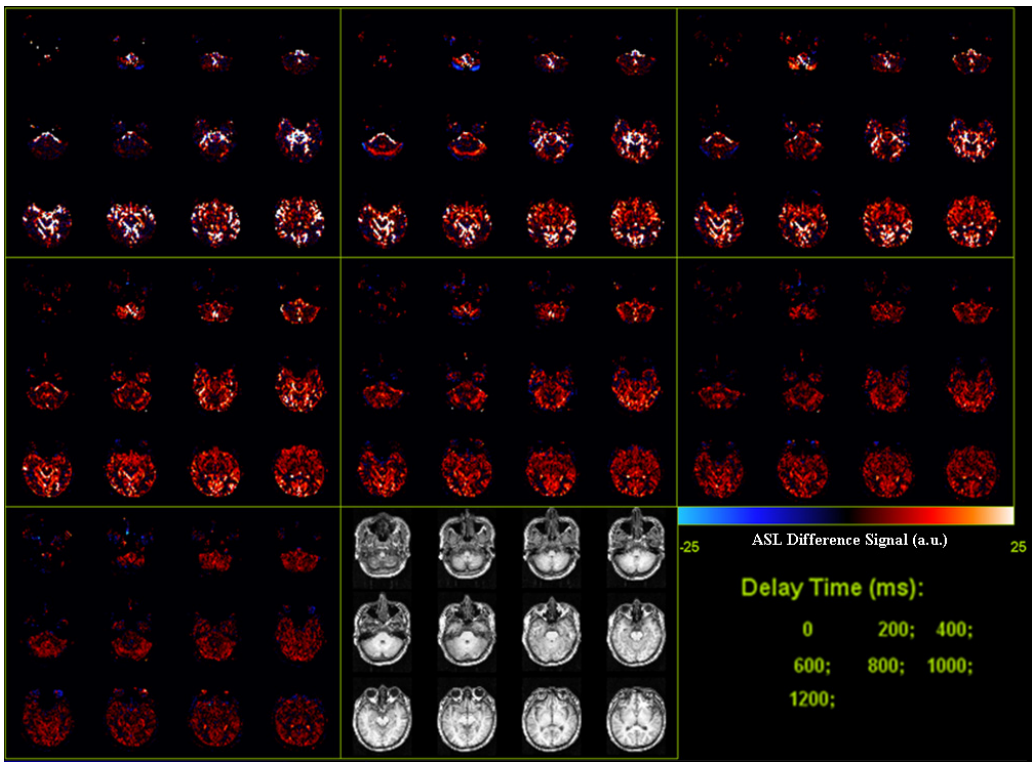

Figure 5-9 One typical subject's perfusion-weighted imaging maps from multiple post-bolus delay experiment and co-registered anatomic images.

To further evaluate the proper post-bolus delay time from another point of view, inter-subject variability and spatial variability of cerebellum CBF measurements for both grey and white matters were calculated and presented in Figure 5-10. At post-bolus delay around 1000 ms, the inter-subject variability is the lowest and the CBF maps became more uniform at 1000 ms for grey matter and 1200 ms for white matter.

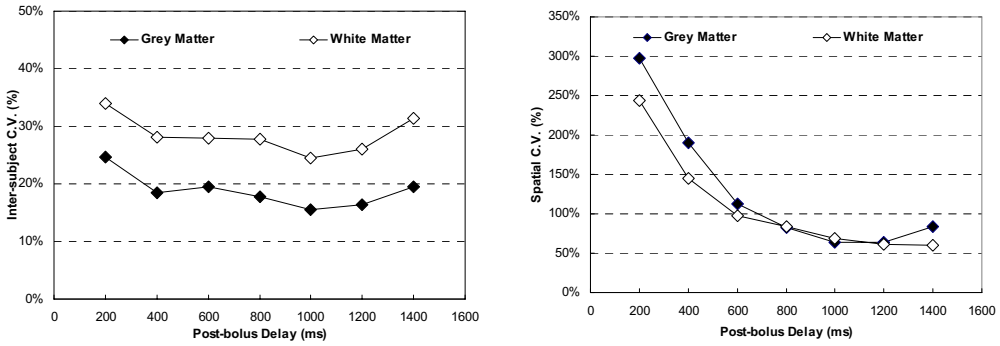

Figure 5-10 Inter-subject variability and spatial variability as a function of post-bolus delay for CBF measurements of cerebellum grey matter and white matter (C.V. for coefficient of variance)

The calculated CBF ratio between grey matter and white matter tends to decrease with increased post-bolus delay as showed in Figure 5-11. This is reasonable because at longer post-bolus delay time, more labeled blood will flow through grey matter tissue into white matter. However, the calculated CBF ratio in the cerebellum is lower than that in the superior part of the brain (The CBF ratio in superior cortex is usually much larger than 2). This may be due to

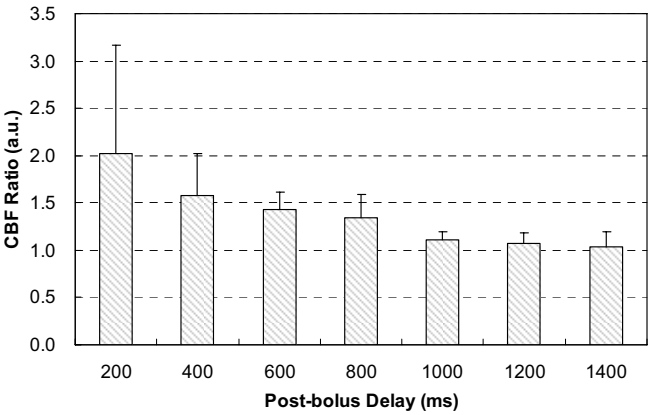

Figure 5-11 Cerebellum CBF ratio between grey matter and white matter as a function of post-bolus delay

the fact that compared to superior cortex, the partial volume effects in the cerebellum is much larger, the cerebellum has much thinner grey matter layer and more CSF around its smaller branches.

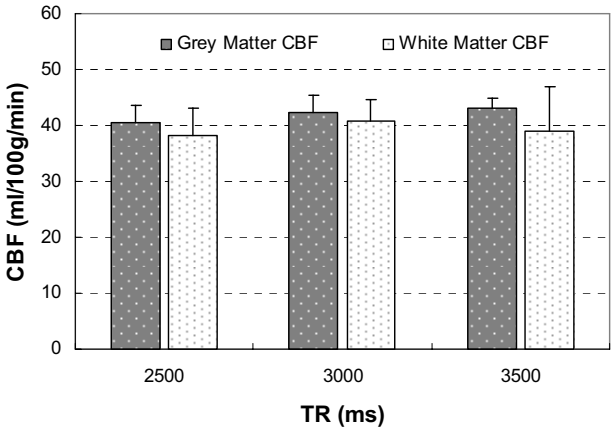

Figure 5-12 CBF measurements using difference TR values

Conclusions

For cerebellum perfusion studies on healthy adults, post-bolus delay equal to 1000 ms is proper for cerebellum grey matter while post-bolus delay equal to 1200 ms can be more proper for cerebellum white matter. For elder subjects, longer post-bolus delay had better be used for both grey matter and white matter. To compensate the signal decay due to longer post-bolus delay, more signal averaging is necessary. Due to larger partial volume effects, the CBF ratio between grey matter and white matter in cerebellum area is smaller than that in superior cortex.

5.1.3 TR Effects Evaluation and Estimation of Necessary Number of Inferior Saturation Pulses

Materials and Methods

In these two studies, the same imaging parameters were used as those in the previous study in addition to the parameters mentioned in the following. In the TR effects evaluation study, three TR values were used in a random order across subjects: 2.5 s, 3.0 s and 3.5 s. Temporal bolus width was equal to 800 ms, and post-bolus delay 1000 ms.

Totally 40 inferior saturation pulses with 25 ms interval were performed during the whole post-bolus delay. In the other study, TR equal to three seconds was used and the number of inferior saturation pulses ranged from 0 to 40 using 10 as an increment.

Results and Discussion

CBF measurements using different TR values are displayed in Figure 5-12. The group mean CBF for cerebellum grey and white matter are very comparable across TR values. Therefore, short TR can be used for cerebellum perfusion studies.

Based on the CBF measurements using different number of inferior saturation pulses as showed in Figure 5-13, the minimal number of inferior saturation pulses can be 20 or 30 to ensure complete suppression of labeled blood residuals. CBF measurements for cerebellum grey matter significantly decreased when inferior saturation pulses were applied. The p value is equal to 0.025 for one-tailed paired t test between the CBF measurements using 10 inferior saturation pulses and those without inferior saturation pulses. No significant differences were found between CBF measurements using 10 inferior saturation pulses and the other number of inferior saturation pulses. One typical subject's perfusion-weighted imaging maps using different

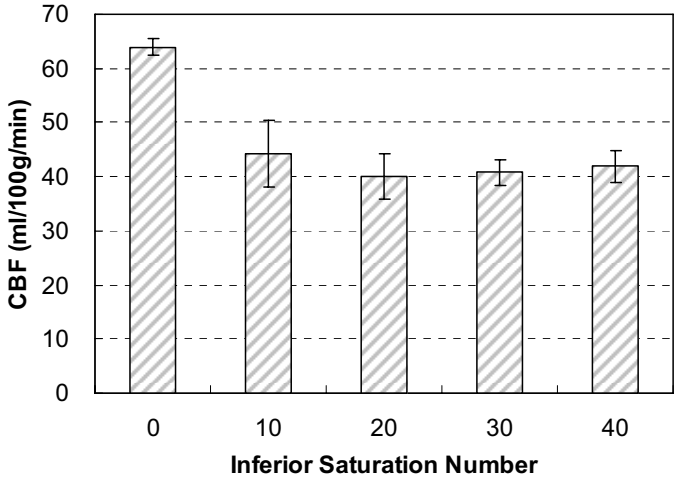

Figure 5-13 Cerebellum CBF changes with the number of inferior saturation pulses for grey matter

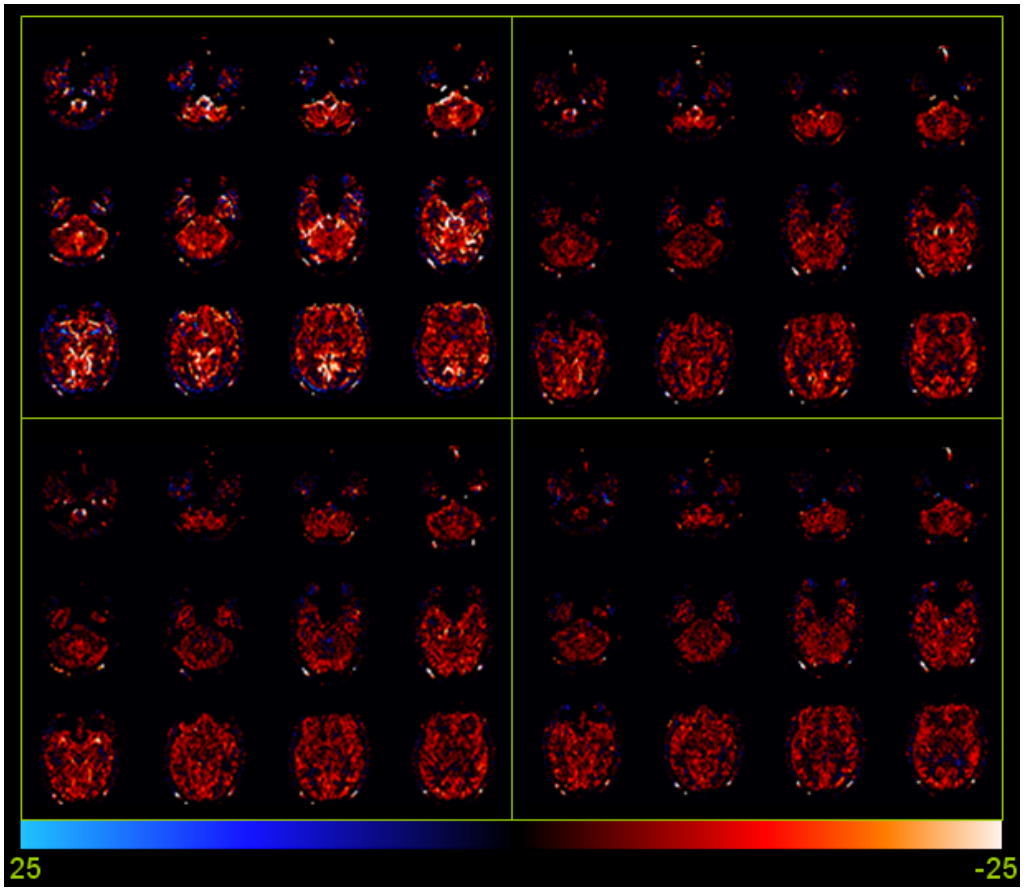

Figure 5-14 Perfusion-weighted imaging maps using fixed temporal bolus width (TI_1 = 800 ms) and different number of inferior saturation pulses: 0 (top left), 10 (top right), 20 (bottom left) and 30 (bottom right)

number of inferior saturation pulses are displayed in Figure 5-14. No spurious intravascular signals were observed when 20 or more inferior saturation pulses were used. to be safe, 20 inferior saturation pulses had better be used for healthy adults. For elder subjects, maybe 30 inferior saturation pulses should be used. In fact, no SAR issue was found in the TR effects study where the maximal number of inferior saturation pulses that fit the post-bolus delay was used. Therefore, it is safe to perform inferior saturation pulses during the whole post- bolus delay.

Conclusions

No TR effects were found in the TR effects evaluation studies using FAIR ASST with Q2TIPS. For healthy adults, 20 inferior saturation pulses are enough to ensure complete suppression of labeled blood residues.

5.1.4 Summary

These performed perfusion studies gave us initial rough ideas about the physiological characteristics of cerebellum perfusion and proper ASL parameters for the following quantitative cerebellum perfusion studies: temporal bolus width = 800 ms, post-bolus delay = 1000 ms, necessary inferior saturation pulse number = 20 or 30, and shorter TR (e.g. 2500 ms) can be used.

5.2 QUANTITATIVE CEREBELLUM PERFUSION STUDIES

Materials and Methods

Five healthy male adults (age range, 27-40 years) were recruited for this quantitative cerebellum perfusion study. The ASL imaging slices were positioned to have the first inferior slice cover the lower edge of cerebellum, oriented to be parallel to the longer dimensions of white matter (anterior to posterior direction) to minimize partial volume effect between grey matter and white matter.

The general MRI parameters for both FAIR ASST and PICORE were as follows: FOV = 180 x 180 mm^2, matrix size = 72 x 72, slice thickness/gap = 3.5/0.7 mm, the number of imaging slices = 16, imaging resolution = 2.5 x 2.5 x 3.5 (+0.7 mm slice gap) mm^3, TR/TE = 2500/12 ms, the number of measurements = 180, iPAT GRAPPA factor = 2 with 24 reference lines using CP mode, partial Fourier (PF) = 7/8, acquisition order = ascending (foot to head), temporal bolus width (TI_1) /post-bolus delay = 800/1000 ms, inferior saturation number = 20 with 25 ms interval using 20 mm saturation slab.

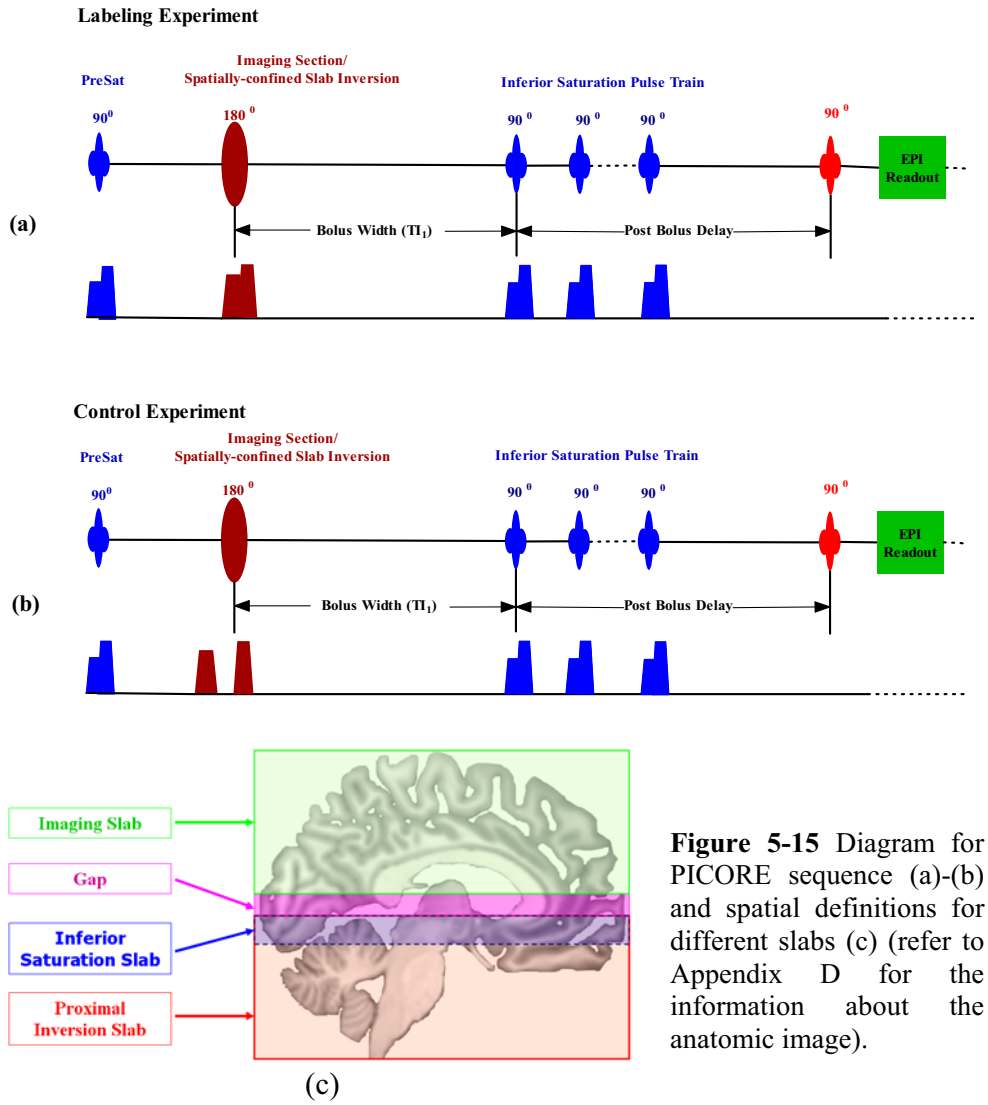

Figure 5-15 Diagram for PICORE sequence (a)-(b) and spatial definitions for different slabs (c) (refer to Appendix D for the information about the anatomic image).

For FAIR ASST, superior saturation slab size was equal to 100 mm, the imaging section inversion and spatially confined inversion slabs were defined as imaging slab size plus 20 mm and 200 mm respectively. The effective labeling size for FAIR ASST, in fact, is 90 mm by excluding 10 mm gap.

The pulse sequence diagram for PICORE is showed in Figure 5-15. In this implementation of PICORE, the same hyperbolic secant RF pulse as in FAIR sequence was used. The implemented PICORE technique is the same as those in literature (Wong, Buxton et al. 1997) in addition to one inserted eddy current compensation gradient in the control imaging that can help to minimize the gradient waveform difference between labeling and control experiments. For eddy current compensation purpose, playing the same gradient wave form as that in selective inversion imaging (control) at different time during non-selective inversion imaging (labeling) for FAIR has ever been used (Kwong, Chesler et al. 1995). The eddy current compensation gradient can be turned on or off via protocol user interface. To make sure both labeling and control experiments have the same preparation time before EPI readout, extra time equal to the duration of eddy current compensation gradient in control experiment was inserted before the 180-degree inversion pulse in labeling experiment. When this eddy current gradient is turned off, the extra time inserted in labeling experiment will be removed automatically.

For quantification purpose, Q2TIPS has been incorporated into PICORE. In the cerebellum perfusion study using PICORE, the same labeling size was used for the proximal inversion. To avoid the interference between imaging slab and the proximal inversion, a 15 mm gap was used, which was determined by evaluation tests using water phantom. The eddy current compensation was turned off in this study.

Please refer to the general descriptions about data processing and ROI-based CBF analysis. For each subject, overall cerebellum grey matter and white matter CBF estimations were obtained from the two PASL techniques. Group analysis was performed and mean CBF and standard error for cerebellum grey matter and white matter were

calculated. Inter-subject variability was evaluated for the two PASL methods by using coefficient of variance. The across-slice uniformity of CBF values was compared between the two PASL methods for grey matter and white matter using two methods.

In method one, for each subject the mean CBF and standard variance for each slice were calculated for each PASL method, and the across-slice CBF mean, across-slice standard variance and coefficient of variance were calculated. Group averaging was then performed to yield group mean, standard error and coefficient of variance for across-slice CBF values.

In method two, group mean and standard variance were first calculated for each slice from individual subject data. These slice-wise CBF values were then averaged across slices to obtain group CBF mean and standard variance across slices. The across-slice variability of group mean CBF values was estimated as the across-slice coefficient of variance, and across-subject variability of each slice mean CBF was calculated as across-subject coefficient of variance. Then an overall mean of across-subject coefficient of variance of all slices was calculated.

To evaluate the stability of CBF measurements using two PASL methods (FAIR ASST and PICORE), temporal coefficient of variance (tC.V.) of CBF measurements was calculated for grey matter and white matter of two selected imaging slices for each method. These two selected imaging slices are near the transverse sinuses. tC.V. is defined as the ratio between temporal standard variance over temporal mean of CBF measurements. Comparisons were performed between the two techniques using one-tailed paired t-test. The reduction of temporal variability of ASL signals by FAIR ASST was calculated as relative percentage change.

For all t tests performed in this study, p value less than 0.05 was used as the threshold of statistically significant difference.

Results

Figure 5-16 shows the co-registered high-resolution anatomic images, segmentation masks for cerebellum grey matter and white matter, and corresponding perfusion-weighted imaging maps using FAIR ASST and PICORE from a representative subject.

In Table 5-1, CBF estimations for overall cerebellum grey matter and white matter using two PASL methods are listed for each subject. Group mean and standard deviation, as well as the coefficient of variance across subjects, are also presented. No significant differences were found for the performed two-tailed paired t tests between the CBF measurements of cerebellum grey matter and white matter, and the CBF ratio for the two methods with the data from the five subjects. The overall mean CBF for cerebellum grey matter is about 43.8 ± 5.1 mL/100g/min, which is very close to what was obtained by using PICORE: 40.35 ± 8.5 mL/100g/min. For cerebellum white matter, the overall mean CBF from FAIR ASST is about 27.6 ± 4.5 mL/100g/min. PICORE gave a little lower CBF estimations for cerebellum white matter: 23.7 ± 7.5 mL/100g/min. For cerebellum tissue, the CBF ratios obtained using two PASL methods are similar and less than two. CBF analysis results using method one (across-slice analysis followed by group analysis) and method two (group analysis for each slice followed by across-slice analysis) are displayed in Figure 5-17 and Figure 5-18 respectively. The results of performed one-tailed paired t tests are also displayed in Figures 5-17 and 5-18 to compare two PASL methods.

In Figure 5-19, the analysis of temporal stability of cerebellum grey matter and white matter ASL signals for two image slices near or containing transverse sinuses obtained with two PASL techniques are presented along with p values from one-tailed paired t tests for comparing the two PASL methods.

Table 5-5 Overall cerebellum CBF measurements by using two PASL methods

Subject No.	FAIR ASST			PICORE		
	CBF_{GM}	CBF_{WM}	$\frac{CBF_{GM}}{CBF_{WM}}$	CBF_{GM}	CBF_{WM}	$\frac{CBF_{GM}}{CBF_{WM}}$
1	42.58	29.56	1.44	41.97	33.5	1.25
2	45.07	28.63	1.57	44.47	28.89	1.54
3	37.89	20.48	1.85	30.28	19.04	1.59
4	41.82	26.62	1.57	33.59	14.71	2.28
5	51.57	32.53	1.59	51.45	22.51	2.29
Mean ± STD	**43.78 ± 5.06**	**27.56 ± 4.49**	**1.60 ± 0.15**	**40.35 ± 8.52**	**23.73 ± 7.53**	**1.79 ± 0.47**
C.V. (%)	**11.6%**	**16.3%**	**9.4%**	**21.1%**	**31.7%**	**26.3%**

CBF_{GM}: grey matter CBF; CBF_{WM}: white matter CBF; C.V.: coefficient of variance. No significant differences were found between two sets of cerebellum CBF measurements using FAIR ASST 112 and PICORE. The unit of CBF is mL/100g/min.

Discussions

As indicated by perfusion-weighted imaging maps from one typical subject's data (Figure 5-16), perfusion weighted imaging maps from PICORE tend to have more negative values (especially for distal slices), implying more subtraction errors. It is also observed that for PICORE technique, the perfusion-weighted map intensities decrease from the inferior slices to the superior slices, while perfusion-weighted imaging maps from FAIR ASST are much more uniform across slices. This is maybe due to the different methods for the control of MT effects. These results imply that for multiple-slice perfusion studies, FAIR ASST is superior to PICORE. CBF estimates from the two PASL techniques are very close, especially for cerebellum grey matter. However, inter-

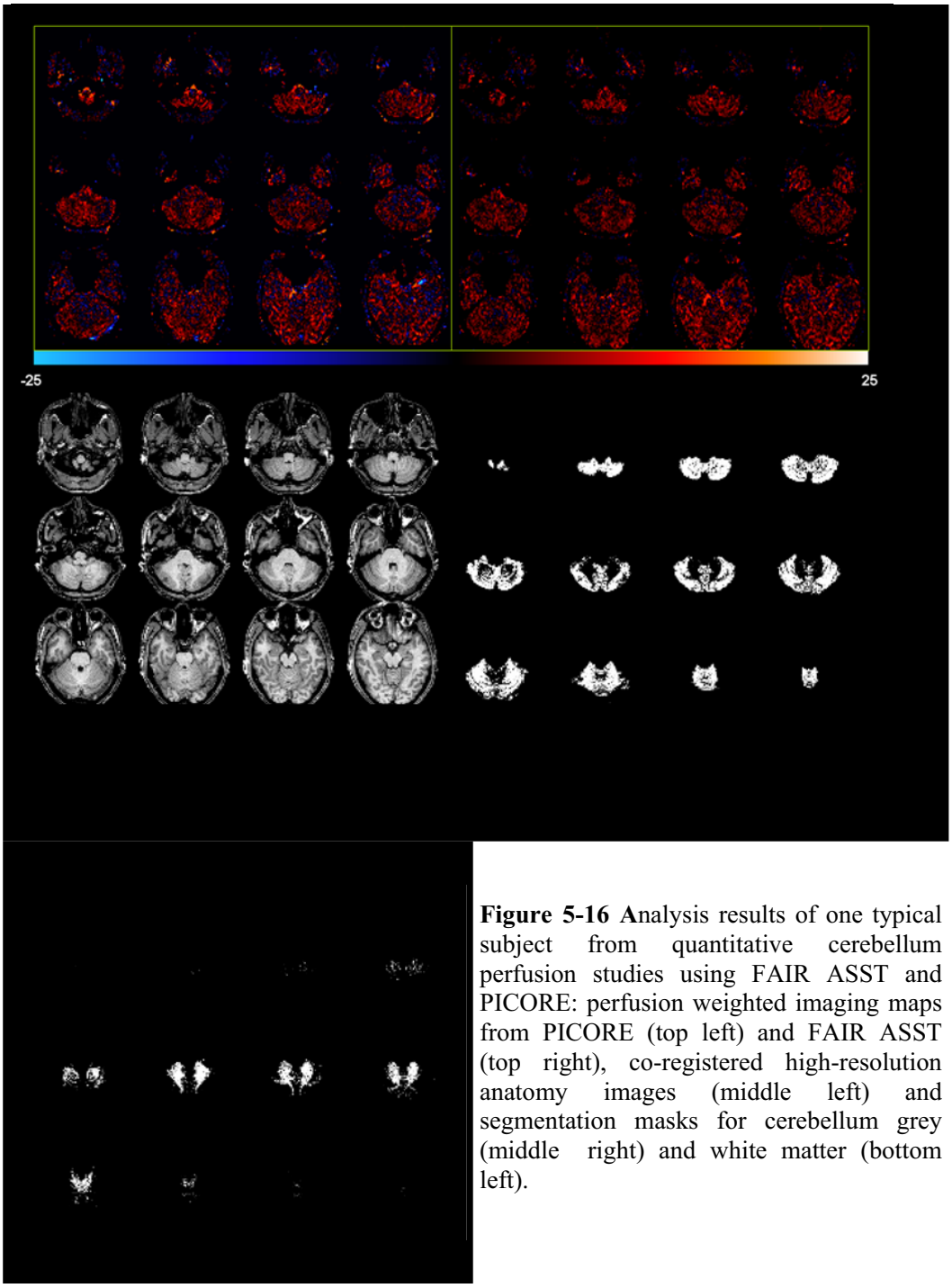

Figure 5-16 Analysis results of one typical subject from quantitative cerebellum perfusion studies using FAIR ASST and PICORE: perfusion weighted imaging maps from PICORE (top left) and FAIR ASST (top right), co-registered high-resolution anatomy images (middle left) and segmentation masks for cerebellum grey (middle right) and white matter (bottom left).

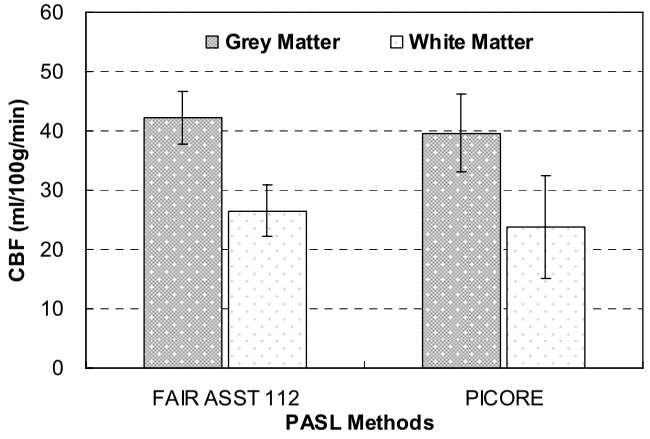

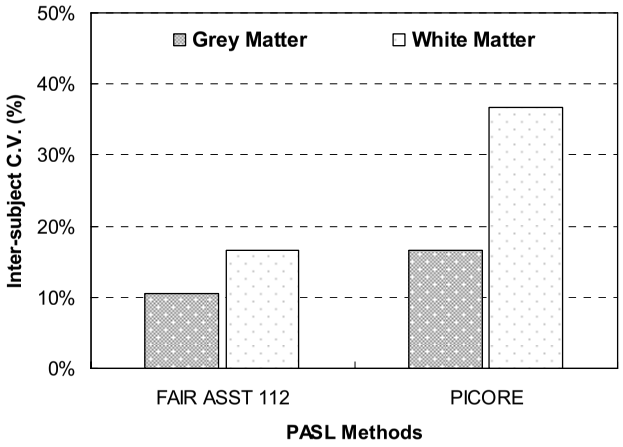

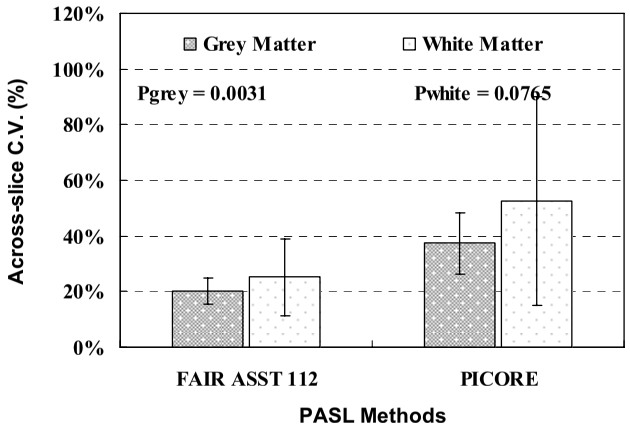

Figure 5-17 CBF analysis results using method one (across-slice analysis followed by group analysis): group mean CBF of across-slice mean CBF estimations (standard error bar here represents the across-subject variability) (top left), inter-subject variability evaluation using coefficient of variance of across-slice mean CBF estimations (top right) and group analysis results for across-slice coefficient of variance (error bar represents the variance across subjects, one-tailed paired t test results are also displayed for both grey matter and white matter (bottom left).

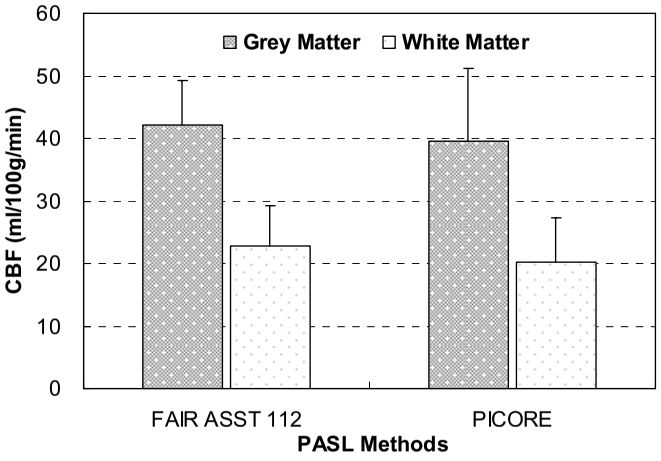

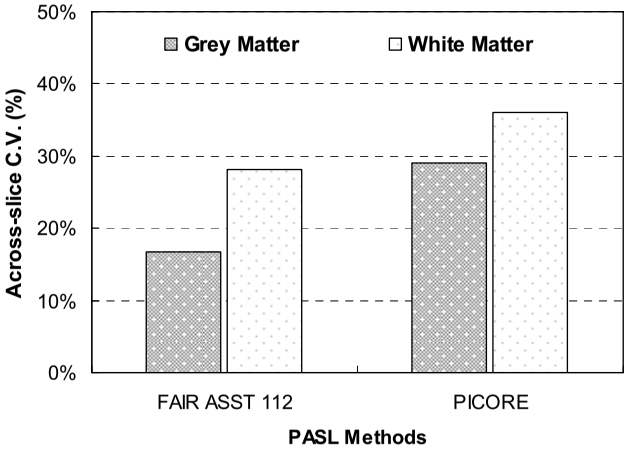

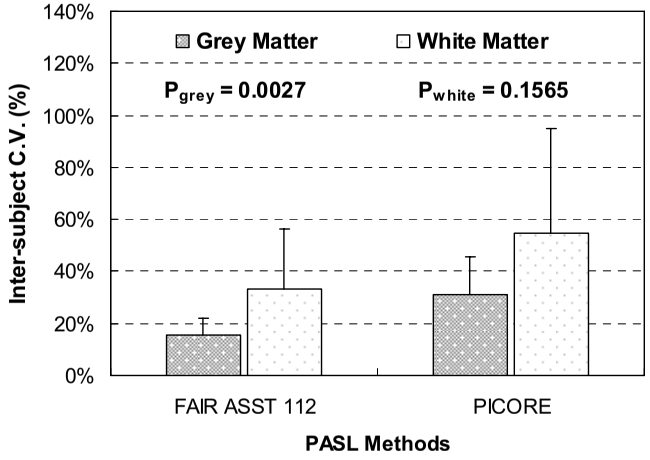

Figure 5-18 CBF analysis results using method two (group analysis for each slice followed by across-slice analysis): across-slice mean of group mean CBF estimations for each slice (error bar represents the variance across slices) (top left), across-slice variability evaluation using coefficient of variance for group mean CBF of each slice (top right) and across-slice mean of coefficient of variances of all slices' inter-subject variability analysis results (error bar represents the variance across slice; one-tailed paired t tests results between the two PASL methods are displayed for both grey matter and white matter) (bottom left)

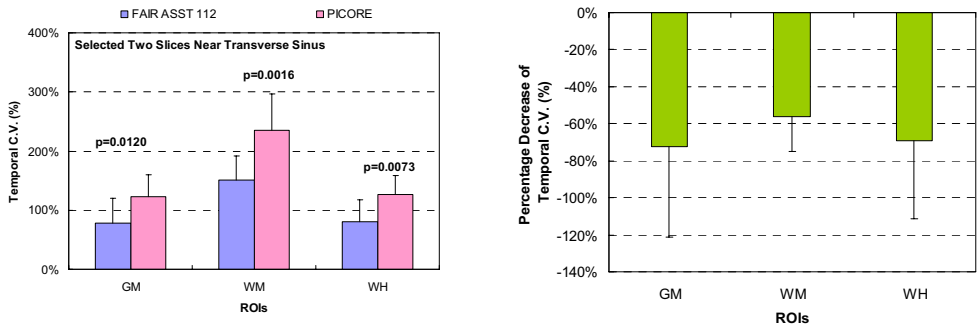

Figure 5-19 Comparison of the temporal stability of ASL signals using FAIR ASST and PICORE: temporal coefficient of variance (left) and calculated reduction of temporal variability (right) by FAIR ASST relative to PICORE for cerebellum grey matter, white matter and overall cerebellum tissue of two selected slices near transverse sinuses. P values from one-tailed paired t tests are also presented. GM represents grey matter, WM represents white matter and WH represents overall cerebellum tissue.

subject variability evaluated by coefficient of variance (C.V.) is consistently lower for CBF measurements using FAIR ASST.

Across-slice CBF analysis results using the first method (Figure 5-17, top right) also indicate that FAIR ASST has less inter-subject variability of CBF measurements than PICORE. Significant differences were found for the group analysis for across-slice variability of slice mean CBF between FAIR ASST and PICORE for both cerebellum grey matter and white matter (Figure 5-17, bottom left). This result is consistent with what was observed from perfusion-weighted imaging maps (Figure 5-16). For the second method (Figure 5-18, top right), across-slice variability of CBF measurements using FAIR ASST is also lower than that using PICORE, which is consistent with the across-slice analysis results using the first analysis method, where slices were averaged across subjects first. For cerebellum grey matter, significantly less inter-subject variability was produced by FAIR ASST than by PICORE. The temporal stability analysis results imply

that the inflow of superior venous blood can also adversely affect the robustness of the ASL technique. Because the superior inflow of venous blood is suppressed at the outset in FAIR ASST, confounding venous inflow effects are minimized, resulting in artifact-free perfusion images and more stable ASL signals. However, in PICORE, effects of superior inflow of venous blood are greater, generating more label-control subtraction errors and temporal variance and instability of perfusion values.

Conclusions

The quantitative cerebellum perfusion studies using FAIR ASST 112 and PICORE showed that FAIR ASST can give more stable CBF measurements with decreased temporal variability, more reliable CBF estimations with less subtraction errors, and more sensitivity to CBF changes with lowered inter-subject variability.

5.3 SUMMARY

Based on ASL optimization study results, proper temporal bolus width and post-bolus delay for cerebellum perfusion studies can be 800 ms and 1000 ms respectively. Shorter TR can be used without TR effects on CBF estimations. Although performing inferior saturation pulses during the completely post-bolus delay is safe, to reduce RF radiation, the estimated necessary minimal number of inferior saturation pulses, twenty, can be used. The estimations for cerebellum perfusion from FAIR ASST method and PICORE are comparable. However, FAIR ASST can give more stable and reliable CBF measurements with lower inter-subject variability.

CHAPTER 6 OPTIMAL FAIR and Cerebellum Perfusion Studies

OPTIMAL FAIR (Orthogonally Positioned Tagging Imaging Method for Arterial Labeling of FAIR) is a new PASL method developed upon FAIR technique, in which the imaging slices are perpendicular to the labeling slab. In this chapter, after the technical descriptions about OPTIMAL FAIR, the initial applications of this technique for cerebellum perfusion studies will be reported.

6.1 OPTIMAL FAIR SEQUENCE

As demonstrated before, the superior labeling of traditional FAIR will generate adverse venous artifacts in cerebellum perfusion studies, making CBF estimations for the cerebellum unreliable. To avoid this problem, coronal imaging slices can be used for cerebellum perfusion studies because the relatively larger FOV can help push the superior labeling slab outside the brain, resulting in no effective superior labeling. Furthermore, transit time within coronal slices can be more uniform for quantitative cerebellum perfusion study, which has

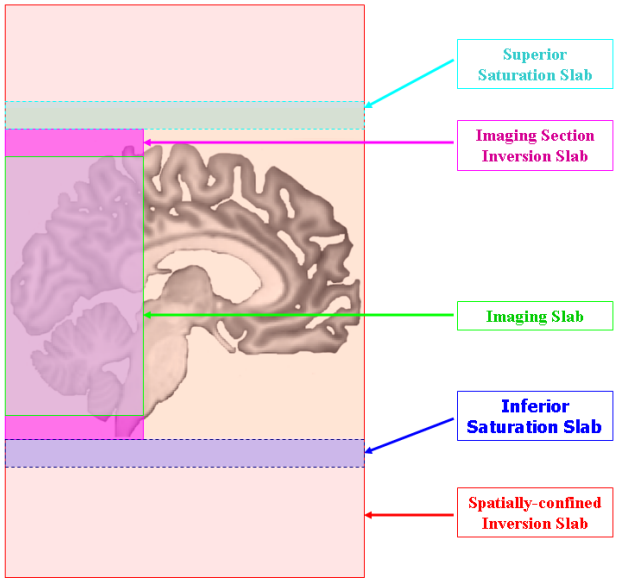

Figure 6-1 Spatial definitions for different slabs of MDS OPTIMAL FAIR sequence (refer to Appendix D for the information about the anatomic image).

been mentioned in Chapter one and indicated by the study results from multiple inversion cerebellum perfusion experiments using FAIR ASST. In principle, imaging acquisition along the major blood flow direction for the interested tissue and more uniform transit time within imaging slices should give more consistent or reliable CBF estimations. In addition, by orienting imaging slices specifically according to the specific anatomic characteristics of the interested brain region, partial volume effects can be also minimized.

OPTIMAL FAIR is a new PASL sequence based on FAIR technique to address the above mentioned issues. In this new sequence, labeling slab is kept as usual along horizontal direction (axial slab) while the imaging slab is rotated 90 degrees to be perpendicular to the labeling slab. This technique is called OPTIMAL FAIR to represent "orthogonally positioned tagging imaging method for arterial labeling of FAIR". When subject's head is very large and larger than the used coronal imaging slice FOV, some venous blood can also be labeled with generated artifacts. Since the effective superior labeling size is small under such a situation, MDS FAIR method will be good enough to suppress these venous bolus. Therefore, in the real implementation, MDS FAIR II was used as the basic sequence for this modification, and the implemented technique can be called OPTIMAL MDS FAIR II. However, for most subjects, even when very small field of view (128 x 128 mm^2) is used, the superior labeling slab will be pushed outside the brain, resulting in no effective superior labeling. Therefore, the superior saturation pulse train of OPTIMAL MDS FAIR can be turned off for most cases. To be simple, this implemented technique will be called OPTIMAL FAIR in the following and the superior saturation pulse train will be off when no specific declaration is made. The spatial definitions of different slabs for this new technique are illustrated in Figure 6-1. As

showed in Figure 6-1, to remove the transition effects of the imaging section inversion RF pulse, the imaging section inversion slab is a little larger (10 mm gap added on each side of imaging slab) than the field of view.

6.2 ASL OPTIMIZATION STUDIES USING OPTIMAL FAIR

Before performing quantitative cerebellum perfusion studies using OPTIMAL FAIR, similar methods as those described in the previous chapter were used to have rough ideas about bolus duration, transit time and so on. These study results are presented in Appendix C for further reference.

The study results from these experiments indicated that 800 ms bolus is still good for temporal bolus width in quantitative cerebellum perfusion studies using OPTIMAL FAIR. Twenty inferior saturation pulses are enough to suppress the residual of labeled blood. Although no multiple post-bolus delay experiments were performed, since the acquisition of OPTIMAL FAIR will follow the major blood supply direction of the cerebellum, late arrived labeled blood at the posterior part of the cerebellum will have more time to travel down vascular tree into small arterioles or capillary bed. Therefore, for quantitative cerebellum perfusion studies, 1000 ms post bolus delay should be also proper, which can be supported by the study results from multiple inversion experiments and also verified later by the performed quantitative cerebellum perfusion in which no spurious intravascular artifacts were observed for obtained perfusion-weighted imaging maps.

Because of the orthogonal position between the imaging slices and labeling slab, in the perfusion studies of whole cerebellum, the acquisition of anterior part of the cerebellum using coronal slices can saturate the arterial blood in vertebral or basilar

arteries. Due to the lower blood velocity and many turbulent flows in these arteries, the saturated blood cannot be cleared quickly from these arteries before the next labeling, and labeling efficiency will be much lowered.

There are two ways to avoid this problem. One way is to avoid the saturation of major blood supply arteries, which can be achieved by performing cerebellum perfusion study with partial coverage as illustrated in Figure 6-2. As the results from the evaluation study indicated (Figure C-6), under such a situation, no obvious TR effects was observed, meaning labeling efficiency will not be affected. The shortcoming of the method is that the anterior tips of the cerebellum are excluded from perfusion study. The other way is to use longer TR values to allow the saturated blood completely cleared from the proximal arteries. If complete coverage of the cerebellum has to be achieved and shorter TR value has to be used, a new labeling efficiency had better be estimated for this situation to compensate the adverse effects from the interference, and due to the lower SNR from lowered labeling efficiency, larger number of measurements had better be used.

6.3 QUANTITATIVE CEREBELLUM PERFUSION STUDIES

Five healthy male adults (age range, 35~37 years) were recruited for the two-session quantitative cerebellum perfusion studies. Totally four experiments were performed during these two sessions: (1) quantitative cerebellum perfusion study with partial coverage (the middle and posterior parts of the cerebellum) in both sessions, (2) quantitative cerebellum perfusion study using single slice and varied isotropic resolution in session one, (3) quantitative cerebellum perfusion study using multiple slices with fixed slice thickness and varied in-plane resolution in session two and (4) whole cerebellum perfusion study in session one.

Materials and Methods

MRI parameters for experiment one are as the following: TR/TE = 2500/14 ms, FOV = 128 x 128 mm^2, matrix size = 64 x 64, slice thickness/slice gap = 5/1 mm, the number of imaging slices = 8, imaging resolution = 2 x 2 x 5 (+1 mm gap) mm^3; phase encoding direction = left to right with 20% phase over sampling, partial Fourier (PF) = 6/8, iPAT GRAPPA factor = 2 with 24 reference lines, slice acquisition order along anterior to posterior direction, imaging section inversion slab size = FOV + 20 mm, spatially-confined inversion slab size = FOV + 200 mm, the number of measurements = 100, TI_1/post-bolus delay = 800/1000 ms, 20 inferior saturation pulses with 25 mm slab size and 25 ms interval. The superior saturation pulse train was turned off since the used FOV is large enough to cover all subjects' heads. Two M_0 images were acquired for each delay time for quantitative CBF estimation. The slice position used for this two-session quantitative cerebellum perfusion study is illustrated in Figure 6-2. Although eight slices were used but only seven imaging slices mainly contain cerebellum tissue.

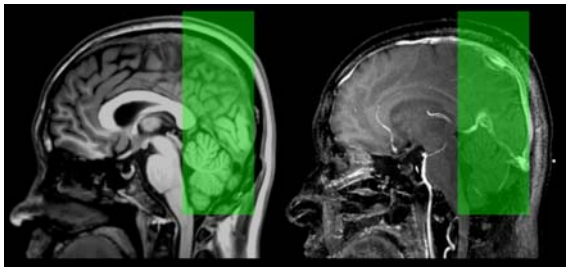

Figure 6-2 Slice position for experiment one (please refer to appendix D for the information about anatomy image and angiography image)

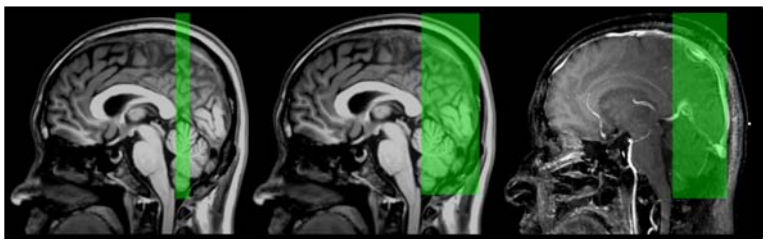

Figure 6-3 Slice(s) positions for experiment two (left) and experiment three (middle and right) (please refer to appendix D for the information about anatomy image and angiography image)

In experiment two, five different isotropic resolutions were used: 2.5 x 2.5 x 2.5 mm^3, 3.0 x 3.0 x 3.0 mm^3, 3.5 x 3.5 x 3.5 mm^3, 5.0 x 5.0 x 5.0 mm^3, and 7.0 x 7.0 x 7.0 mm^3. To achieve these resolutions, the following fields of view (FOVs) were used with fixed matrix size 64 x 64: 160 x 160 mm^2, 192 x 192 mm^2, 224 x 224 mm^2, 320 x 320 mm^2, and 448 x 448 mm^2. To ensure enough SNR for ASL signals, the number of measurements varied for different resolutions: 230, 134, 84, 30, and 10. Other MRI parameters were kept the same for different resolutions: TR/TR = 2500/14 ms, partial Fourier (PF) = 7/8, iPAT GRAPPA factor = 2 with 24 reference lines, phase encoding direction = left to right, the number of imaging slices = one, imaging section inversion slab size = FOV + 20 mm, spatially-confined inversion slab size = FOV + 200 mm, temporal bolus width (TI_1) /post-bolus delay = 800/1000 ms, 20 inferior saturation pulses with 25 mm slab size and 25 ms interval. Superior saturation pulse train was turned off too in this study. Although the slice thickness was varied for different isotropic resolutions, the slice center was kept the same for all different resolutions as indicated in Figure 6-3.

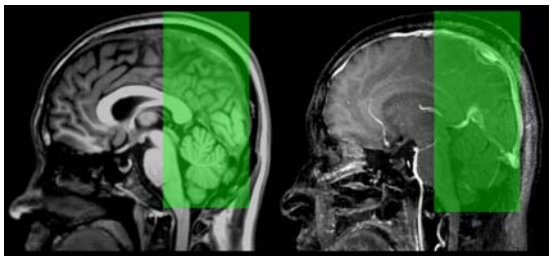

Figure 6-4 Slice position for whole cerebellum perfusion study (please refer to appendix D for the information about anatomy image and angiography image)

In experiment three, twelve imaging slices were used with fixed imaging slice thickness equal to 3.0 mm and 20% slice gap. Five different in-plane resolutions were used: 2.5 x 2.5 mm^2, 3.0 x 3.0 mm^2, 3.5 x 3.5 mm^2, 5.0 x 5.0 mm^2, and 7.0 x 7.0 mm^2. To achieve these resolutions, the same series of fields of view (FOVs) as before were used

with fixed matrix size 64 x 64: 160 x 160 mm^2, 192 x 192 mm^2, 224 x 224 mm^2, 320 x 320 mm^2, and 448 x 448 mm^2. To ensure enough SNR for ASL signals, the number of measurements varied for different resolutions: 230, 160, 120, 60, and 30. All other parameters were kept the same as those used in experiment two. The slice position used in this study is displayed in Figure 6-3.

MRI parameters used for experiment four are exactly the same as those used in experiment one except that the imaging slice position was different (Figure 6-4) and 12 imaging slices were used. Only 10 imaging slices mainly contain cerebellum tissue.

To improve the co-registration between high-resolution anatomy and ASL series, GRE images were acquired for each ASL series with matched slice orientation and center position of imaging slices. The MRI parameters used for GRE images that matched each ASL series are described in the appendix C. For all other aspects of these studies, data processing and ROI-based analysis please refer to Chapter 2.

Results and Discussion

Study results from experiment one are displayed in Figures 6-5 and 6-6. The cerebellum CBF estimations from this two-session perfusion study are also listed in Table 6-1 for the five subjects. The estimated CBF for cerebellum grey matter is 33.3 ± 3.1 (mL/100g/min) for the first session and 34.6 ± 2.4 (mL/100g/min) for the second session. For cerebellum white matter, CBF measurements for the first and second sessions are 21.8 ± 3.3 (mL/100g/min) and 21.2 ± 1.8 (mL/100g/min) respectively. CBF ratios are much less than 2, which is consistent to what I obtained in cerebellum perfusion studies using FAIR ASST. Cerebellum grey matter CBF estimations have better reproducibility than white matter CBF estimations, but the inter-subject variability of the evaluated

reproducibility for cerebellum grey matter is larger than that for white matter. The inter-subject variability of cerebellum grey matter CBF measurements is smaller than that of cerebellum white matter CBF measurements.

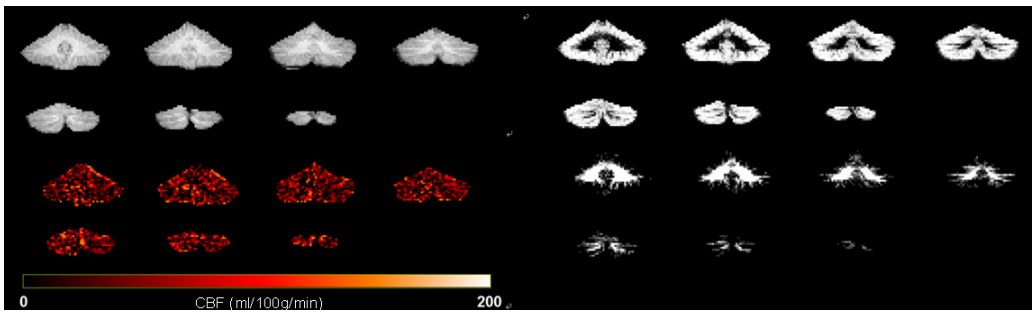

Figure 6-5 Co-registered high-resolution cerebellum anatomy images (left top), CBF maps (left bottom), segmented cerebellum grey matter masks (right top) and segmented cerebellum white matter masks (right bottom) from one typical subject of two-session quantitative cerebellum perfusion study

The study results from experiment two and three are showed in Figures 6-7 to 6-10. These study results indicated that higher resolution tends to give higher CBF estimations for both cerebellum grey matter and white matter. In principle, when higher resolution images are used, the mixture between grey matter and white matter will be reduced with increased CBF estimations for grey matter and decreased CBF estimations for white matter. The obtained results here showed that both grey matter and white matter CBF estimations were increased due to the increase of imaging resolution. This is maybe due to that the fact that for cerebellum tissue, at the surface, the separation of cerebellum grey and white matter is very difficult since the layer of grey matter is very thin (even less than 0.5 mm) and the large amount of CSF can be the major contributions for the partial volume effects. In addition, the obtained CBF estimations for cerebellum white matter using single slice and isotropic resolutions are consistently higher than those using multi-

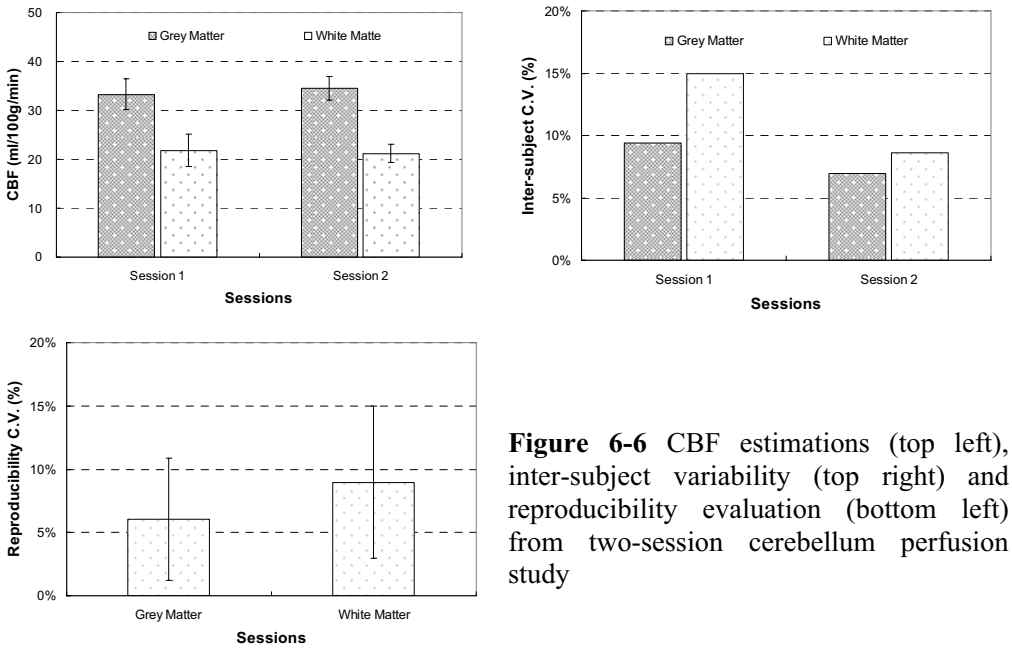

Figure 6-6 CBF estimations (top left), inter-subject variability (top right) and reproducibility evaluation (bottom left) from two-session cerebellum perfusion study

slice with fixed slice thickness and five different in-plane resolutions. This is may be because the position of the used single slice had been placed intentionally to void ventricle CSF for relatively pure cerebellum white matter tissue. The CBF estimations for cerebellum grey matter from both resolution dependency studies are very comparable. Due to the nice cooperation of these volunteers, the motions from these subjects are all very small: around 0.2 mm translation along any of the three axis and 0.2 degree of rotation around any of the three axis.

Although the resolution dependency study results indicated that higher imaging resolution gave us higher CBF estimations for both grey and white matter, the higher imaging resolution, especially the thinner imaging slices, the more sensitive to subject motion. Therefore, for future applications, intermediate imaging resolution had better be

Table 6-6 CBF estimations and reproducibility of CBF measurements from two-session quantitative cerebellum perfusion studies

Subject No.	CBF Measurements (ml/100g/min)						Reproducibility C.V. (%)	
	Session I			Session II				
	CBF_{GM}	CBF_{WM}	$\frac{CBF_{GM}}{CBF_{WM}}$	CBF_{GM}	CBF_{WM}	$\frac{CBF_{GM}}{CBF_{WM}}$	GM	WM
1	29.6	21.4	1.38	35.5	24.2	1.47	12.8%	8.5%
2	35.4	25.9	1.37	34.1	20.0	1.70	2.6%	18.1%
3	31.6	18.3	1.73	36.0	20.5	1.75	9.2%	8.3%
4	32.5	19.3	1.69	30.6	19.6	1.56	4.1%	1.1%
5	37.5	24.4	1.53	36.7	21.6	1.70	1.4%	8.8%
Mean ± STD	**33.3 ± 3.1**	**21.8 ± 3.3**	**1.54 ± 0.17**	**34.6 ± 2.4**	**21.2 ± 1.8**	**1.64 ± 0.12**	**6.0% ±4.8%**	**9.0% ± 6.0%**
Inter-subject Variability C.V. (%)	**9.4%**	**14.9%**	**10.9%**	**7.0%**	**8.6%**	**7.2%**	**79.7%**	**67.1%**

GM represents grey matter, and WM represents white matter. C.V. is the coefficient of variance calculated for CBF measurements across two sessions.

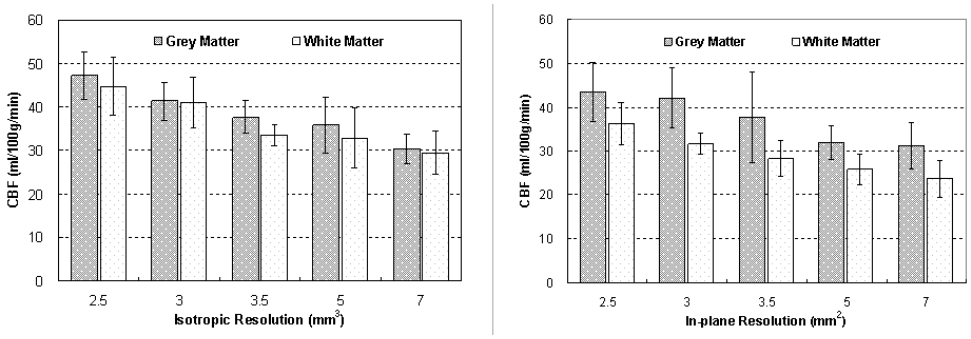

Figure 6-7 Cerebellum CBF measurements using single imaging slice with different isotropic resolution (left) and multiple imaging slice with different in-plane resolutions and fixed slice thickness (right)

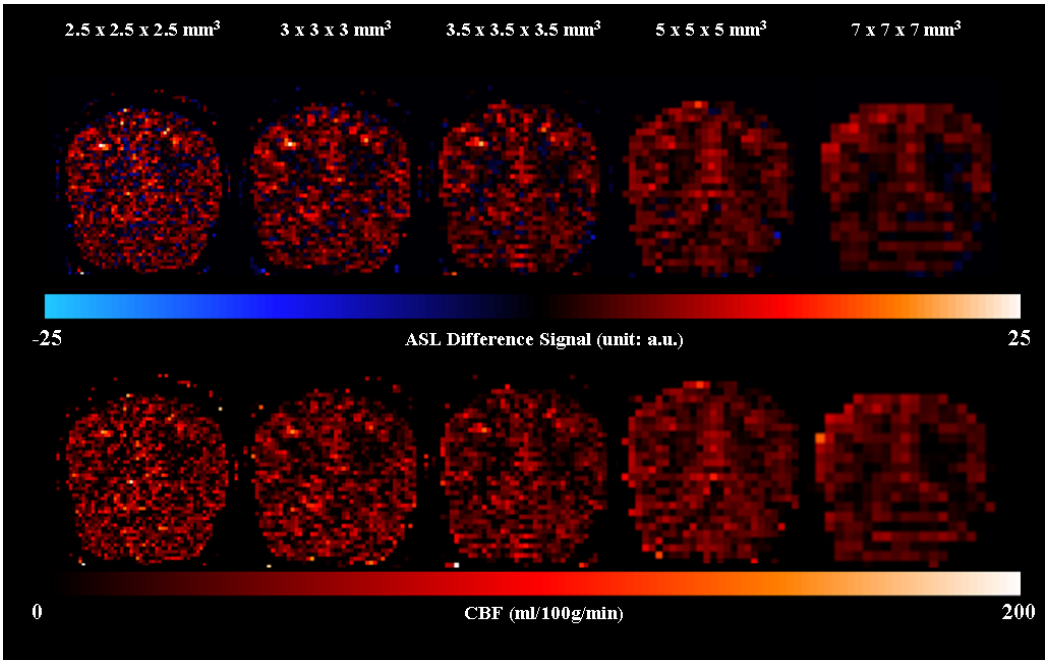

Figure 6-8 One typical subject's perfusion-weighted images (top) and corresponding CBF maps (bottom with the unit mL/100g/min) from cerebellum perfusion study using single slice and five different isotropic resolutions (from left to right: 2.5 x 2.5 x 2.5 mm^3, 3 x 3 x 3 mm^3, 3.5 x 3.5 x 3.5 mm^3, 5 x 5 x 5 mm^3 and 7 x 7 x 7 mm^3)

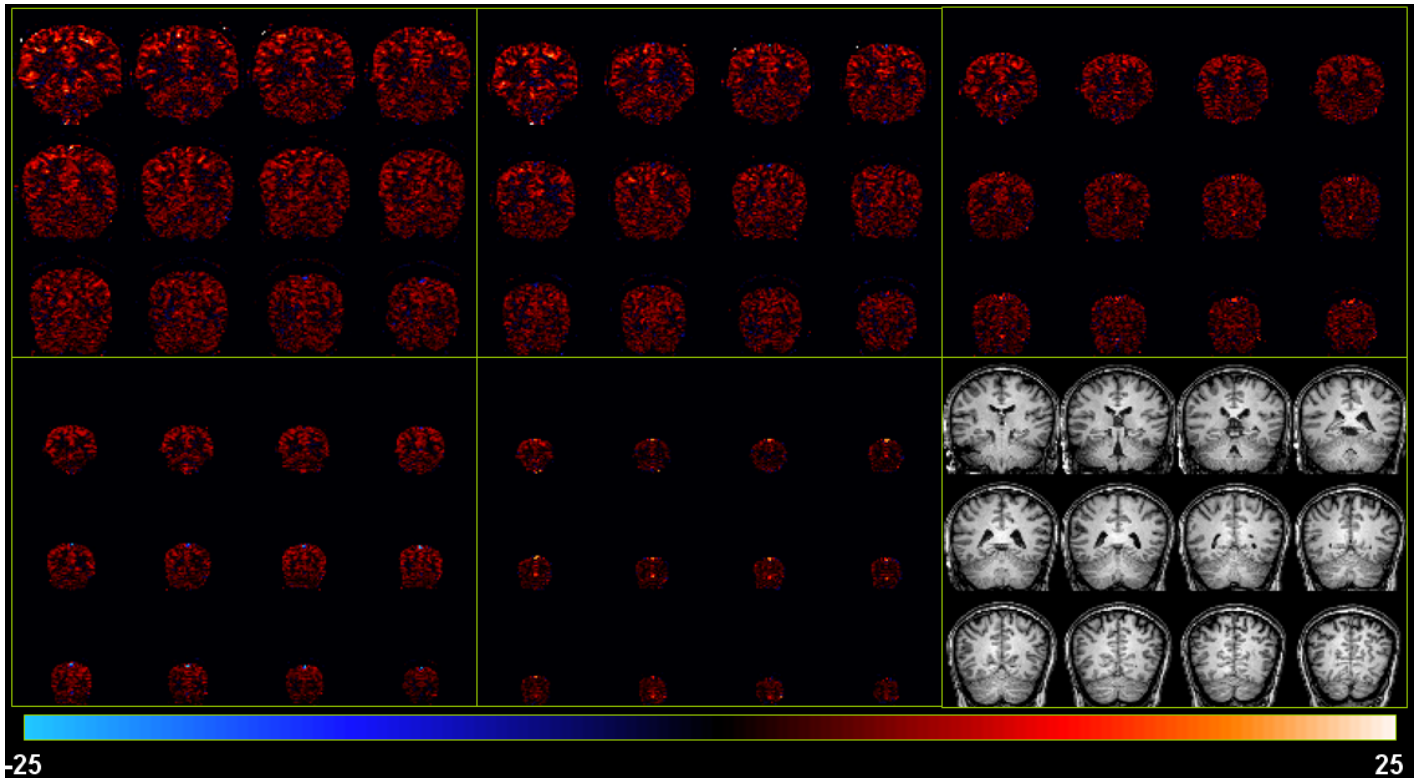

Figure 6-9 One representative subject's perfusion-weighted images from experiment three using multiple slices with fixed slice thickness and five different in-plane resolutions, and co-registered high-resolution anatomy images for the cerebellum perfusion scan using the highest imaging resolution

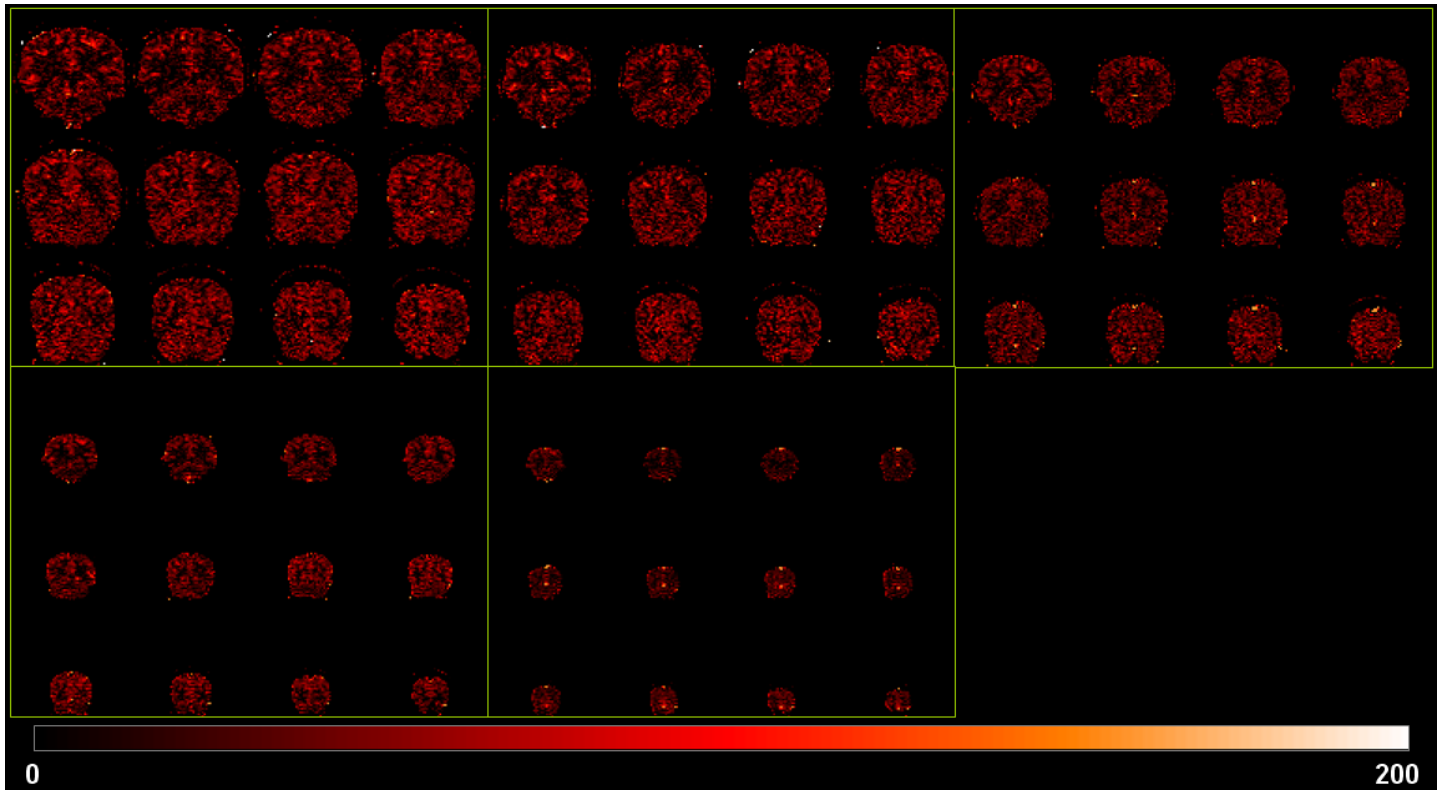

Figure 6-10 One representative subject's CBF maps (with unit mL/100g/min) from experiment three using multiple slices with fixed slice thickness and five different in-plane resolutions

.used. The estimated cerebellum perfusion level of the cerebellum is obvious lower than that of superior cortex. As I mentioned earlier, this may be due to the larger partial volume effects in the cerebellum area.

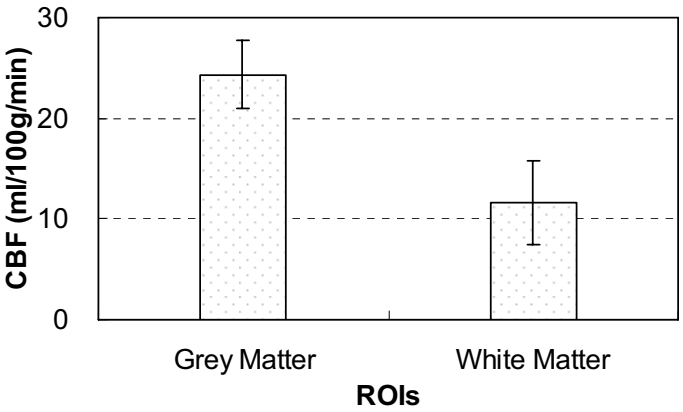

Figure 6-11 Cerebellum CBF estimations from cerebellum perfusion study with whole coverage

The study results from experiment four are showed in Figure 6-11. The group mean CBF estimations for cerebellum grey matter and white matter are all lower than those obtained in experiments one. Performed two-tailed paired t tests for both cerebellum grey matter and white matter CBF estimations between experiment one and experiment four showed significant differences. P values from two-tailed paired t tests for cerebellum grey matter and white matter CBF estimations between session one of experiment one and experiment four are 0.0142 and 0.0141. P values of two-tailed paired t tests for cerebellum grey matter and white matter CBF estimations between session two of experiment one and experiment four are 0.00357 and 0.00461 respectively. These study results implied that the acquisition of slices that cover the anterior part of the cerebellum has saturation effects on arterial blood in major blood supply arteries, making the labeling efficiency decreased greatly. The deceased labeling efficiency lowered the measured ASL signals. When the CBF reconstruction was performed using the default

labeling efficiency (0.95), the estimated CBFs for both cerebellum grey and white matters should be artificially lower. To avoid this problem, a much longer TR had better be used to allow saturated arterial blood cleared from the labeling site before the next labeling action. To correct the error for cerebellum CBF estimations, new labeling efficiency value should be used. By assuming cerebellum grey matter perfusion is uniform and comparing the cerebellum grey matter CBF estimations from experiment one of session one and experiment four, the labeling efficiency for cerebellum perfusion using OPTIMAL FAIR with whole cerebellum coverage is about 0.7 instead of 0.95.

The partial volume effects can be reduced by positioning the slice perpendicular to the horizontal 'axis' of the cerebellum, along which the shape changes of cerebellum tissue are relatively slow. By using high in-plane resolution, the mixture between cerebellum grey and white matter can be reduced.

The cerebellum CBF measurements by OPTIMAL FAIR are significantly lower than the CBF measurements using FAIR ASST (p value = 0.00614 for two-tailed unpaired t test). This can be due to the fact that using the same post-bolus delay (1000 ms), compared to perfusion studies using OPTIMAL FAIR, more labeled blood can still stay in bigger arteries in the posterior part of the cerebellum at the imaging slice acquisition time for cerebellum perfusion studies using FAIR ASST.

Conclusions

The two-session quantitative cerebellum perfusion study using OPTIMAL FAIR indicated that compared to cerebellum white matter, cerebellum grey matter has both higher reproducibility and lower inter-subject variability. Higher imaging resolution can

give higher CBF estimations for the cerebellum, but the estimated overall perfusion level of the cerebellum is relatively lower than the perfusion level of superior cortex, which may be due to the larger extend of partial volume effects in cerebellum area. Due to the interference between the imaging and labeling of OPTIMAL FAIR, labeling efficiency is lower in quantitative cerebellum perfusion studies using OPTIMAL FAIR with whole cerebellum coverage. This interference can be avoided or new calibrated labeling efficiency values can be obtained for whole cerebellum perfusion studies.

6.4 SUMMARY

OPTIMAL FAIR technique can effectively avoid venous artifacts and associated contaminations from the superior labeling of FAIR technique. Because imaging slices were particularly oriented to be perpendicular to the immediate blood supply arterial direction for the cerebellum, the homogeneity of transit time within coronal imaging slices was improved. Therefore, in principle, more reliable CBF can be obtained with the coronal images of OPTIMAL FAIR than with the axial images of traditional FAIR.

CHAPTER 7 Hippocampus Perfusion Studies Using OPTIMAL FAIR

As another application of OPTIMAL FAIR technique, hippocampus perfusion studies were performed using this technique. As what has been done for quantitative cerebellum perfusion studies, before the quantitative hippocampus perfusion studies, ASL optimization studies were conducted to obtain initial ideas about some specific physiological aspects of hippocampus perfusion.

7.1 ASL OPTIMIZATIONS FOR HIPPOCAMPUS PERFUSION STUDY

To have initial idea about some important physiological aspects associated with hippocampus perfusion, similar optimization studies as performed for the cerebellum were conducted: (1) multiple inversion experiment, (2) multiple post-bolus delay experiment and (3) the evaluation of TR effects and the estimation of the necessary minimal number of the inferior saturation pulses. Totally four healthy adults (age range, 26-39 years) have taken part in the three-session optimization studies. To minimize the study time for each session, thicker imaging slices were used.

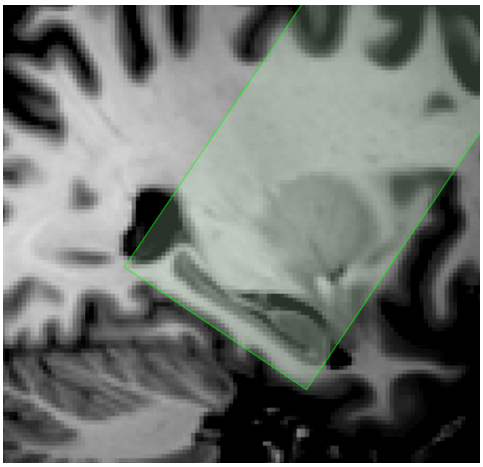

Figure 7-1 Imaging slab position for hippocampus perfusion studies using OPTIMAL FAIR (refer to Appendix D for the information about the anatomic image)

7.1.1 Multiple Inversion Experiment

Materials and Methods

MRI Parameters

In this study, the following ASL parameters were used: TR/TE = 4000/14 ms, FOV = 128 x 128 mm^2, matrix size = 64 x 64; slice thickness/slice gap = 8/1.6 mm, the number of imaging slices = 6, imaging resolution = 2.0 x 2.0 x 8.0 (+1.6 mm slice gap) mm^3, left to right phase encoding direction with 20% phase over sampling, partial Fourier (PF) = 6/8, imaging section inversion slab = FOV + 20 mm, spatially-confined inversion slab = FOV + 200 mm, the number of measurements = 110, iPAT GRAPPA factor = 2 with 24 reference lines, imaging acquisition order following anterior to posterior parts of the brain. Inferior saturation pulse train was turned off to utilize the whole bolus. The following multiple inversion times were used in this study and randomized for each subject: 300 ms, 600 ms, 900 ms, 1200 ms, 1500 ms, 1800 ms, 2100 ms, 2400 ms and 2700 ms.

Oblique coronal slices were used with the first slice beginning at hippocampus head (Figure 7-1). The use of coronal imaging slices can not only minimize the partial volume effects and follow the major blood flow direction for the hippocampus (body and tail), but also help avoid the interference between the arterial labeling and the slice imaging of OPTIMAL FAIR.

Oblique coronal imaging slices using GRE were acquired using the following parameters: TR/TE = 50/3.7 ms, FOV = 128 x 128 mm^3, matrix size = 192 x 192, the number of imaging slices = 6, slice thickness/slice gap = 8.0/1.6 mm, in-plane resolution = 0.7 x 0.7 mm^2, FA = 70 degrees, right to left phase encoding direction with 25% over sampling, averages = 3, concatenation = 1, bandwidth = 330 Hz/Px. The acquired GRE images were particularly positioned to match the ASL series in terms of slice orientation and the center of imaging slab.

Data Processing and ROI-based Analysis

The perfusion-weighted images were generated for the measurement at each inversion time. The methods for ROI-based analysis and iterative model fitting were described in Chapter 2.

Since the blood supplies for the hippocampus are from two different sources of arterial blood, the transit time or bolus duration for different regions of the hippocampus may be different. To have some idea about these characteristics, the segmented hippocampus regions were divided into 3 segments by assigning different slices into 3 slice groups: anterior segment, middle segment and posterior segment. Assigning imaging slices to three segments are based on individual subject's hippocampus structure by visual inspection. The first two slices containing hippocampus tissue are thought as the anterior segment of the hippocampus, the second two slices as the middle segment of the hippocampus, and the last slice as the posterior segment of the hippocampus. Averaging ASL signals using two slices can help further increase the SNR and stability of ASL signals due to the increase of the number of imaging voxels.

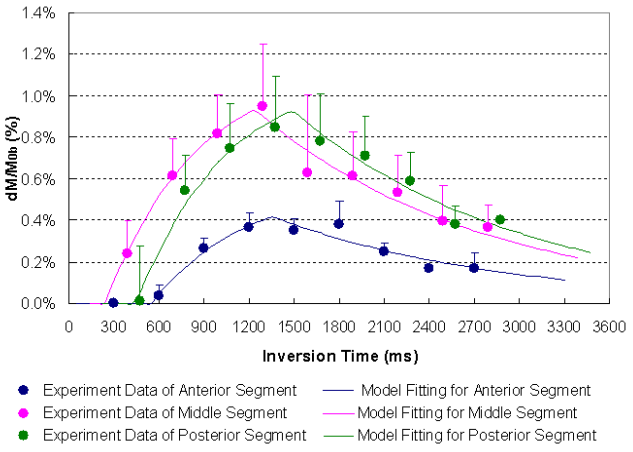

Figure 7-2 The dynamic changes of group mean ASL signals with inversion time for the defined three segments of the hippocampus region.

For each subject, the mean ASL signals were generated for each segment of the hippocampus region. Iterative model-fitting using single blood compartment model was performed for the mean ASL signals of each segment. Group analysis was performed for the estimated parameters.

Results and Discussion

Figure 7-2 shows the obtained dynamic curves for group mean ASL signals in each segment of the hippocampus region. ASL signals in the anterior segment are consistently lower than ASL signals in the other two segments of the hippocampus region. The across-subject variations of ASL signals in the anterior segment are consistently smaller than those in the other two segments. ASL signals in the other two segments have similarly higher level of CBF estimations and larger inter-subject variability. By comparing the times for the ASL signals to begin to rise as indicated by the model-fitting curves, it is obvious that the anterior segment of the hippocampus region has the longest transit time. For the other two segments, the transit time increases from the middle segment to the posterior segment. The group analysis results for the estimated parameters are showed in Figure 7-3. The estimated M_{0b} is around 1500 for the overall hippocampus region. The estimated bolus durations for the used labeling size are around or larger than 800 ms for the three defined segments. As indicated by Figure 7-3 (b), the inter-subject variability is relatively large across the four subjects. To be conservative, 600 ms bolus width had better be used for the following quantitative hippocampus perfusion studies.

Significant differences ($p<0.05$) were found by the performed two-tailed paired t tests for the estimated transit time and CBF values between the anterior segment and the other two segments. The p values are 0.011 and 0.040 for the performed t tests for the

estimated transit times between the anterior and middle segment, and between the anterior and posterior segment respectively. The p values from the performed t tests for the estimated CBF are 0.0019 and 0.02 respectively for the same two comparisons.

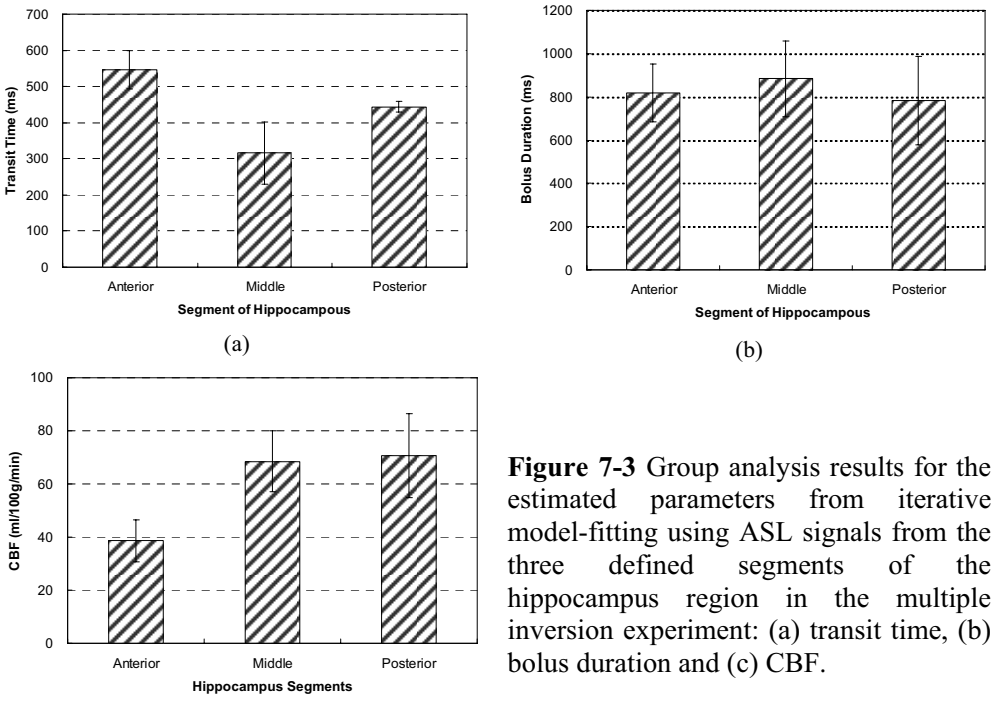

Figure 7-3 Group analysis results for the estimated parameters from iterative model-fitting using ASL signals from the three defined segments of the hippocampus region in the multiple inversion experiment: (a) transit time, (b) bolus duration and (c) CBF.

The longest transit time for the anterior segment may be due to the fact that the blood supply for this segment comes from the branches of anterior choroidal arteries, the labeled arterial blood spins from the carotid arteries have to go up and then curve back to irrigate the anterior part of the hippocampus region.

Conclusions

Based on the multiple inversion experiment results, temporal bolus width equal to 600 ms should be conservatively proper for quantitative hippocampus perfusion study using single subtraction method and single blood compartment model. Compared to the

middle and posterior segments of the hippocampus region, the anterior segment has both significantly lower perfusion and significantly longer transit time.

7.1.2 Multiple Post-bolus Delay Experiment

Materials and Methods

The same parameters as those in the previous study were used except the following ones: TR = 3000 ms, sequence-defined temporal bolus width (TI_1) = 600 ms. The following delay times were used in a randomized way across subjects: 0 ms, 400 ms, 800 ms, 1000 ms, 1200 ms, 1400 ms and 1800 ms. The maximal number of inferior saturation pulses that fits each post-bolus delay was used with usual parameters: saturation slab size equal to 20 mm with 25 ms interval. Two M_0 images were acquired for each delay time for quantitative CBF estimation.

For GRE imaging and data pre-processing, please refer to the descriptions of the previous study. In this study, quantitative CBF estimations were obtained at each inversion time by using single blood compartment model.

Results and Discussion

In Figure 7-4, the dynamic changes of group mean CBF with the post-bolus delay time are displayed for the three segments and overall hippocampus region. For the anterior segment, the estimated CBF increased slowly and basically reached the plateau at the post-bolus delay equal to 1200 ms. Especially, no very high perfusion level was observed at short delay time for the anterior segment. For the middle and posterior segments, CBF measurements had much higher levels at short delay time equal to 400 ms and returned to relatively flat or stable level after 1200 ms delay. In addition, CBF measurements at shorter inversion time have larger inter-subject variability.

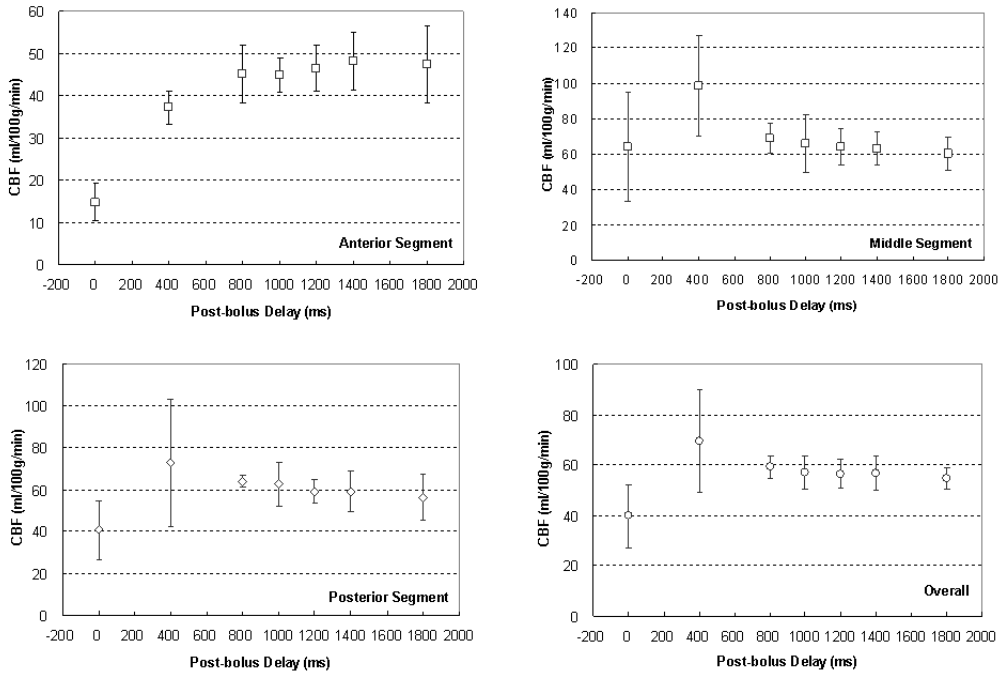

Figure 7-4 Hippocampus CBF changes with post-bolus delay.

The difference of CBF changes with post-bolus delay between the anterior segment and the other two segments may be due to the difference of the vascular characteristics of their blood supply arteries. For hippocampus body and tail, there are many relatively larger surface arteries, through which labeled blood will travel for distal imaging voxels. At short delay time, such as 400 ms, due to the large amount of intravascular labeled blood, CBF can be overestimated. The arteries around the anterior segment of the hippocampus region may be only smaller ones and blood supplies from these small arteries are mainly for the perfusion of the anterior segments.

One representative subject's perfusion-weighted imaging maps and CBF maps are presented in Figure 7-5, in which only signals in the segmented hippocampus areas are displayed. From these maps, it is noticeable that after 1000 ms, no spurious ASL signals

can be observed, and the perfusion signals in the segmented hippocampus areas became more uniform.

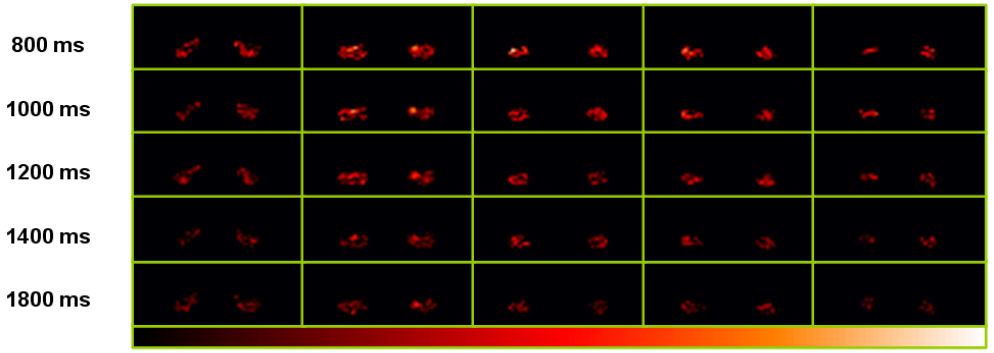

(a)

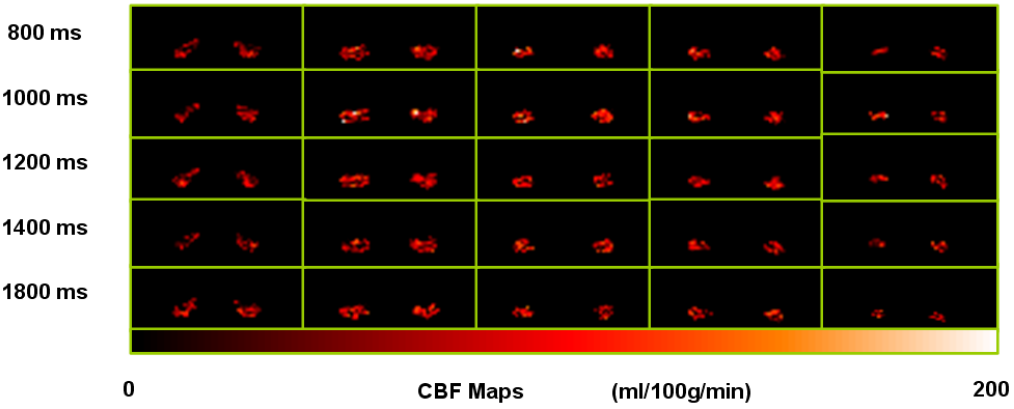

(b)

Figure 7-5 One representative subject's perfusion-weighted imaging maps (a) and CBF maps (b) for the hippocampus region from multiple post-bolus delay perfusion study

Conclusions

The multiple post-bolus delay study results indicated that to avoid intravascular artifacts and have more stable CBF estimations across subjects, longer post-bolus delay, such as 1200 ms, had better be used.

7.1.3 TR effects Evaluation and Estimation of Necessary Number of Inferior Saturation Pulses

Materials and Methods

In the TR effects evaluation study, quantitative perfusion studies were performed using the same parameters as in the previous studies but with varied TR values (2.5 s, 3.0 s, 3.5 s and 4.0 s). The selected sequence-defined bolus width (TI_1) and post-bolus delay are 600 ms and 1200 ms respectively. For the inferior saturation pulses, saturation slab size equal to 20 mm with 25 ms interval was used. The inferior saturation was performed during the whole post-bolus delay by using 48 pulses. Two M0 images were acquired for each delay time for quantitative CBF evaluation.

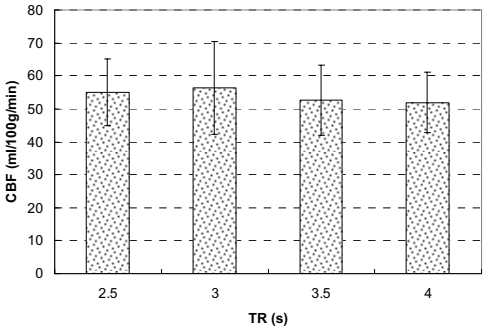

Figure 7-6 TR effects on hippocampus CBF measurements

For the study to estimate the necessary minimal number of inferior saturation pulses, all other MRI parameters were kept the same as those in previous studies except that the number of inferior saturation pulses were varied using the following saturation numbers: 0, 10, 20, 30, 40 and 48, and TR was fixed as 3 seconds.

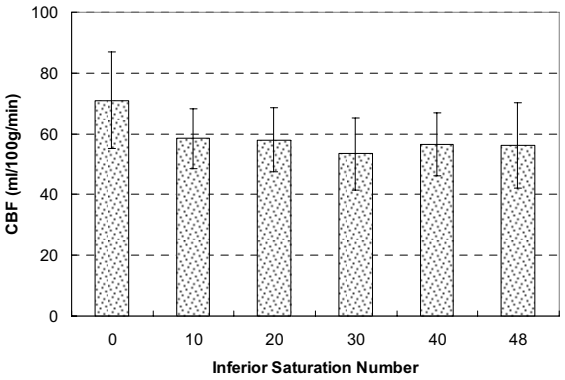

Figure 7-7 Hippocampus CBF changes as a function of inferior saturation pulse number

For GRE imaging and data pre-processing, please refer to the descriptions of the previous study. In this study, quantitative CBF estimations were obtained at each inversion time by using single blood compartment model.

Results and Discussion

The results from the TR effects evaluation study are presented in Figure 7-6. The CBF measurements using different TR values are very comparable. As mentioned in the previous chapter, there exists interference between the imaging and the labeling for OPTIMAL FAIR technique, and if the RF pulse for imaging slice acquisition can saturate the arterial blood in the major blood supply arteries, labeling efficiency can be decreased, especially for perfusion study using shorter TR values. However, in hippocampus perfusion study, due to the use of oblique coronal imaging slices, the acquisition of the imaging slices can avoid the saturation of the blood from major arteries (carotid, vertebral and basilar arteries), resulting in no adverse effects on the labeling efficiency.

In Figure 7-7, CBF measurements using different number of inferior saturation pulses are displayed. It showed that CBF measurements remained similar when the inferior saturation number is larger than 30. Forty inferior saturation pulses should be good enough. Visual inspection of perfusion-weighted imaging maps from this study also verified the same conclusion. In Figure 7-8, one representative subject's perfusion weighted imaging maps obtained by using different number of inferior saturation pulses are displayed. The perfusion-weighted imaging maps became more uniform when 40 inferior saturation pulses were used.

Conclusions

No TR effects were found for perfusion studies of the hippocampus using

OPTIMAL FAIR. To minimize study time and motions, shorter TR had better be used. To minimize intravascular artifacts from the residues of labeled blood, 40 inferior saturation pulses are good enough for healthy adults.

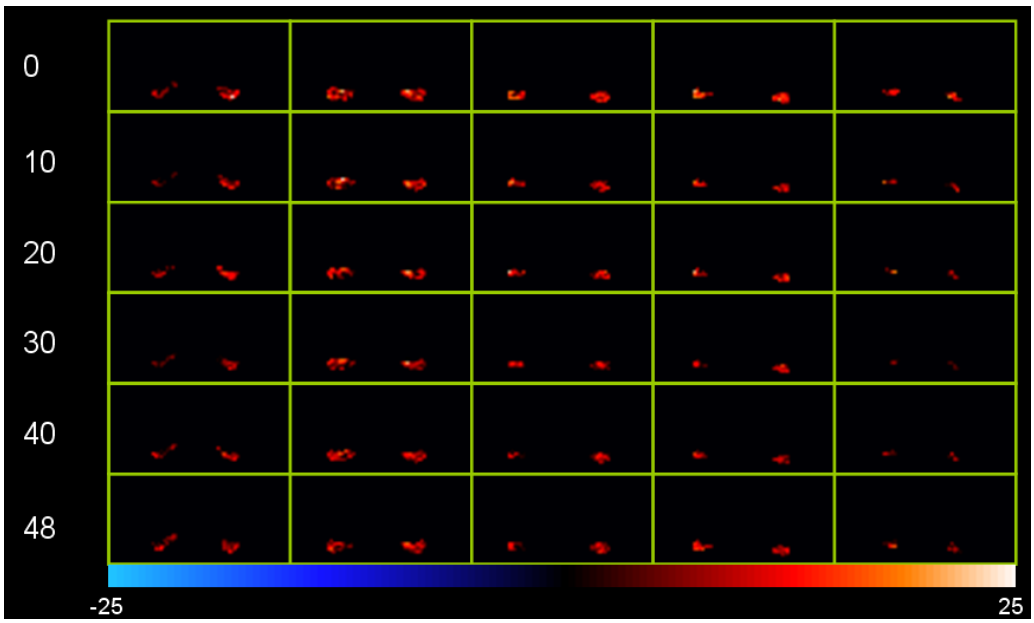

Figure 7-8 Perfusion-weighted imaging maps acquired with different inferior saturation pulse number.

7.2 QUANTITATIVE HIPPOCAMPUS PERFUSION STUDIES

Based on the performed ASL optimization studies, proper ASL parameters were used in quantitative hippocampus perfusion studies. Totally six healthy adults (one female at 26 years old, and five males with age range: 27-42 years) took part in this study.

Materials and Methods

In this study, two imaging resolutions were used for the quantitative perfusion studies of the hippocampus: 2.0 x 2.0 x 5.0 (+1 mm slice gap) mm^3 and 3.0 x 3.0 x 3.0 (+0.6 mm slice gap) mm^3. For resolution 2.0 x 2.0 x 5.0 (+1.0 mm slice gap) mm^3, the following MRI parameters were used: TR/ TE = 3000/14 ms, FOV = 128 x 128 mm^2,

matrix size = 64 x 64, slice thickness/gap = 5.0/1.0 mm, the number of imaging slices = 10, left to right phase encoding direction with 20% phase over sampling, partial Fourier (PF) = 6/8, imaging section inversion slab = FOV + 20 mm, spatially-confined inversion slab = FOV + 200 mm, the number of measurements = 200, iPAT GRAPPA factor = 2 with 24 reference lines, imaging acquisition order following anterior to posterior direction, the number of inferior saturation pulses = 40 with 20 mm slab size and 25 ms interval, the sequence-defined temporal bolus width (TI_1) = 600 ms and the post-bolus delay = 1200 ms. The superior saturation pulse train was off.

For the resolution 3.0 x 3.0 x 3.0 (+0.6 mm slice gap) mm^3, all other MRI parameters were kept the same as those above except the following ones: TR/TE = 3000/11 ms, FOV = 192 x 192 mm^2, slice thickness/gap = 3.0/0.6 mm, the number of imaging slices = 16, no phase over sampling, partial Fourier (PF) = 7/8, and the number of measurements = 160.

Corresponding to two imaging resolutions used for quantitative hippocampus perfusion studies, two sets of GRE images were acquired with matched slice orientation and position.

For the resolution 2.0 x 2.0 x 5.0 (+1 mm slice gap) mm^3, the following MRI parameters were used for the corresponding GRE images: TR/TE = 81/3.7 ms, the number of imaging slices = 10, slice thickness/slice gap = 5.0/1.0 mm, FOV = 128 x 128 mm^3, matrix size = 192 x 192, in-plane resolution = 0.7 x 0.7 mm^2, FA = 70 degrees, right to left phase encoding direction with 25% over sampling, averages = 3, concatenation = 1, bandwidth = 330 Hz/Px.

For the resolution 3.0 x 3.0 x 3.0 (+0.6 mm slice gap) mm^3, the following MRI parameters were used for corresponding GRE images: TR/TE = 65/3.7 ms, the number of imaging slices = 16, slice thickness/slice gap = 3.0 /0.6 mm, FOV = 192 x 192 mm^3, matrix size = 192 x 192, in-plane resolution = 1.0 x 1.0 mm^2, FA = 70 degrees, right to left phase encoding direction with no over sampling, averages = 3, concatenation = 2, bandwidth = 330 Hz/Px.

In the CBF analysis, similar method was used to assign slices into three segments of the hippocampus. For perfusion study using 2.0 x 2.0 x 5.0 (+1 mm slice gap) mm^3, for most subjects, the first 3 slices containing hippocampus tissue were taken as the anterior segment of the hippocampus region, the next two slices the middle segment, and the left slices the posterior segment. For perfusion study using 3.0 x 3.0 x 3.0 (+0.6 mm slice gap) mm^3, for most subjects, the first five slices containing hippocampus tissue were taken as the anterior segment of the hippocampus region, the next three slices the middle segment, and the left slices the posterior segment.

The same data pre-processing and ROI-based analysis methods were used as in the previous studies.

Results and Discussion

The study results from the quantitative hippocampus perfusion studies are showed in Tables 7-1 and 7-2 respectively for 2 different imaging resolutions. Two-tailed paired t tests were performed for different kinds of the comparisons of the measured hippocampus CBF values and showed in Tables 7-3 and 7-4. In these two tables, p values listed in the upper part of the table are t test results performed between the left and the right hemispheres for each segment and the overall hemisphere, and p values in the lower part

Table 7-7 Hippocampus CBF measurements using resolution 2 x 2 x 5 mm^3

Hippocampus CBF measurements using resolution 2 x 2 x 5 mm^3

Subject No.	Left Hemisphere				Right Hemisphere				Two Hemispheres			
	Anterior	Middle	Posterior	Whole	Anterior	Middle	Posterior	Whole	Anterior	Middle	Posterior	Whole
1	42.36	46.18	46.87	45.14	39.83	68.40	55.20	54.48	41.10	57.29	51.03	49.81
2	51.74	71.02	56.69	59.81	51.66	69.39	50.75	57.27	51.70	70.20	53.72	58.54
3	53.15	63.14	61.59	59.29	48.38	79.21	61.24	62.94	50.76	71.17	61.41	61.12
4	42.21	71.46	51.02	54.90	40.08	57.37	58.53	51.99	41.14	64.42	54.78	53.45
5	48.23	58.06	50.02	52.10	41.95	59.37	51.23	50.85	45.09	58.72	50.62	51.48
6	47.59	53.02	53.01	51.21	45.68	51.88	48.54	48.70	46.64	52.45	50.77	49.95
Mean	**47.55**	**60.48**	**53.20**	**53.74**	**44.60**	**64.27**	**54.25**	**54.37**	**46.07**	**62.37**	**53.72**	**54.06**
STD	**4.58**	**10.05**	**5.24**	**5.52**	**4.81**	**9.91**	**4.94**	**5.14**	**4.56**	**7.49**	**4.14**	**4.73**
C.V.	**0.10**	**0.17**	**0.10**	**0.10**	**0.11**	**0.15**	**0.09**	**0.09**	**0.10**	**0.12**	**0.08**	**0.09**

Anterior: anterior segment; Middle: middle segment; Posterior: posterior segment; Whole: whole hemisphere(s).

Table 7-8 Hippocampus CBF measurements using resolution 3 x 3 x 3 mm^3

Hippocampus CBF measurements using resolution 3 x 3 x 3 mm^3

Subject No.	Left Hemisphere				Right Hemisphere				Two Hemispheres			
	Anterior	Middle	Posterior	Whole	Anterior	Middle	Posterior	Whole	Anterior	Middle	Posterior	Whole
1	36.21	63.27	62.73	54.07	55.75	64.69	62.61	61.01	45.98	63.98	62.67	57.54
2	46.86	72.68	44.38	54.64	40.62	65.56	60.24	55.48	43.74	69.12	52.31	55.06
3	62.44	64.61	83.17	70.07	46.23	72.87	66.70	61.93	54.34	68.74	74.93	66.00
4	36.79	58.27	59.99	51.68	42.53	48.77	67.11	52.80	39.66	53.52	63.55	52.24
5	42.87	38.32	58.20	46.46	32.84	52.14	58.30	47.76	37.86	45.23	58.25	47.11
6	40.03	42.19	50.18	44.13	42.10	45.28	40.88	42.75	41.06	43.73	45.53	43.44
Mean	**44.20**	**56.56**	**59.77**	**53.51**	**43.34**	**58.22**	**59.31**	**53.62**	**43.77**	**57.39**	**59.54**	**53.57**
STD	**9.77**	**13.50**	**13.32**	**9.13**	**7.51**	**10.99**	**9.67**	**7.49**	**5.93**	**11.48**	**10.13**	**7.98**
C.V.	**0.22**	**0.24**	**0.22**	**0.17**	**0.17**	**0.19**	**0.16**	**0.14**	**0.14**	**0.20**	**0.17**	**0.15**

Anterior: anterior segment; Middle: middle segment; Posterior: posterior segment; Whole: whole hemisphere(s).

Table 7-9 P values of performed t tests for the following comparisons of hippocampus CBF measurements using resolution 2 x 2 x 5 mm^3

Comparisons between two hemispheres				
	Anterior	**Middle**	**Posterior**	**Whole**
	0.023	0.513	0.684	0.767

Comparisons between different segments						
	Left Hemisphere		**Right Hemisphere**		**Two Hemispheres**	
	Middle	**Posterior**	**Middle**	**Posterior**	**Middle**	**Posterior**
Anterior	**0.022**	**0.003**	**0.003**	**0.025**	**0.001**	**0.008**
Middle		0.094		**0.028**		**0.007**

P values smaller than 0.05 are highlighted in bold. All the performed t tests are two-tailed paired t tests.
Anterior: anterior segment; Middle: middle segment; Posterior: posterior segment; Whole: whole hemisphere.

Table 7-10 P values of performed t tests for the following comparisons of hippocampus CBF measurements using resolution 3 x 3 x 3 mm^3

Comparisons between Two Hemispheres				
	Anterior	**Middle**	**Posterior**	**Whole**
	0.876	0.667	0.924	0.958

Comparisons between Different Segments						
	Left Hemisphere		**Right Hemisphere**		**Two Hemispheres**	
	Middle	**Posterior**	**Middle**	**Posterior**	**Middle**	**Posterior**
Anterior	0.082	**0.016**	**0.015**	**0.015**	**0.009**	**0.004**
Middle		0.673		0.791		0.642

P values smaller than 0.05 are highlighted in bold. All the performed t tests are two-tailed paired t tests.
Anterior: anterior segment; Middle: middle segment; Posterior: posterior segment; Whole: whole hemisphere.

of the table represent t test results between one of the segments listed in column and one of the segments listed in the row.

For quantitative perfusion study using resolution 2.0 x 2.0 x 5.0 (+1.0 mm slice gap) mm3, overall CBF estimations for the left and right hemispheres of the hippocampus region are 53.74 ± 5.52 (mL/100g/min) and 54.37 ± 5.14 (mL/100g/min). The mean CBF for two hemispheres is 54.06 ± 4.74 (mL/100g/min). The CBF measurements for the anterior segments of the hippocampus are significantly lower than the CBF estimations for the middle and posterior segments for both left and right hemispheres (Table 7-3).

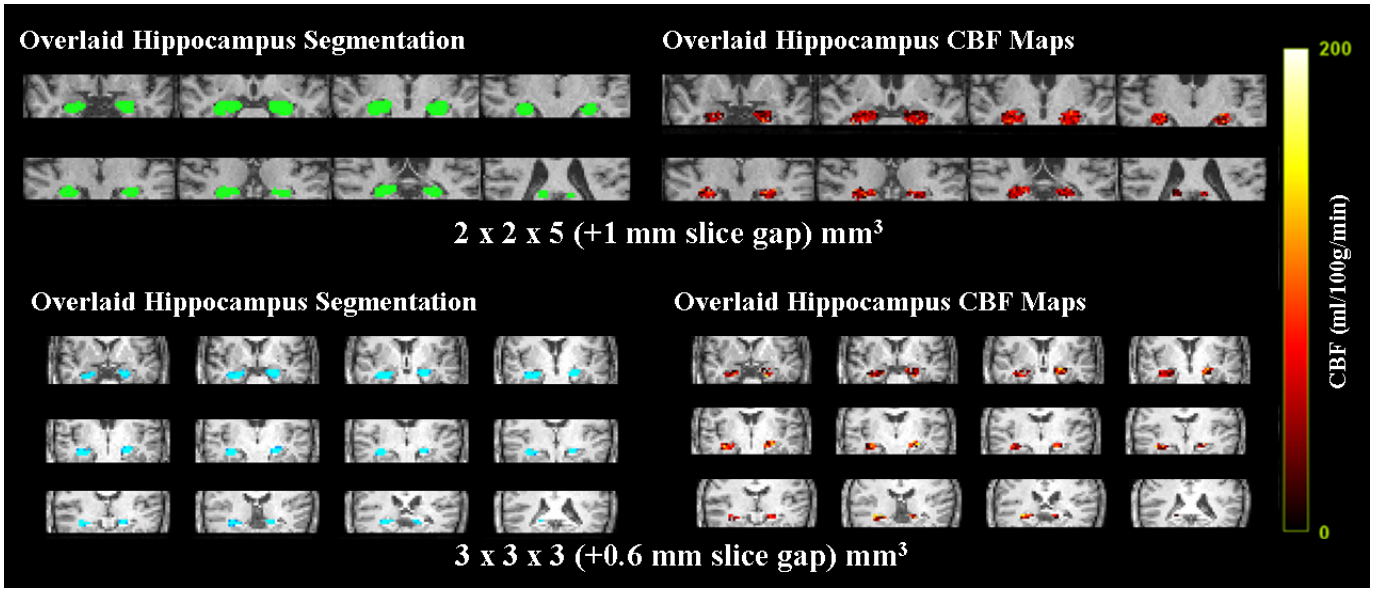

Figure 7-9 Segmented ROIs for the hippocampus (left) and corresponding CBF maps (right) overlaid on co-registered T_1-weighted images from one typical subject of hippocampus perfusion studies.

significant difference was observed for the anterior segments between the left and right hemispheres too.

For quantitative perfusion study using resolution 3 x 3 x 3 (+0.6 mm slice gap) mm^3, the overall CBF estimations for the left, the right and two hemispheres are very comparable to what were obtained by using resolution 2.0 x 2.0 x 5.0 (+1.0 mm slice gap) mm^3: 53.51 ± 9.13 (mL/100g/min), 53.62 ± 7.49 (mL/100g/min) and 53.57 ± 7.98 (mL/100g/min). The estimated CBF values for the anterior segments are also lower than those for the middle and posterior segments although no significant differences were found between the anterior segment and the middle or posterior segments for the left hemisphere. Two-tailed paired t tests were also performed between the CBF estimations by using two resolutions for the left, the right and two hemispheres, and no significant differences were found. In Figures 7-9, co-registered high-resolution anatomic images with overlaid segmented hippocampus ROIs and regional CBF maps are displayed for one representative subject's data. The comparisons of inter-subject variability between CBF measurements using two different imaging resolutions were performed for the left, the right and two hippocampus hemisphere(s) and are presented in Figure 7-10. It indicated that CBF measurements using larger voxel size gave larger inter-subject variability. This may be because larger voxels can give different extends of partial volume effects across subjects.

Conclusions

Initial hippocampus perfusion studies using OPTIMAL FAIR technique further indicated that compared to the middle and posterior segments of the hippocampus, the anterior segment of the hippocampus has lowest perfusion level. Perfusion study on the

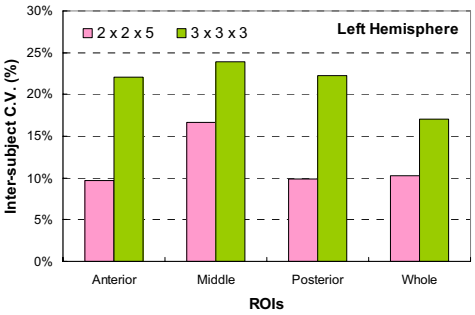

(a)

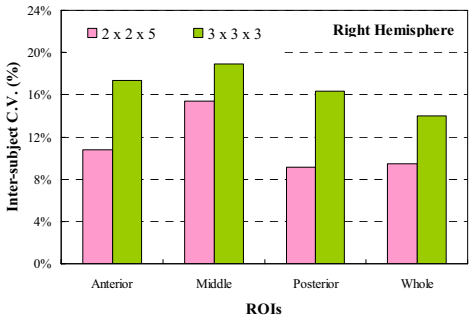

(b)

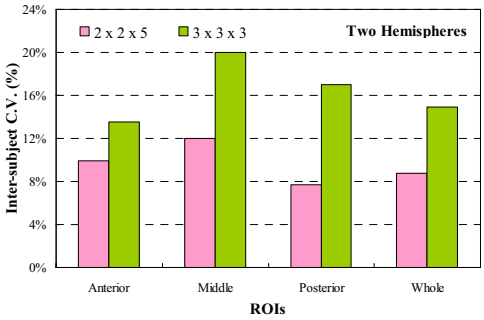

(c)

Figure 7-10 Inter-subject variability comparisons between CBF measurements using two imaging resolutions: (a) left hemisphere, (b) right hemisphere and (c) two hemispheres. C.V. represents the coefficient of variance for the inter-subject variability.

hippocampus region using resolution 2.0 x 2.0 x 5.0 (+1 mm slice gap) mm^3 gave us lower inter-subject variability.

7.3 SUMMARY

It is feasible to perform hippocampus perfusion study using OPTIMAL FAIR technique. The use of oblique coronal imaging slices for hippocampus perfusion study can avoid the adverse interference effects between the labeling and the imaging of OPTIMAL FAIR.

The optimization studies indicated that the anterior segment of the hippocampus region has lowest perfusion level and longest transit time. For quantitative hippocampus perfusion studies, based on optimization study results, 600 ms can be proper for the temporal bolus width, 1200 ms for post-bolus delay, and 40 for the number of inferior

saturation pulses. Shorter TR can be used since no TR effects were found. Compared to perfusion imaging resolution 3.0 x 3.0 x 3.0 (+0.6 mm slice gap) mm^3, imaging resolution 2.0 x 2.0 x 5.0 (+1.0 mm slice gap) mm^3 can give us lower inter-subject variability in the quantitative hippocampus perfusion studies. The quantitative hippocampus perfusion study further verified that the perfusion level in the anterior segment is lower than that in the middle or posterior segments.

To the best of our knowledge, it is the first time that quantitative CBF estimations have been performed separately for the anterior segment, the middle segment and the posterior segment of hippocampus region. It is also the first time that the perfusion level of the anterior segment of the hippocampus is found to be lower than the perfusion levels of the other two segments. All of the new knowledge can be valuable to help us understand the physiological state of the hippocampus, and the potential reason why hippocampus head tends to have atrophy or degenerative effects with aging.

CHAPTER 8 Summaries

Optimizing parameters and developing ASL methods for quantifying perfusion in specific brain regions is important to accurately characterize their function in health and in disease. This region-targeted approach to perfusion studies was developed and its advantages were demonstrated with perfusion studies of the cerebellum and the hippocampus.

To minimize or eliminate the venous artifacts found in cerebellum perfusion studies using traditional FAIR, MDS FAIR (modulated dual saturation for FAIR) and FAIR ASST (FAIR with active suppression of superior tagging) were implemented and evaluated.

MDS FAIR uses a train of period RF saturation pulses to suppress labeled venous blood before the acquisition of imaging slices. Two versions of MDS FAIR were implemented: MDS FAIR I, in which the periodic superior saturation RF pulse train begins just after temporal bolus width is defined and lasts until the beginning of image acquisition, and MDS FAIR II, in which the periodic superior saturation pulse train begins immediately after the inversion RF pulses and lasts until the beginning of image acquisition. Comparative evaluation studies indicated that although MDS FAIR II is superior to MDS FAIR I in terms of the suppression of venous artifacts, MDS FAIR II can only be effective for perfusion studies using smaller coverage, and is more likely to inadvertently saturate the inferior bolus. The cerebellum perfusion studies using MDS FAIR I and II with limited coverage indicated that MDS FAIR II tends to give less inter-subject variability than MDS FAIR I.

In contrast, FAIR ASST destroys superior labeling effects of the FAIR technique by performing pre-inversion and post-inversion superior saturations at the labeling stage. From a total of 23 methods preliminarily tested using different combinations and types of pre-inversion and post-inversion superior saturation pulses, three representatively effective methods (FAIR ASST 012, 112 and 211) were more extensively compared by performing quantitative perfusion studies with imaging slabs in the superior, deep and inferior brain regions. The study results indicated that FAIR ASST methods 112 and 211 were very comparable, gave better venous artifacts suppression and less inter-subject variability than FAIR ASST 012. Further quantitative cerebellum perfusion studies using FAIR ASST 112 and PICORE showed that FAIR ASST gives more stable CBF measurements with decreased temporal variability, more reliable CBF estimations with less subtraction errors, and more sensitivity to CBF changes with lowered inter-subject variability.

OPTIMAL FAIR (orthogonally-positioned tagging imaging method for arterial labeling of FAIR) was initially proposed to eliminate venous artifacts found in the cerebellum perfusion studies using traditional FAIR and later applied to quantitative hippocampus perfusion studies. The major advantages of OPTIMAL FAIR technique include reducing the heterogeneity of transit time within imaging slices and minimizing partial volume effects. In some cases, such as whole cerebellum perfusion study, care must be taken to avoid interference between the labeling and imaging slices which would affect the default labeling efficiency assumed for the hyperbolic secant RF pulse and adversely affect the corresponding CBF estimations. Alternatively, calibration studies can be performed to estimate the new labeling efficiency empirically.

Before performing quantitative perfusion studies for the cerebellum and the hippocampus, studies were performed to obtain estimations of physiological parameters needed to optimize the ASL parameters.

All these studies show the benefits of both optimizing ASL parameters and improving on techniques or introducing novel imaging schemes tailored for perfusion studies of specific brain regions. Brain region-targeted ASL techniques make perfusion studies of specific brain regions more reliable - with more accurate and artifact-free CBF measurements, more efficient - by using more suitable slice geometry and placement, and more sensitive to CBF changes - due to reduced partial volume effects and lower variability.

The major achievements of the thesis work are: (1) two new FAIR-based PASL techniques, FAIR ASST and OPTIMAL FAIR, were developed to reduce venous artifacts and improve CBF quantification accuracy; (2) for the first time, systematic quantitative perfusion studies of the cerebellum and the hippocampus were performed; (3) validation of the importance and usefulness of brain region-targeted ASL in cerebellum and hippocampus indicates that it should be more generally applicable to other regions.

OPTIMAL FAIR has been used for dynamic physostigmine perfusion studies of hippocampus on normal healthy controls. The study results showed that OPTIMAL FAIR can detect small significant CBF changes due to physostigmine challenge (unpublished data). In the future, these novel ASL techniques can be used for diverse clinic applications or neuroscience research studies. For example, although these novel ASL techniques were implemented for more reliable perfusion studies of specific brain regions (important for Gulf War Syndrome), they should also be very valuable for perfusion

studies of other organs or tissue, such as kidney, liver and muscle. They also have potential for improving techniques other than FAIR; for example, CASL (continuous arterial spin labeling) and pCASL (pseudo-continuous arterial spin labeling) should both benefit from this region-targeted approach.

APPENDIX A Supplementary Results from FAIR ASST Evaluation Studies

A.1. CBF ESTIMATIONS AND PERFORMED T TESTS RESULTS

In the comparison analysis for the following presented study results, one-tailed paired t tests were performed between traditional FAIR method (FAIR ASST 000) and anyone of the other three FAIR ASST methods (012, 112 and 211) while two-tailed paired t tests were performed between any two of the three FAIR ASST methods 012, 112 and 211.

Table A-1-1
Cerebellum CBF measurements by different FAIR methods

Subject No.	CBF (ml/100g/min)											
	000			012			112			211		
	GM	WM	Ratio	GM	WM	Ratio	GM	WM	Ratio	GM	WM	Ratio
1	64.38	36.14	1.78	39.77	25.45	1.56	41.34	25.50	1.62	45.30	23.11	1.96
2	47.46	33.05	1.44	47.71	40.89	1.17	43.71	34.16	1.28	48.67	38.12	1.28
3	35.90	31.93	1.12	29.79	25.43	1.17	34.29	21.58	1.59	26.85	19.23	1.40
4	60.07	37.78	1.59	46.75	33.68	1.39	49.40	29.84	1.66	46.75	29.60	1.58
5	65.54	40.14	1.63	45.01	24.68	1.82	50.71	22.59	2.24	56.19	18.87	2.98
Mean	**54.67**	**35.81**	**1.51**	**41.81**	**30.03**	**1.42**	**43.89**	**26.73**	**1.68**	**44.75**	**25.79**	**1.84**
± STD	**± 12.71**	**± 3.37**	**± 0.25**	**± 7.38**	**± 7.11**	**± 0.28**	**± 6.63**	**± 5.25**	**± 0.35**	**± 10.85**	**± 8.13**	**± 0.69**

GM: grey matter; WM: white matter; Ratio: CBF ratio between grey matter and white matter

Table A-1-2
P values from t tests between cerebellum CBF measurements by different FAIR methods

	012			112			211		
	GM	WM	Ratio	GM	WM	Ratio	GM	WM	Ratio
000	**0.024**	0.107	0.185	**0.025**	**0.020**	0.179	**0.020**	**0.041**	0.143
012				0.283	**0.042**	**0.027**	0.298	**0.006**	0.094
112							0.751	0.521	0.393

GM: grey matter; WM: white matter; Ratio: CBF ratio between grey matter and white matter. The significant results (P<0.05) are highlighted in bold.

Table A-1-3

Spatial variability analysis for cerebellum grey matter CBF measurements using different FAIR methods

Subject No.	Coefficient of Variance			
	000	**012**	**112**	**211**
1	3.24	0.86	1.02	0.90
2	2.21	0.59	0.75	0.71
3	5.28	1.66	1.91	3.61
4	4.14	0.71	1.86	1.37
5	2.80	1.12	1.21	1.33
Mean ± STD	**3.53 ± 1.20**	**0.99 ± 0.42**	**1.35 ± 0.52**	**1.58 ± 1.17**

Table A-1-4

P values from t tests between cerebellum spatial variability of grey matter CBF measurements using different FAIR methods

	012	**112**	**211**
000	**0.002**	**0.002**	**0.001**
012		0.142	0.170
112			0.577

The significant results (P<0.05) are highlighted in bold.

Table A-1-5

Spatial variability analysis for cerebellum white matter CBF measurements using different FAIR methods

Subject No.	Coefficient of Variance			
	000	**012**	**112**	**211**
1	0.96	1.09	1.13	1.28
2	1.14	0.77	0.82	0.76
3	1.05	1.13	1.35	1.48
4	5.33	0.55	0.64	0.76
5	0.93	1.17	1.35	1.53
Mean ± STD	**1.88 ± 1.93**	**0.94 ± 0.27**	**1.06 ± 0.32**	**1.16 ± 0.38**

Table A-1-6

P values from t tests for the spatial variability of cerebellum white matter CBF measurements between different FAIR methods

	012	**112**	**211**
000	0.192	0.223	0.251
012		**0.031**	**0.030**
112			0.070

The significant results (P<0.05) are highlighted in bold.

Table A-1-7

CBF measurements in the inferior part of the brain using different FAIR methods

Subject No.	CBF (ml/100g/min)											
	000			**012**			**112**			**211**		
	GM	**WM**	**Ratio**	**GM**	**WM**	**Ratio**	**GM**	**WM**	**Ratio**	**GM**	**WM**	**Ratio**
1	81.84	25.09	3.26	38.59	21.46	1.80	39.50	19.35	2.04	41.99	21.19	1.98
2	55.93	25.81	2.17	51.35	19.73	2.60	48.05	21.16	2.27	49.52	22.20	2.23
3	65.89	29.07	2.27	37.09	23.03	1.61	34.94	20.13	1.74	30.61	20.75	1.47
4	87.05	30.74	2.83	50.03	27.75	1.80	52.20	26.63	1.96	49.97	23.58	2.12
5	104.39	24.66	4.23	47.14	26.14	1.80	50.57	25.12	2.01	62.57	23.96	2.61
Mean ± STD	**79.02 ± 18.85**	**27.07 ± 2.68**	**2.95 ± 0.84**	**44.84 ± 6.59**	**23.62 ± 3.30**	**1.92 ± 0.39**	**45.05 ± 7.48**	**22.48 ± 3.21**	**2.00 ± 0.19**	**46.93 ± 11.74**	**22.34 ± 1.42**	**2.08 ± 0.41**

GM: grey matter; WM: white matter; Ratio: CBF ratio between grey matter and white matter

Table A-1-8

P values from t tests between CBF measurements using different FAIR methods in the inferior part of the brain

	012			112			211		
	GM	WM	Ratio	GM	WM	Ratio	GM	WM	Ratio
000	**0.009**	**0.033**	**0.047**	**0.006**	**0.019**	**0.035**	**0.004**	**0.013**	**0.019**
012				0.876	0.192	0.486	0.602	0.316	0.473
112							0.541	0.879	0.624

GM: grey matter; WM: white matter; Ratio: CBF ratio between grey matter and white matter. The significant results (P<0.05) are highlighted in bold.

Table A-I-9

Spatial variability analysis for grey matter CBF measurements in the inferior part of the brain using different FAIR methods

Subject No.	Coefficient of Variance			
	000	012	112	211
1	4.18	1.14	1.55	1.10
2	2.61	0.60	0.76	0.70
3	4.38	1.46	1.88	2.17
4	4.45	1.12	1.52	1.34
5	3.88	1.78	1.55	1.53
Mean ± STD	**3.90 ± 0.75**	**1.22 ± 0.43**	**1.45 ± 0.41**	**1.37 ± 0.55**

Table A-1-10

P values from t tests for the spatial variability of grey matter CBF measurements in the inferior part of the brain between different FAIR methods

	012	112	211
000	**0.0003**	**0.0001**	**0.0002**
012		0.1377	0.4094
112			0.5223

The significant results (P<0.05) are highlighted in bold.

Table A-1-11

Spatial variability analysis for white matter CBF measurements in the inferior part of the brain using different FAIR methods

Subject No.	Coefficient of Variance			
	000	012	112	211
1	2.20	1.45	1.68	1.49
2	2.66	1.60	1.37	1.39
3	1.85	1.27	1.67	1.55
4	4.62	1.29	1.76	1.57
5	2.30	1.22	1.30	1.73
Mean ± STD	**2.73 ± 1.10**	**1.37 ± 0.16**	**1.56 ± 0.21**	**1.55 ± 0.12**

Table A-I-12

P values from t tests for the spatial variability of white matter CBF measurements in the inferior part of the brain between different FAIR methods

	012	112	211
000	**0.027**	**0.033**	**0.038**
012		0.203	0.216
112			0.936

The significant results (P<0.05) are highlighted in bold.

Table A-1-13

Deep brain region CBF measurements using different FAIR methods

Subject No.	CBF (ml/100g/min)											
	000			012			112			211		
	GM	WM	Ratio	GM	WM	Ratio	GM	WM	Ratio	GM	WM	Ratio
1	59.14	21.43	2.76	48.12	20.60	2.34	47.30	23.04	2.05	48.88	20.47	2.39
2	58.44	29.86	1.96	54.49	24.57	2.22	51.10	26.03	1.96	51.74	21.04	2.46
3	58.46	13.75	4.25	50.79	13.76	3.69	51.80	19.44	2.66	55.89	19.98	2.80
4	74.71	23.94	3.12	56.69	24.17	2.35	52.95	24.77	2.14	56.28	25.47	2.21
5	77.52	25.92	2.99	60.65	19.77	3.07	59.44	23.06	2.58	52.29	18.96	2.76
Mean	**65.66**	**22.98**	**3.02**	**54.15**	**20.57**	**2.73**	**52.52**	**23.27**	**2.28**	**53.01**	**21.18**	**2.52**
± STD	**± 9.61**	**± 6.01**	**± 0.82**	**± 4.91**	**± 4.36**	**± 0.63**	**± 4.41**	**± 2.48**	**± 0.32**	**± 3.09**	**± 2.51**	**± 0.25**

GM: grey matter; WM: white matter; Ratio: ratio between grey matter CBF and white matter CBF.

Table A-1-14

P values from t-tests between deep brain region CBF measurements using different FAIR methods

	012			112			211		
	GM	WM	Ratio	GM	WM	Ratio	GM	WM	Ratio
000	**0.006**	**0.077**	0.111	**0.006**	0.437	**0.026**	**0.018**	0.231	0.142
012				0.136	**0.037**	**0.039**	0.636	0.901	0.630
112							0.816	0.149	0.034

GM: grey matter; WM: white matter; Ratio: ratio between grey matter CBF and white matter CBF. The significant results (P<0.05) are highlighted in bold.

Table A-1-15

Spatial variability analysis for grey matter CBF measurements in the deep brain region using different FAIR methods

Subject No.	Coefficient of Variance			
	000	012	112	211
1	2.66	0.77	0.85	0.92
2	1.67	0.70	0.84	0.63
3	1.01	0.79	0.73	0.92
4	2.79	0.94	0.93	1.01
5	2.21	0.73	0.76	1.13
Mean ± STD	**2.07 ± 0.74**	**0.79 ± 0.09**	**0.82 ± 0.08**	**0.92 ± 0.18**

Table A-1-16

P values from t tests for the spatial variability of grey matter CBF measurements in the deep brain region between differenet FAIR methods

	012	112	211
000	**0.007**	**0.007**	**0.010**
012		0.358	0.150
112			0.349

The significant results (P<0.05) are highlighted in bold.

Table A-1-17

Spatial variability analysis for white matter CBF measurements in the deep brain region using different FAIR methods

Subject No.	Coefficient of Variance			
	000	012	112	211
1	1.48	1.42	1.28	1.60
2	1.04	1.08	1.01	1.25
3	2.06	2.07	1.45	2.30
4	1.89	1.31	1.44	1.40
5	1.43	1.70	1.41	1.70
Mean ± STD	1.58 ± 0.4	1.52 ± 0.38	1.32 ± 0.19	1.65 ± 0.4

Table A-1-18

P values from t tests for the spatial variability of white matter CBF measurements in the deep brain region between different FAIR methods

	012	112	211
000	0.336	0.044	0.324
012		0.189	**0.029**
112			0.083

The significant results (P<0.05) are highlighted in bold.

Table A-1-19

CBF measurements in the superior brain region using different FAIR methods

Subject No.	CBF (ml/100g/min)											
	000			012			112			211		
	GM	WM	Ratio	GM	WM	Ratio	GM	WM	Ratio	GM	WM	Ratio
1	45.95	25.38	1.81	50.85	23.50	2.16	50.79	23.11	2.20	47.11	23.46	2.01
2	44.73	23.94	1.87	43.32	23.14	1.87	45.66	23.87	1.91	45.93	23.58	1.95
3	58.11	25.43	2.29	56.44	25.57	2.21	55.50	23.96	2.32	56.10	25.69	2.18
4	53.17	22.97	2.31	53.88	19.89	2.71	55.36	20.43	2.71	55.24	19.92	2.77
5	61.10	32.25	1.89	59.30	29.54	2.01	52.29	18.96	2.76	59.44	23.06	2.58
Mean	**52.61**	**25.99**	**2.03**	**52.76**	**24.33**	**2.19**	**51.92**	**22.07**	**2.38**	**52.76**	**23.14**	**2.30**
± STD	**± 7.23**	**± 3.65**	**± 0.24**	**± 6.13**	**± 3.55**	**±0.32**	**± 4.04**	**± 2.25**	**± 0.36**	**± 5.93**	**± 2.07**	**± 0.36**

GM: grey matter; WM: white matter; Ratio: CBF ratio between grey matter and white matter.

Table A-1-20

P values from t tests between CBF measurements in the superior brain region using different FAIR methods

	012		112		211	
	GM	WM	GM	WM	GM	WM
000	0.914	0.049	0.784	0.174	0.863	0.166
012			0.637	0.346	0.996	0.422
112					0.656	0.275

GM: grey matter; WM: white matter; Ratio: ratio between grey matter CBF and white matter CBF.

Table A-1-21

Spatial variability analysis for grey matter CBF measurements in the superior brain region using different FAIR methods

Subject No.	Coefficient of Variance			
	000	012	112	211
1	0.62	0.49	0.50	0.51
2	0.49	0.57	0.49	0.50
3	0.48	0.48	0.51	0.49
4	0.47	0.47	0.43	0.44
5	0.41	0.44	0.48	0.41
Mean ± STD	**0.49 ± 0.08**	**0.49 ± 0.05**	**0.48 ± 0.03**	**0.47 ± 0.04**

Table A-1-22

P values from t tests for the spatial variability of grey matter CBF measurements in the superior brain region using different FAIR methods

	012	112	211
000	0.914	0.730	0.350
012		0.742	0.283
112			0.485

The significant results (P<0.05) are highlighted in bold.

Table A-1-23

Spatial variability analysis for white matter CBF measurements in the superior brain region using different FAIR methods

Subject No.	Coefficient of Variance			
	000	012	112	211
1	0.95	0.95	0.96	0.96
2	0.82	0.92	0.9	0.85
3	0.92	0.92	1.01	0.97
4	1.05	1.19	1.23	1.18
5	0.78	0.86	1.23	1.41
Mean ± STD	**0.9 ± 0.11**	**0.97 ± 0.13**	**1.07 ± 0.15**	**1.07 ± 0.22**

Table A-1-24

P values from t tests for the spatial variability of white matter CBF measurements in the superior brain region between different FAIR methods

	012	112	211
000	0.083	0.103	0.219
012		0.236	0.400
112			0.864

The significant results (P<0.05) are highlighted in bold.

Table A-1-25

Asymmetry index (A.I.) analysis for CBF measurements from four slices that cover the middle region of cerebellum using different FAIR methods

Subject No.	|Asymmetric Index (%)|							
	000		012		112		211	
	GM	WM	GM	WM	GM	WM	GM	WM
1	16.7	1.8	4.1	1.6	5.2	8.5	3.3	6.3
2	11.6	6.1	0.1	6.9	1.1	7.2	1.4	5.6
3	19.0	19.7	3.8	2.2	4.6	3.0	4.4	0.4
4	7.6	13.3	2.4	14.6	5.8	8.4	4.3	11.2
5	23.5	25.0	10.2	1.8	2.3	2.1	12.0	12.7
Mean ± STD	**15.7 ± 6.2**	**13.2 ± 9.5**	**4.1 ± 3.7**	**5.4 ± 5.6**	**3.8 ± 2.0**	**5.9 ± 3.1**	**5.1 ± 4.1**	**7.3 ± 4.0**

GM: grey matter; WM: white matter

Table A-1-26
P values from t tests for A.I. analysis of cerebellum CBF measurements in the middle of the cerebellum between different FAIR methods

	012		112		211	
	GM	WM	GM	WM	GM	WM
000	**0.001**	0.105	**0.010**	0.126	**0.003**	0.120
012			0.875	0.845	0.124	0.527
112					0.580	0.603

GM: grey matter; WM: white matter. The significant results (P<0.05) are highlighted in bold.

A.2 ANALYSIS RESULTS OF MOTIONS

The motions in the FAIR ASST evaluation studies have been evaluated for each subject and each scan. The group analysis results of the motions are presented in the following Figures A-1-1 to A-1-3. Due to the good cooperation of the subjects, the motions in the performed studies are all very small.

In the analysis, three-dimension (3D) translation was used to measure the total translation distance of the motion in space and calculated as the root of the sum of the independent translation's square along each axis. The rotations along the three axes are evaluated separately and indicated by using the same names as those used in SPM software: pitch, roll and yaw.

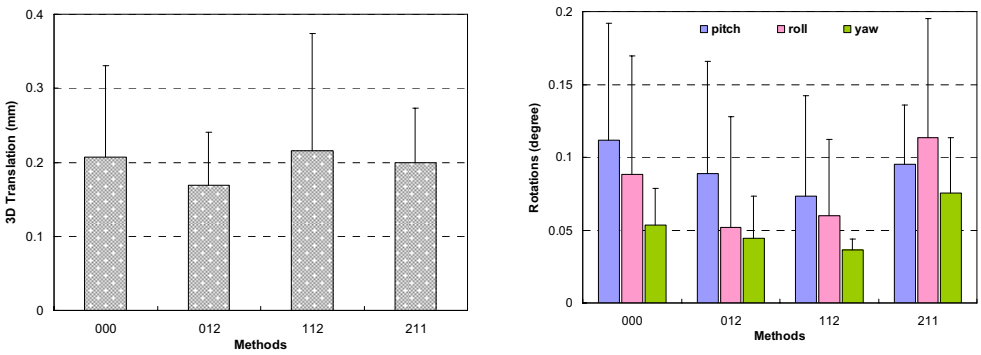

Figure A-1-1 Motion evaluation results for perfusion studies in the inferior part of the brain: (a) 3D translations and (b) rotations along three axis

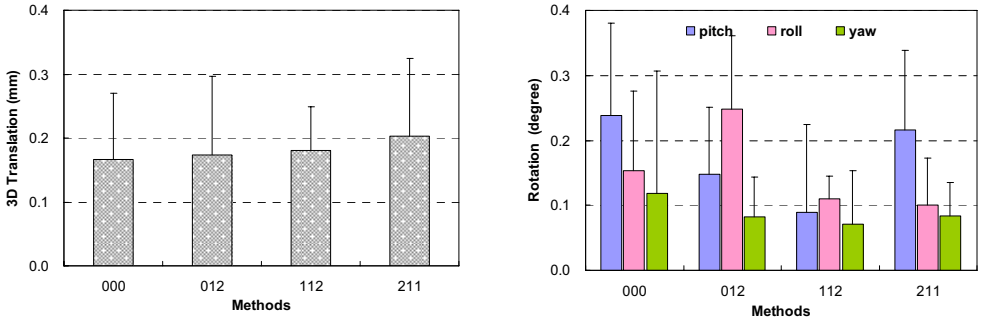

Figure A-1-2 Motion evaluation results for perfusion studies in the deep brain region from: (a) 3D translations and (b) rotations along three axis

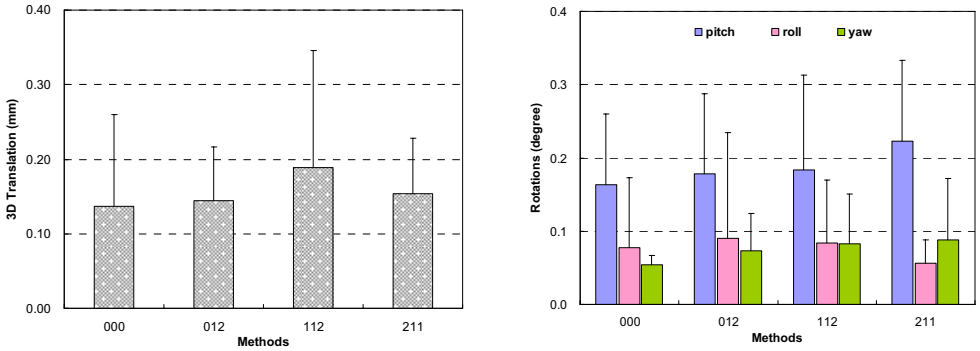

Figure A-1-3 Motion evaluation results for perfusion studies in the superior part of the brain: (a) 3D translations and (b) rotations along three axis

Two-tailed paired t tests did not show significant differences for all aspects of the motions (3D translation, pitch, roll and yaw) between any two of those scans using four FAIR methods for each study region.

APPENDIX B Supplementary for ASL Optimization Studies Using FAIR ASST

Study results from the multiple inversion experiment of cerebellum perfusion study showed that transit time was not consistently increased from the inferior to superior slices. Particularly, transit time for grey matter of slices 7 and 8 is shorter than that of the middle slices 5 and 6. This may be due to the fact that blood velocity in large vertical arteries, vertebral and basilar arteries, is higher than that in small horizontal arteries that are branches of vertebral and basilar arteries. This also implies that transit time difference across axial slices can be smaller than the transit time difference between the anterior and posterior parts of the cerebellum.

To verify this assumption, grey matter ASL signals were analyzed in the following. The transit times for the anterior and posterior parts of axial slices were analyzed for cerebellum grey matter by dividing axial slices into anterior and posterior parts and performing an iterative model fitting for each part. One subject's ROI for the anterior part of the cerebellum, the experiment data for the anterior and posterior parts as well as the corresponding model-fitting results are showed in Figure B-1. These plots indicated that transit time differences between axial slices are relatively smaller than those between the anterior and posterior parts of the cerebellum. Especially for the middle and superior slices, the transit time differences between the anterior and posterior parts of the cerebellum became larger. For comparison purpose, the experiment data for the overall inferior and superior parts of the cerebellum and for the overall anterior and posterior

parts of the cerebellum were also analyzed by performing model fitting. These analysis results are showed in Figure B-2.

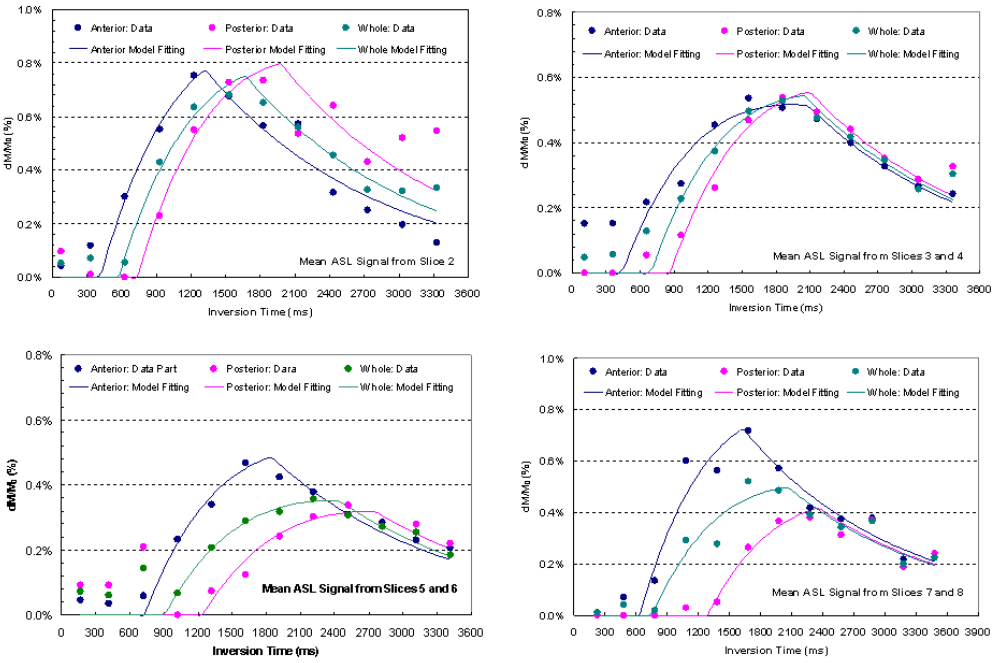

Figure B-1 ASL signal changes with the inversion time for the anterior part, posterior part and the overall of cerebellum grey matter and the ROI defined for the anterior part of cerebellum for one subject from multiple inversion experiments

It is obvious that transit time difference between the inferior and superior parts of cerebellum is smaller than that between the divided anterior and posterior parts of the cerebellum. In the above analysis, the estimated transit time for the posterior part of cerebellum is mainly determined by the transit time of the anterior portion of the

posterior part. The transit time for cerebellum tissue near the posterior end of the

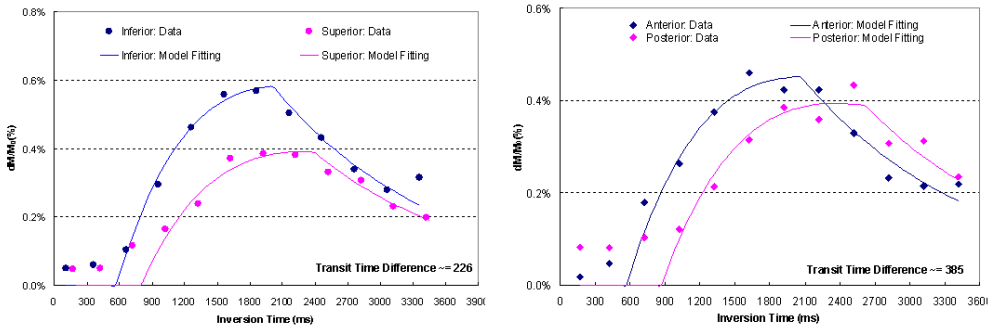

Figure B-2 ASL signal changes with inversion time for the inferior and superior parts of cerebellum grey matter (Inferior part: slices 2-4 and superior part: slices 5-7)

cerebellum will have much longer transit time. This means transit time within axial slice has much larger heterogeneity.

The group analysis results for transit time differences between the inferior and superior parts of the cerebellum are presented in Figure B-3. Along the inferior-superior direction of the cerebellum, transit time differences are showed as the transit time differences between that of the first inferior slice (slices 1-2) and those of other imaging slices. These results further confirmed that transit time within axial slices has larger heterogeneity. In principle, uniform transit time within imaging slices will give more reliable and accurate CBF estimations since all labeled blood will arrive at small arterioles or capillary bed at close times, minimizing confounding effects from the possible exchange and signal decay with tissue T_1.

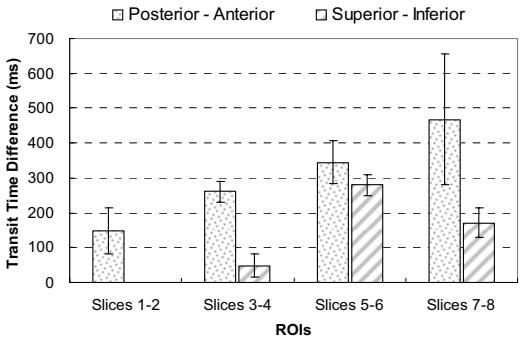

Figure B-3 Group analysis results for transit time differences

In summary, based on the above analysis results, transit time within axial imaging slices has larger heterogeneity.

APPENDIX C Supplementary Materials for Cerebellum Perfusion Studies Using OPTIMAL FAIR

In this appendix, ASL optimization study results using OPTIMAL FAIR will be presented in the first section. In the second section, GRE imaging parameters are provided for all acquired GRE images in the cerebellum perfusion using OPTIMAL FAIR.

Three healthy male adults (age range, 37-39 years) have taken part in these optimization studies. All three subjects took part in the multiple inversion experiment. Two subjects took part in the estimation of the minimal number of inferior saturation pulses and the TR effects evaluation study for perfusion study using partial cerebellum coverage.

C.1 ASL OPTIMIZATION STUDIES USING OPTIMAL FAIR

C.1.1 Multiple Inversion Experiment

Materials and Methods

The following MRI parameters were used in the multiple inversion experiment: TR/TE = 4000/9.6 ms, FOV = 220 x 220 mm^2, matrix size = 74 x 74, slice thickness/slice gap = 5/1 mm, imaging resolution = 3 x 3 x 5 (+1 mm slice gap) mm^3; partial Fourier (PF) = 7/8, iPAT GRAPPA factor = 2 with 24 reference lines using CP mode, the number of measurements = 60. Slices were acquired along anterior to posterior direction with the position using the following methods: the first coronal slice was positioned at the beginning of anterior tip of the cerebellum. Twelve imaging slices were used to assure complete coverage for the cerebellum for all subjects. The gap between the orthogonal labeling and the imaging section is 10 mm on each side of the imaging section. Imaging

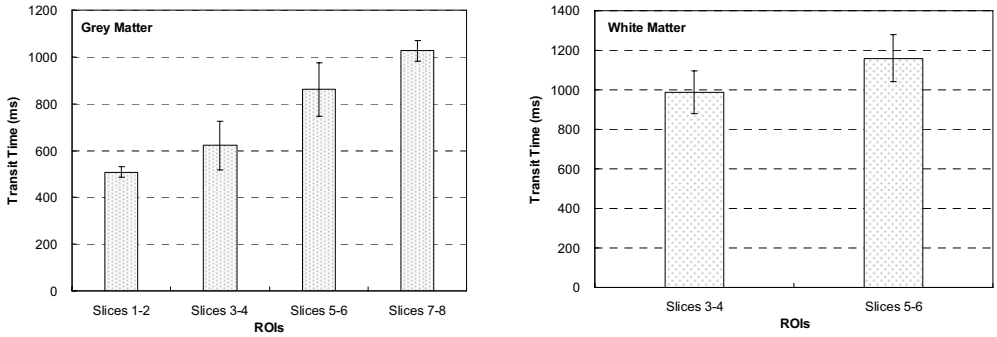

Figure C-1 Estimated transit times by performing iterative model-fitting of multiple inversion experiment data

section inversion slab size is equal to FOV plus 20 mm. Spatially-confined inversion slab size is equal to FOV plus 200 mm. When the FOV completely covers the whole head, making the superior labeling slab outside of the brain, no superior saturation pulses need be performed. The inferior saturation pulse train was turned off to utilize the whole amount of labeled blood. The inversion time was varied randomly across subjects using 50 ms, 300 ms, 600 ms, 900 ms, 1200 ms, 1500 ms, 1800 ms, 2100 ms, 2400 ms, 2700 ms, 3000 ms and 3300 ms.

For GRE images, the following MRI parameters were used: TR/TE = 150/3.7 ms, the number of imaging slices = 32, slice thickness = 6 mm, FOV = 220 x 220 mm^3, matrix size = 256 x 256, in-plane resolution = 0.86 x 0.86 mm^2, FA = 90 degrees, right to left phase encoding direction, averages = 2, concatenation = 1, bandwidth = 330 Hz/Px. The central twelve slices matched the ASL series in terms of slice orientation and imaging slab center.

Due to subject-dependent geometry difference, for some subjects with smaller cerebellum, only 8 slices contain cerebellum tissue. Therefore, only the first eight slices

were used for the data analysis. For information about the data processing, model fitting and ROI-based analysis, please refer to Chapter 2.

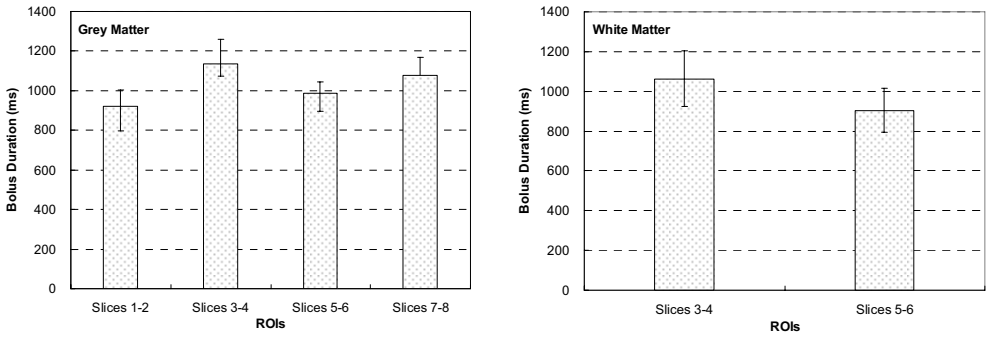

Figure C-2 Estimated bolus duration by performing iterative model fitting of multiple inversion experiment data

Results and Discussion

In Figure C-1, the group analysis results of estimated transit time are presented for both grey and white matters. It is obvious that the estimated transit times increased consistently for both grey and white matters from anterior to posterior slices. The transit time difference between the anterior slices and posterior slices is larger than 400 ms for cerebellum grey matter. In Figure C-2, the group analysis results for the estimated bolus duration are displayed for both grey and white matters. The dynamic ASL signal (in percentage) changes with the inversion time are plotted in Figure C-3 ((a) and (b)) for both grey and white matters. One representative subject's perfusion weighted imaging maps for six selected inversion times are also presented (Figure B-3 (c)). It showed that the bolus duration is larger than 800 ms. From those displayed perfusion weighted imaging maps, it is clear that after inversion time equal to 1800 ms, ASL signals have become uniform with no obvious spurious signals in cerebellum area. Since the estimated bolus duration is larger than 800 ms, when 800 ms temporal bolus width (TI_1) is defined

in ASL sequence by using inferior saturation pulses in the quantitative cerebellum perfusion studies, 1000 ms post-bolus delay should be good enough.

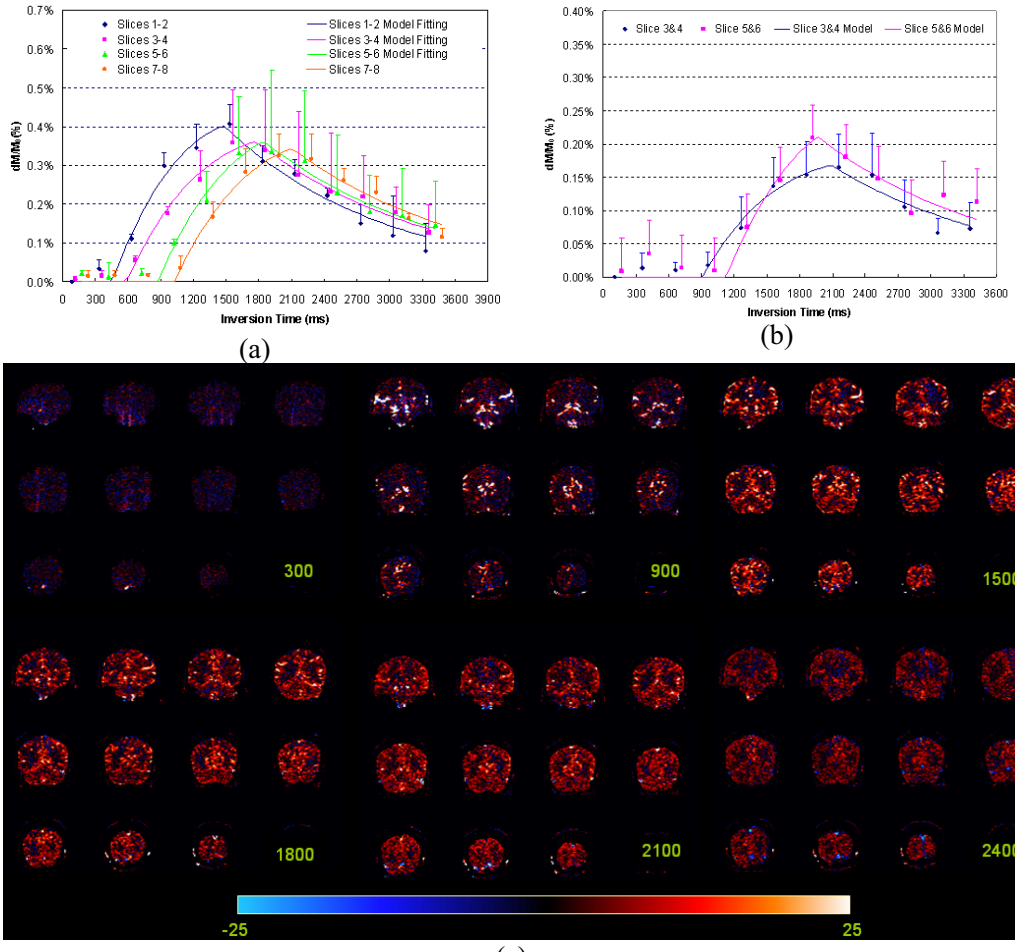

(a) (b)

(c)

Figure C-3 Study results from multiple inversion experiments: dynamic ASL signal changes with the inversion time and corresponding model fitting results for grey matter (a) and white matter (b), and one typical subject's perfusion weighted imaging maps for six selected inversion times

From this study, the estimated CBF for cerebellum grey and white matters are 35.92 ± 6.8 (mL/100g/min) and 21.62 ± 1.9 (mL/100g/min) respectively. The estimated M_0 of the blood is 1496.91 ± 0.48.

C.1.2 Results from Other Performed Optimization Studies

C.1.2.1 The estimation of the minimal number of inferior saturation pulses

The same ASL parameters as those in the previous study were used in the study for the estimation of the minimal number of inferior saturation pulses except the following ones: temporal bolus width (TI_1) = 800 ms, post-bolus delay = 1000 ms, the number of inferior saturation pulses varied from 0 to 40 by using 10 as an increment. The order of the applied number of inferior saturation pulses was randomized across the two subjects.

The study results presented in Figure C-4 showed that ten inferior saturation pulses are enough to suppress the residuals of labeled blood. To be safe, twenty inferior saturation pulses can be used in the following quantitative cerebellum perfusion studies.

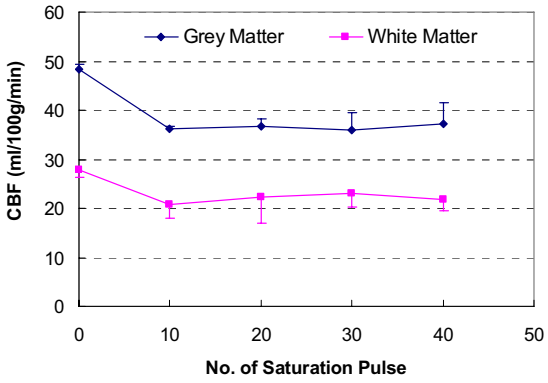

Figure C-4 CBF changes with the number of inferior saturation pulses

C.1.2.2 TR effects for cerebellum perfusion studies using partial coverage

To verify that the cerebellum perfusion studies using partial coverage can avoid the TR effects due to the interference between the labeling and the imaging of OPTIMAL FAIR, two subjects took part in the TR effects evaluation. All other MRI parameters used in this study were kept the same as those used in the two-session quantitative cerebellum perfusion study (experiment one in section 6.2.2) except that TR was varied from the

shortest TR equal to 2400 ms to a little longer TR value 3200 ms. The study results are presented in Figure C-5. The coefficients of variance for two CBF measurements of cerebellum grey matter are 4% and 2.36% respectively for two subjects. These coefficients of variance are much smaller than the typical coefficients of variance for PASL scans within one session (Jahng, Song et al. 2005), which means there is no significant difference between these two CBF measurements.

C.2 GRE IMAGING PARAMETERS IN QUANTITATIVE CEREBELLUM PERFUSION STUDIES

In the performed cerebellum perfusion studies, the number of imaging slices of GRE imaging is larger than the number of perfusion imaging slices, which, based on our experience, can help improve the accuracy of the co-registration. The center of GRE imaging slab matched the center of ASL imaging slab.

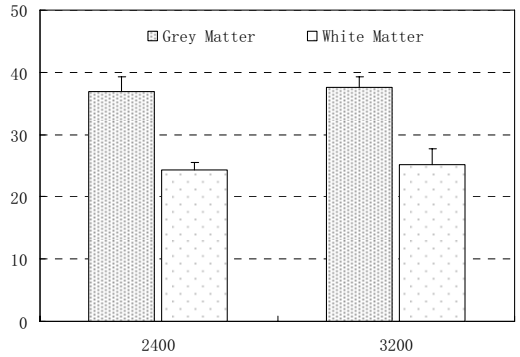

Figure C-5 CBF Measurements using two different TR values

C.2.1 GRE Imaging Parameters for Two-session Quantitative Cerebellum Perfusion Study

The following MRI parameters were used in this study: TR/TE = 80/5.2 ms, FOV = 128 x 128 mm^2, matrix size = 192 x 192, the number of imaging slices = 24, slice thickness = 6.0 mm, imaging resolution = 0.67 x 0.67 x 6.0 mm^3, flip angle = 80 degree, averages = 2, concatenations = 4, bandwidth = 160 Hz/Px.

C.2.2 GRE Imaging Parameters for Perfusion Studies Using Single Slice and Isotropic Resolution

(1) For resolution 2.5 x 2.5 x 2.5 mm^3, GRE imaging parameters are as the following: TR/TE = 102/6.9 ms, FOV = 160 x 160 mm^2, matrix size = 192 x 192, the number of imaging slices = 27, slice thickness = 2.5 mm, in-plane resolution = 0.84 x 0.84 mm^2, flip angle = 90, averages = 3, concatenations = 4, bandwidth = 120 Hz/Px.

(2) For resolution 3.0 x 3.0 x 3.0 mm^3, GRE imaging parameters are as the following: TR/TE = 120/5 ms, FOV = 192 x 192 mm^2, matrix size = 256 x 256, the number of imaging slices = 21, slice thickness = 3 mm, in-plane resolution = 0.75 x 0.75 mm^2, flip angle = 90, averages = 2, concatenations = 2, bandwidth = 180 Hz/Px.

(3) For resolution 3.5 x 3.5 x 3.5 mm^3, GRE imaging parameters are as the following: TR/TE = 85/4.84 ms, FOV = 224 x 224 mm^2, matrix size = 320 x 320, the number of imaging slices = 19, slice thickness = 3.5 mm, in-plane resolution = 0.7 x 0.7 mm^2, flip angle = 70, averages = 2, concatenations = 3, bandwidth = 180 Hz/Px.

(4) For resolution 5.0 x 5.0 x 5.0 mm^3 , GRE imaging parameters are as the following: TR/TE = 82/4.5 ms, FOV = 320 x 320 mm^2, matrix size = 448 x 448, the number of imaging slices = 15, slice thickness = 5 mm, in-plane resolution = 0.71 x 0.71 mm^2, flip angle = 80, averages = 2, concatenations = 2, bandwidth = 200 Hz/Px.

(5) For resolution 7.0 x 7.0 x 7.0 mm^3, GRE imaging parameters are as the following: TR/TE = 60/4.4 ms, FOV = 448 x 448 mm^2, matrix size = 512 x 512, the number of imaging slices = 9, slice thickness = 7 mm, in-plane resolution = 0.88 x 0.88 mm^2, flip angle = 70, averages = 1, concatenations = 2, bandwidth = 220 Hz/Px.

C.2.3 GRE Imaging Parameters for Perfusion Studies Using Multiple Slices

(1) For in-plane resolution 2.5 x 2.5 mm^2, GRE imaging parameters are as the following: TR/TE = 125/4.45 ms, FOV = 160 x 160 mm^2, matrix size = 192 x 192, the number of imaging slices = 24, slice thickness = 3.5 mm, in-plane resolution = 0.83 x 0.83 mm^2, flip angle = 90, averages = 2, concatenations = 2, bandwidth = 200 Hz/Px.

(2) For in-plane resolution 3.0 x 3.0 mm^3, all other imaging parameters are the same as those described in (1) in addition to the following ones: FOV = 192 x 192 mm^2, matrix size = 256 x 256, in-plane resolution = 0.75 x 0.75 mm^2.

(3) For in-plane resolution 3.5 x 3.5 mm^3, all other imaging parameters are the same as those described in (1) in addition to the following ones: FOV = 224 x 224 mm^2, matrix size = 256 x 256, in-plane resolution = 0.88 x 0.88 mm^2.

(4) For in-plane resolution 5.0 x 5.0 mm^3, all other imaging parameters are the same as those described in (1) in addition to the following ones: TR/TE = 112/4.25 ms, FOV = 320 x 320 mm^2, matrix size = 320 x 320, in-plane resolution = 1.0 x 1.0 mm^2.

(5) For in-plane resolution 7.0 x 7.0 mm^3, all other imaging parameters are the same as those described in (1) in addition to the following ones: TR/TE = 94/3.42 ms, FOV = 448 x 448 mm^2, matrix size = 448 x 448, in-plane resolution = 1.0 x 1.0 mm^2, bandwidth = 360 Hz/Px.

C.2.4 GRE Imaging Parameters for Perfusion Studies Using Whole Cerebellum Coverage

Exactly the same parameters as those in the two-session quantitative cerebellum perfusion study were used in this study.

APPENDIX D Anatomic and Angiography Images Used for Illustrations

D.1 ANATOMIC IMAGES USED FOR ILLUSTRATION

The anatomy images used for the illustrations were the averaged images from 30 co-registered and normalized anatomy images obtained across 30 sessions from one subject using Siemens' T_1-weighted imaging sequence MPRAGE with the typical imaging parameters described in Chapter 2. The co-registration and normalization were performed by using SPM 2. The final interpolated resolution of the averaged anatomic images is 1.0 x 1.0 x 1.0 mm^3.

Some images used in the illustration contain only brain tissue. These images were generated by using skull strip tool. Intensity threshold was used to remove voxels that mainly contain CSF. The skull was stripped by using Steve Smith's Brain Extraction Tool (BET) with fractional intensity equal to 0.6. These generated anatomic images were further cleaned in Adobe Photoshop CS 2. The selected slice used for the demonstration of the slab positions of pulse sequences is one slice on the left side of the brain with 4 mm away from the middle sagittal plane. For the illustration of imaging slice position in the hippocampus perfusion study, one slice from the left hemisphere was selected. The imaging slice used for the illustration of the slice positions used in cerebellum perfusion studies is from one imaging slice 2 mm away from the middle sagittal plane.

D.2 ANGIOGRAPHY IMAGES USED FOR ILLUSTRATIONS IN CEREBELLUM PERFUSION STUDIES

The MRI parameters used for the acquisition of 3D angiograph images are listed in the following: TR/TE = 20/4.2 ms, the number of slabs = 2, distance factor = -11.11%,

slice orientation = sagittal, phase encoding direction = anterior to posterior, the number of imaging slices per slab = 36, FOV in readout direction = 280 mm, FOV in phase encoding direction = 90%, slice thickness = 2.0 mm, concatenations = 2, flip angle = 20 degree, base resolution = 320, phase resolution = 68%, slice partial Fourier = 6/8, bandwidth = 120 Hz/Px.

The image used for the illustration of the slice position in cerebellum perfusion studies was generated by using maximum intensity projection method for the acquired 3D angiography volume.

BIBLIOGRAPHY

Alsop, D. C., M. Casement, et al. (2008). "Hippocampal hyperperfusion in Alzheimer's disease." Neuroimage.

Alsop, D. C. and J. A. Detre (1996). "Reduced transit-time sensitivity in noninvasive magnetic resonance imaging of human cerebral blood flow." J Cereb Blood Flow Metab **16**(6): 1236-49.

Alsop, D. C. and J. A. Detre (1998). "Multisection cerebral blood flow MR imaging with continuous arterial spin labeling." Radiology **208**(2): 410-6.

Berr, S. S., K. D. Hagspiel, et al. (1999). "Perfusion of the kidney using extraslice spin tagging (EST) magnetic resonance imaging." J Magn Reson Imaging **10**(5): 886-91.

Berr, S. S. and V. M. Mai (1999). "Extraslice spin tagging (EST) magnetic resonance imaging for the determination of perfusion." J Magn Reson Imaging **9**(1): 146-50.

Blaha, M., V. Benes, et al. (2007). "The effect of caffeine on dilated cerebral circulation and on diagnostic CO2 reactivity testing." J Clin Neurosci **14**(5): 464-7.

Boss, A., P. Martirosian, et al. (2007). "FAIR-TrueFISP imaging of cerebral perfusion in areas of high magnetic susceptibility differences at 1.5 and 3 Tesla." J Magn Reson Imaging **25**(5): 924-31.

Buxton, R. B. (2001). Introduction to Functional Magnetic Resonance Imaging: Principles and Techniques Cambridge University Press.

Buxton, R. B. (2005). "Quantifying CBF with arterial spin labeling." J Magn Reson Imaging **22**(6): 723-6.

Buxton, R. B., L. R. Frank, et al. (1998). "A general kinetic model for quantitative perfusion imaging with arterial spin labeling." Magn Reson Med **40**(3): 383-96.

Cameron, O. G., J. G. Modell, et al. (1990). "Caffeine and human cerebral blood flow: a positron emission tomography study." Life Sci **47**(13): 1141-6.

Campbell, A. M. and C. Beaulieu (2006). "Pulsed arterial spin labeling parameter optimization for an elderly population." J Magn Reson Imaging **23**(3): 398-403.

Detre, J. A., J. S. Leigh, et al. (1992). "Perfusion imaging." Magn Reson Med **23**(1): 37-45.

Donahue, M. J., H. Lu, et al. (2006). "An account of the discrepancy between MRI and PET cerebral blood flow measures. A high-field MRI investigation." NMR Biomed **19**(8): 1043-54.

Duhamel, G., C. de Bazelaire, et al. (2003). "Evaluation of systematic quantification errors in velocity-selective arterial spin labeling of the brain." Magn Reson Med **50**(1): 145-53.

Duvernoy, H. M. (2005). "The Human Hippocampus Functional Anatomy, Vascularization and Serial Sections with MRI." Springer-Verlag Berlin Heideiberg New York **Third Edition**

Edelman, R. R. and Q. Chen (1998). "EPISTAR MRI: multislice mapping of cerebral blood flow." Magn Reson Med **40**(6): 800-5.

Edelman, R. R., B. Siewert, et al. (1994). "Qualitative mapping of cerebral blood flow and functional localization with echo-planar MR imaging and signal targeting with alternating radio frequency." Radiology **192**(2): 513-20.

Ewing, J. R., Y. Cao, et al. (2001). "Single-coil arterial spin-tagging for estimating cerebral blood flow as viewed from the capillary: relative contributions of intra- and extravascular signal." Magn Reson Med **46**(3): 465-75.

Fernandez-Seara, M. A., J. Wang, et al. (2007). "Imaging mesial temporal lobe activation during scene encoding: Comparison of fMRI using BOLD and arterial spin labeling." Hum Brain Mapp **28**(12): 1391-400.

Fernandez-Seara, M. A., Z. Wang, et al. (2005). "Continuous arterial spin labeling perfusion measurements using single shot 3D GRASE at 3 T." Magn Reson Med **54**(5): 1241-7.

Field, A. S., P. J. Laurienti, et al. (2003). "Dietary caffeine consumption and withdrawal: confounding variables in quantitative cerebral perfusion studies?" Radiology **227**(1): 129-35.

Fox, S. I. (2006). Human Physiology, McGraw-Hill Science/Engineering/Math; 9 edition.

Frackowiak, R. S., G. L. Lenzi, et al. (1980). "Quantitative measurement of regional cerebral blood flow and oxygen metabolism in man using 15O and positron emission tomography: theory, procedure, and normal values." J Comput Assist Tomogr **4**(6): 727-36.

Frank, L. R., E. C. Wong, et al. (1997). "Slice profile effects in adiabatic inversion: application to multislice perfusion imaging." Magn Reson Med **38**(4): 558-64.

Golay, X., M. Stuber, et al. (1999). "Transfer insensitive labeling technique (TILT): application to multislice functional perfusion imaging." J Magn Reson Imaging **9**(3): 454-61.

Gunther, M., K. Oshio, et al. (2005). "Single-shot 3D imaging techniques improve arterial spin labeling perfusion measurements." Magn Reson Med **54**(2): 491-8.

Haase, A., D. Matthaei, et al. (1986). "Dynamic digital subtraction imaging using fast low-angle shot MR movie sequence." Radiology **160**(2): 537-41.

Haines, D. E. (2004). "Neuroanaotmy An atlas of Structures, Sections, and Systems." Lippincott Williams & Wilkins A Wolters Kluwer Company **Sixth Edition**.

Haley, R. W. (1999). "Is there a Gulf War syndrome?" Lancet **354**(9190): 1645-6.

Hennig, J., A. Nauerth, et al. (1986). "RARE imaging: a fast imaging method for clinical MR." Magn Reson Med **3**(6): 823-33.

Hom, J., R. W. Haley, et al. (1997). "Neuropsychological correlates of Gulf War syndrome." Arch Clin Neuropsychol **12**(6): 531-44.

Ishii, K., M. Sasaki, et al. (1998). "Paradoxical hippocampus perfusion in mild-to-moderate Alzheimer's disease." J Nucl Med **39**(2): 293-8.

Ito, H., K. Inoue, et al. (2006). "Database of normal human cerebral blood flow measured by SPECT: I. Comparison between I-123-IMP, Tc-99m-HMPAO, and Tc-99m-ECD as referred with O-15 labeled water PET and voxel-based morphometry." Ann Nucl Med **20**(2): 131-8.

Jagust, W. J., J. L. Eberling, et al. (1993). "The cortical topography of temporal lobe hypometabolism in early Alzheimer's disease." Brain Res **629**(2): 189-98.

Jahng, G. H., E. Song, et al. (2005). "Human brain: reliability and reproducibility of pulsed arterial spin-labeling perfusion MR imaging." Radiology **234**(3): 909-16.

Jahng, G. H., X. P. Zhu, et al. (2003). "Improved perfusion-weighted MRI by a novel double inversion with proximal labeling of both tagged and control acquisitions." Magn Reson Med **49**(2): 307-14.

Kety, S. S. and C. F. Schmidt (1948). "The Nitrous Oxide Method for the Quantitative Determination of Cerebral Blood Flow in Man: Theory, Procedure and Normal Values." J Clin Invest **27**(4): 476-83.

Kim, S. G. (1995). "Quantification of relative cerebral blood flow change by flow-sensitive alternating inversion recovery (FAIR) technique: application to functional mapping." Magn Reson Med **34**(3): 293-301.

Kim, S. G. and N. V. Tsekos (1997). "Perfusion imaging by a flow-sensitive alternating inversion recovery (FAIR) technique: application to functional brain imaging." Magn Reson Med **37**(3): 425-35.

Kubota, T., Y. Ushijima, et al. (2005). "Diagnosis of Alzheimer's disease using brain perfusion SPECT and MR imaging: which modality achieves better diagnostic accuracy?" Eur J Nucl Med Mol Imaging **32**(4): 414-21.

Kwong, K. K., J. W. Belliveau, et al. (1992). "Dynamic magnetic resonance imaging of human brain activity during primary sensory stimulation." Proc Natl Acad Sci U S A **89**(12): 5675-9.

Kwong, K. K., D. A. Chesler, et al. (1995). "MR perfusion studies with T1-weighted echo planar imaging." Magn Reson Med **34**(6): 878-87.

Lai, S., J. Wang, et al. (2001). "FAIR exempting separate T (1) measurement (FAIREST): a novel technique for online quantitative perfusion imaging and multi-contrast fMRI." NMR Biomed **14**(7-8): 507-16.

Lars Edvinsson, D. N. K. (2002). Cerebral Blood Flow and Metabolism. Philadelphia, PA, LIPPINCOTT WILLIAMS & WILKINS.

Le Bihan, D., E. Breton, et al. (1988). "Separation of diffusion and perfusion in intravoxel incoherent motion MR imaging." Radiology **168**(2): 497-505.

Luh, W. M., E. C. Wong, et al. (1999). "QUIPSS II with thin-slice TI1 periodic saturation: a method for improving accuracy of quantitative perfusion imaging using pulsed arterial spin labeling." Magn Reson Med **41**(6): 1246-54.

Luh, W. M., E. C. Wong, et al. (2000). "Comparison of simultaneously measured perfusion and BOLD signal increases during brain activation with T(1)-based tissue identification." Magn Reson Med **44**(1): 137-43.

Lunt, M. J., S. Ragab, et al. (2004). "Comparison of caffeine-induced changes in cerebral blood flow and middle cerebral artery blood velocity shows that caffeine reduces middle cerebral artery diameter." Physiol Meas **25**(2): 467-74.

Maccotta, L., J. A. Detre, et al. (1997). "The efficiency of adiabatic inversion for perfusion imaging by arterial spin labeling." NMR Biomed **10**(4-5): 216-21.

Mai, V. M. and S. S. Berr (1999). "MR perfusion imaging of pulmonary parenchyma using pulsed arterial spin labeling techniques: FAIRER and FAIR." J Magn Reson Imaging **9**(3): 483-7.

Mai, V. M., K. D. Hagspiel, et al. (1999). "Perfusion imaging of the human lung using flow-sensitive alternating inversion recovery with an extra radiofrequency pulse (FAIRER)." Magn Reson Imaging **17**(3): 355-61.

Manto, M.-U. (2002). The cerebellum and its disorders, Cambridge : Cambridge University Press, 2002.

Marro, K. I., C. E. Hayes, et al. (1997). "A model of the inversion process in an arterial inversion experiment." NMR Biomed **10**(7): 324-32.

Mathew, R. J. and W. H. Wilson (1991). "Substance abuse and cerebral blood flow." Am J Psychiatry **148**(3): 292-305.

Matt A. Bernstein, K. F. K., Xiaohong Joe Zhou (2004). Handbook of MRI Pulse Sequences Section 17.1 Academic Press.

Matthew, E., P. Andreason, et al. (1993). "Reproducibility of resting cerebral blood flow measurements with H2(15)O positron emission tomography in humans." J Cereb Blood Flow Metab **13**(5): 748-54.

Menon, P. M., H. A. Nasrallah, et al. (2004). "Hippocampal dysfunction in Gulf War Syndrome. A proton MR spectroscopy study." Brain Res **1009**(1-2): 189-94.

Ohnishi, T., H. Hoshi, et al. (1995). "High-resolution SPECT to assess hippocampal perfusion in neuropsychiatric diseases." J Nucl Med **36**(7): 1163-9.

Ostergaard, L., A. G. Sorensen, et al. (1996). "High resolution measurement of cerebral blood flow using intravascular tracer bolus passages. Part II: Experimental comparison and preliminary results." Magn Reson Med **36**(5): 726-36.

Ostergaard, L., R. M. Weisskoff, et al. (1996). "High resolution measurement of cerebral blood flow using intravascular tracer bolus passages. Part I: Mathematical approach and statistical analysis." Magn Reson Med **36**(5): 715-25.

Parkes, L. M. (2005). "Quantification of cerebral perfusion using arterial spin labeling: two-compartment models." J Magn Reson Imaging **22**(6): 732-6.

Parkes, L. M. and P. S. Tofts (2002). "Improved accuracy of human cerebral blood perfusion measurements using arterial spin labeling: accounting for capillary water permeability." Magn Reson Med **48**(1): 27-41.

Pekar, J., P. Jezzard, et al. (1996). "Perfusion imaging with compensation for asymmetric magnetization transfer effects." Magn Reson Med **35**(1): 70-9.

Pell, G. S., D. P. Lewis, et al. (2004). "TurboFLASH FAIR imaging with optimized inversion and imaging profiles." Magn Reson Med **51**(1): 46-54.

Pell, G. S., M. F. Lythgoe, et al. (1999). "Reperfusion in a gerbil model of forebrain ischemia using serial magnetic resonance FAIR perfusion imaging." Stroke **30**(6): 1263-70.

Pell, G. S., D. L. Thomas, et al. (1999). "Implementation of quantitative FAIR perfusion imaging with a short repetition time in time-course studies." Magn Reson Med **41**(4): 829-40.

Pruessmann, K. P., X. Golay, et al. (2000). "RF pulse concatenation for spatially selective inversion." J Magn Reson **146**(1): 58-65.

Raichle, M. E., W. R. Martin, et al. (1983). "Brain blood flow measured with intravenous H2(15)O. II. Implementation and validation." J Nucl Med **24**(9): 790-8.

Rempp, K. A., G. Brix, et al. (1994). "Quantification of regional cerebral blood flow and volume with dynamic susceptibility contrast-enhanced MR imaging." Radiology **193**(3): 637-41.

Rodriguez, G., P. Vitali, et al. (2000). "Hippocampal perfusion in mild Alzheimer's disease." Psychiatry Res **100**(2): 65-74.

Sapirstein, L. A. (1958). "Regional blood flow by fractional distribution of indicators." Am J Physiol **193**(1): 161-8.

Schraml, C., A. Boss, et al. (2007). "FAIR true-FISP perfusion imaging of the thyroid gland." J Magn Reson Imaging **26**(1): 66-71.

Schwarzbauer, C. and W. Heinke (1998). "BASE imaging: a new spin labeling technique for measuring absolute perfusion changes." Magn Reson Med **39**(5): 717-22.

Schwarzbauer, C., S. P. Morrissey, et al. (1996). "Quantitative magnetic resonance imaging of perfusion using magnetic labeling of water proton spins within the detection slice." Magn Reson Med **35**(4): 540-6.

Silva, A. C., W. Zhang, et al. (1995). "Multi-slice MRI of rat brain perfusion during amphetamine stimulation using arterial spin labeling." Magn Reson Med **33**(2): 209-14.

Silva, A. C., W. Zhang, et al. (1997). "Estimation of water extraction fractions in rat brain using magnetic resonance measurement of perfusion with arterial spin labeling." Magn Reson Med **37**(1): 58-68.

St Lawrence, K. S., J. A. Frank, et al. (2000). "Effect of restricted water exchange on cerebral blood flow values calculated with arterial spin tagging: a theoretical investigation." Magn Reson Med **44**(3): 440-9.

Stubbs, T. A. and I. A. Macdonald (1995). "Systemic and regional haemodynamic effects of caffeine and alcohol in fasting subjects [corrected]." Clin Auton Res **5**(3): 123-7.

Tanabe, J. L., M. Yongbi, et al. (1999). "MR perfusion imaging in human brain using the UNFAIR technique. Un-inverted flow-sensitive alternating inversion recovery." J Magn Reson Imaging **9**(6): 761-7.

Utting, J. F., D. L. Thomas, et al. (2003). "Velocity-driven adiabatic fast passage for arterial spin labeling: results from a computer model." Magn Reson Med **49**(2): 398-401.

Wang, J., D. C. Alsop, et al. (2002). "Comparison of quantitative perfusion imaging using arterial spin labeling at 1.5 and 4.0 Tesla." Magn Reson Med **48**(2): 242-54.

Wang, J., D. J. Licht, et al. (2003). "Pediatric perfusion imaging using pulsed arterial spin labeling." J Magn Reson Imaging **18**(4): 404-13.

Wang, J., Y. Zhang, et al. (2005). "Amplitude-modulated continuous arterial spin-labeling 3.0-T perfusion MR imaging with a single coil: feasibility study." Radiology **235**(1): 218-28.

Wang, X. S., J. Y. Tang, et al. (2003). "Pediatric cancer pain management practices and attitudes in China." J Pain Symptom Manage **26**(2): 748-59.

Williams, D. S., J. A. Detre, et al. (1992). "Magnetic resonance imaging of perfusion using spin inversion of arterial water." Proc Natl Acad Sci U S A **89**(1): 212-6.

Williams, D. S., D. J. Grandis, et al. (1993). "Magnetic resonance imaging of perfusion in the isolated rat heart using spin inversion of arterial water." Magn Reson Med **30**(3): 361-5.

Wintermark, M., M. Sesay, et al. (2005). "Comparative overview of brain perfusion imaging techniques." J Neuroradiol **32**(5): 294-314.

Wolff, S. D. and R. S. Balaban (1989). "Magnetization transfer contrast (MTC) and tissue water proton relaxation in vivo." Magn Reson Med **10**(1): 135-44.

Wong, E. C., R. B. Buxton, et al. (1997). "Implementation of quantitative perfusion imaging techniques for functional brain mapping using pulsed arterial spin labeling." NMR Biomed **10**(4-5): 237-49.

Wong, E. C., R. B. Buxton, et al. (1998). "Quantitative imaging of perfusion using a single subtraction (QUIPSS and QUIPSS II)." Magn Reson Med **39**(5): 702-8.

Wong, E. C., M. Cronin, et al. (2006). "Velocity-selective arterial spin labeling." Magn Reson Med **55**(6): 1334-41.

Wu, W. C., M. Fernandez-Seara, et al. (2007). "A theoretical and experimental investigation of the tagging efficiency of pseudocontinuous arterial spin labeling." Magn Reson Med **58**(5): 1020-7.

Wu, W. C., Y. Mazaheri, et al. (2007). "The effects of flow dispersion and cardiac pulsation in arterial spin labeling." IEEE Trans Med Imaging **26**(1): 84-92.

Wu, W. C. and E. C. Wong (2006). "Intravascular effect in velocity-selective arterial spin labeling: the choice of inflow time and cutoff velocity." Neuroimage **32**(1): 122-8.

Wu, W. C. and E. C. Wong (2007). "Feasibility of velocity selective arterial spin labeling in functional MRI." J Cereb Blood Flow Metab **27**(4): 831-8.

Yang, Y., J. A. Frank, et al. (1998). "Multislice imaging of quantitative cerebral perfusion with pulsed arterial spin labeling." Magn Reson Med **39**(5): 825-32.

Yazici, B., B. Erdogmus, et al. (2005). "Cerebral blood flow measurements of the extracranial carotid and vertebral arteries with Doppler ultrasonography in healthy adults." Diagn Interv Radiol **11**(4): 195-8.

Ye, F. Q., V. S. Mattay, et al. (1997). "Correction for vascular artifacts in cerebral blood flow values measured by using arterial spin tagging techniques." Magn Reson Med **37**(2): 226-35.

Yongbi, M. N., C. A. Branch, et al. (1998). "Perfusion imaging using FOCI RF pulses." Magn Reson Med **40**(6): 938-43.

Zaharchuk, G., P. J. Ledden, et al. (1999). "Multislice perfusion and perfusion territory imaging in humans with separate label and image coils." Magn Reson Med **41**(6): 1093-8.

Zhang, W., A. C. Silva, et al. (1995). "NMR measurement of perfusion using arterial spin labeling without saturation of macromolecular spins." Magn Reson Med **33**(3): 370-6.

Zhang, W., D. S. Williams, et al. (1992). "Measurement of brain perfusion by volume-localized NMR spectroscopy using inversion of arterial water spins: accounting for transit time and cross-relaxation." Magn Reson Med **25**(2): 362-71.

Zhang, W., D. S. Williams, et al. (1993). "Measurement of rat brain perfusion by NMR using spin labeling of arterial water: in vivo determination of the degree of spin labeling." Magn Reson Med **29**(3): 416-21.

Zhang, X., T. Nagaoka, et al. (2007). "Quantitative basal CBF and CBF fMRI of rhesus monkeys using three-coil continuous arterial spin labeling." Neuroimage **34**(3): 1074-83.

Zhang, Y., H. K. Song, et al. (2005). "Spatially-confined arterial spin-labeling with FAIR." J Magn Reson Imaging **22**(1): 119-24.

Zhou, J., S. Mori, et al. (1998). "FAIR excluding radiation damping (FAIRER)." Magn Reson Med **40**(5): 712-9.

Zhou, J. and P. C. van Zijl (1999). "Perfusion imaging using FAIR with a short predelay." Magn Reson Med **41**(6): 1099-107.

Zhou, J., D. A. Wilson, et al. (2001). "Two-compartment exchange model for perfusion quantification using arterial spin tagging." J Cereb Blood Flow Metab **21**(4): 440-55.